CONTRACT NAS8-2631

DETERMINATION OF LOW-TEMPERATURE FATIGUE PROPERTIES OF ALUMINUM AND TITANIUM ALLOYS

ANNUAL SUMMARY REPORT

JULY 1963

prepared for

NATIONAL AERONAUTICS AND SPACE ADMINISTRATION
GEORGE C. MARSHALL SPACE FLIGHT CENTER

prepared by

MARTIN DENVER

(NASA-CR-63-29) OTS: (cover) Copy No. 11

(NASA Contract NAS8-2631)

DETERMINATION OF LOW-TEMPERATURE FATIGUE PROPERTIES OF ALUMINUM AND TITANIUM ALLOYS, ANNUAL SUMMARY REPORT

July 1963

Authors

F. R. Schwartzberg,
R. D. Keys,
M. J. Brown, and
C. L. Reightler

July 1963 rcgs

Approved

W. H. Clohessy

W. H. Clohessy, Director
Space Research Laboratories

552 8500
~~552 8504~~ marietta corp.

~~MARTIN COMPANY~~
Denver, Colorado
Aerospace Division of Martin-Marietta Corporation

FOREWORD

This report was prepared by Martin-Marietta Corporation under Contract NAS8-2631 for the George C. Marshall Space Flight Center of the National Aeronautics and Space Administration. The work was administered under the technical direction of the Propulsion and Vehicle Engineering Division, Engineering Materials Branch, of the George C. Marshall Space Flight Center, with W. B. McPherson acting as Project Manager.

CONTENTS

		Page
Foreword		ii
Contents		iii
Abstract		viii
I.	Introduction	1
II.	Materials	4
III.	Specimens	8
IV.	Test Apparatus and Facilities	11
	A. Cryostat	13
	B. Alignment and Assembly	17
	C. Automation	22
	D. Facility	25
	E. Performance	28
V.	Test Procedure	29
	A. Tension	29
	B. Fatigue	29
VI.	Experimental Results	31
	A. Tension Tests	31
	B. Fatigue Tests	31
VII.	Discussion of Results	53
	A. Aluminum Alloys	53
	1. Tension Properties	53

2. Fatigue Properties 54

B. Titanium Alloys 63

1. Tension Properties 64

2. Fatigue Properties 67

VIII. Conclusions 72

References 73

Appendix A -- Cryostat Drawings . . . . . A-1 thru A-9

Appendix B -- Tensile Data . . . . . B-1 thru B-8

Appendix C -- Fatigue Data . . . . . C-1 thru C-26

Distribution

Figure

1 Specifications for Tensile Specimen 8

2 Specifications for Fatigue Specimen 9

3 Effect of Misalignment on the Applied Axial Load of 5456-H343 Aluminum Alloy at -423°F . . 10

4 SF 10U Fatigue-Testing Machine 12

5 Cutaway View of Cryostat Assembly Mounted in Fatigue-Testing Machine 14

6 Cryostat Components before Assembly 15

7 Liquid Hydrogen Cryostat Lid Assembly 16

8 View of Cryostat and Mounting Hardware 18

9	Frames from High-Speed Motion Pictures of Misaligned 7075-T6 Aluminum Alloy Fatigue Test	19
10	Frames from High-Speed Motion Picture of Properly Aligned 7075-T6 Aluminum Alloy Fatigue Test	21
11	Liquid Nitrogen Fill Controller	23
12	Liquid Hydrogen Fill Controller	23
13	Schematic Diagram of Liquid Hydrogen Flow System	24
14	Liquid Hydrogen Fatigue-Testing Facility	26
15	Liquid Nitrogen Fatigue-Testing Facility	27
16	Tensile Properties of 2014-T6 Aluminum Alloy at Cryogenic Temperatures	32
17	Tensile Properties of 2219-T87 Aluminum Alloy at Cryogenic Temperatures	33
18	Tensile Properties of 5456-H343 Aluminum Alloy at Cryogenic Temperatures	34
19	Tensile Properties of 2020-T6 Aluminum Alloy at Cryogenic Temperatures	35
20	Tensile Properties of 7075-T6 Aluminum Alloy at Cryogenic Temperatures	36
21	Tensile Properties of 5Al-2.5Sn Titanium Alloy at Cryogenic Temperatures	37
22	Tensile Properties of 6Al-4V Titanium Alloy at Cryogenic Temperatures	38
23	Tensile Properties of 13V-11Cr-3Al Titanium Alloy at Cryogenic Temperatures	39
24	Fatigue Properties of Parent Metal 2014-T6 Aluminum Alloy	40

25	Fatigue Properties of Parent Metal 2219-T87 Aluminum Alloy	41
26	Fatigue Properties of Parent Metal 5456-H343 Aluminum Alloy	42
27	Fatigue Properties of Parent Metal 2020-T6 Aluminum Alloy	43
28	Fatigue Properties of Parent Metal 7075-T6 Aluminum Alloy	44
29	Fatigue Properties of Welded 2014-T6 Aluminum Alloy	45
30	Fatigue Properties of Welded 2219-T87 Aluminum Alloy	46
31	Fatigue Properties of Welded 5456-H343 Aluminum Alloy	47
32	Fatigue Properties of Annealed Parent Metal 5Al-2.5Sn Titanium Alloy	48
33	Fatigue Properties of Solution-Treated and Aged Parent Metal 6Al-4V Titanium Alloy	49
34	Fatigue Properties of Solution-Treated and Aged Parent Metal 13V-11Cr-3Al Titanium Alloy . . .	50
35	Fatigue Properties of Annealed, Welded 5Al-2.5Sn Titanium Alloy	51
36	Fatigue Properties of Solution-Treated and Aged Welded 6Al-4V Titanium Alloy	52
37	Modulus of Elasticity of Five Aluminum Alloys at Cryogenic Temperatures	55
38	Fatigue Strength/Ultimate Strength Ratio for Five Aluminum Alloys	60
39	Fatigue Strength/Yield Strength Ratio for Five Parent Metal Aluminum Alloys	61

40	Effect of Stress Ratio on the Fatigue Properties of Two Aluminum Alloys at -423°F	63
41	Effect of Interstitial Content on the Unnotch Tensile Strength of Ti-5Al-2.5Sn	65
42	Modulus of Elasticity of Three Titanium Alloys at Cryogenic Temperatures	66
43	Fatigue Strength/Tensile Strength Ratio for Three Titanium Alloys	70
44	Fatigue Strength/Yield Strength Ratio for Three Parent Metal Titanium Alloys	71

Table

I	List of Materials Selected for Experimental Program	4
II	Details of Welding Procedure for Aluminum Alloys	6
III	Details of Welding Procedure for Titanium Alloys	6
IV	Chemical Analyses of Titanium Alloy Sheet, Wire, and Weld Bead	7
V	Endurance Limits for Aluminum Alloys	56
VI	Fatigue Strength/Ultimate Strength Ratio for Aluminum Alloys	58
VII	Fatigue Strength/Yield Strength Ratio for Parent Metal Aluminum Alloys	59
VIII	Comparison of Fatigue Strength Ratios with Notch Strength Ratios for Aluminum Alloys . . .	62
IX	Endurance Limits for Titanium Alloys	67
X	Fatigue Strength/Ultimate Strength Ratio of Titanium Alloys	69
XI	Fatigue Strength/Yield Strength Ratio of Parent Metal Titanium Alloys	69

ABSTRACT

11818

The first year's progress on this program is reported.

Two cryogenic fatigue-testing systems were constructed: one for operation at -320°F, one for -423°F testing. Cryostats were designed to permit fully reversed stressing of sheet materials under axial load conditions. A cryostat design incorporating a vacuum-insulated, double-walled, stainless steel container with a tubular loading stem passing through its central axis was used. The cryostat mounts on the reciprocating platen of the test machine and moves with it while the lid and associated lines and instrumentation remain fixed. The equipment techniques developed have demonstrated that by careful alignment, fatigue tests of axial-loaded, flat sheet materials can be effectively accomplished using fully reversed stresses. The apparatus has performed satisfactorily for almost 1 yr despite the severe environmental conditions.

Various aluminum and titanium sheet alloys (0.100-in. nominal thickness), as listed below, were evaluated in the parent metal and, where applicable, welded conditions.

Aluminum	Titanium
2014-T6	Ti-5Al-2.5Sn
2219-T87	Ti-6Al-4V
5456-H343	Ti-13V-11Cr-3Al
2020-T6	
7075-T6	

Properties were determined at 70, -320, -423°F for fatigue life in the 10^3 to 10^7 cycle range. Titanium alloy 5Al-2.5Sn showed outstanding behavior on the basis of fatigue strength/tensile strength ratio values. The Ti-6Al-4V alloy heat-treated to 165,000 psi showed fatigue strength similar to Ti-5Al-2.5Sn, but was poorer on the dynamic/static strength ratio basis. Welded Ti-5Al-2.5Sn also exhibited outstanding properties.

In the aluminum family, 5456-H343 fared very well. Alloys 2014-T6 and 2219-T87 also showed good fatigue properties. The 2020-T6 and 7075-T6 compositions exhibited the lowest properties of all the materials evaluated. Welded 5456, 2014, and 2219 all displayed good fatigue resistance.

The titanium alloys exhibited a much greater ratio of fatigue/ultimate strength than the aluminum alloys.

AUTHOR

I. INTRODUCTION

Because of the behavior of structural materials at low temperatures, selection of the proper materials for booster and space vehicle systems that use cryogenic propellants is a challenge. Routine mechanical properties, such as tensile and compressive strength, modulus of elasticity, and ductility, are usually determined to assess the behavior of a candidate material. Behavior under stress concentration and cyclic loading conditions must also be studied to evaluate adequately a potential material.

Cryogenic literature reveals some data on the routine properties, but there is a significant lack of reliable information on fatigue or cyclic loading. Cryogenic data on welded material are virtually nonexistent. To fill this obvious requirement for sound engineering data, the experimental program presented in this report was prepared.

Fatigue tests can best be described by the method used to apply loads. Repeated loading to both a constant-stress amplitude and a constant-strain amplitude are used. With the first method, direct axial loading is employed, and with the second, bending techniques, either plane or rotational. For axial testing, the entire cross section is uniformly loaded. Stress is determined by load/area. In bending, the stress varies throughout the cross section of the test specimen, from a maximum at the outer fiber through zero at the neutral axis, to a maximum negative value at the opposite outer surface. With this technique, stress must be obtained by calculating from the moment formula $S = (Mc)/I$.

Although these bending tests have been the most popular fatigue techniques in the past, they are being replaced by the axial-loading method because there are certain disadvantages in using bending fatigue.

As shown by the formula, bending stress is calculated using the bending moment and section modulus. The bending moment M is a function of the modulus of elasticity of the test material. Accuracy of the stress calculation is therefore directly proportional to the accuracy of the modulus value. Although moduli of common engineering materials at room temperature are known, there is little information in the literature on values at cryogenic temperatures.

The endurance limit obtained by bending techniques may be as great as 30% higher than values obtained by axial loading. Although

we do not fully understand the reasons for this, certain state-of-stress theories have been proposed. One explanation is the possible development of favorable transverse stresses in the elongated or compressed surface layers and an outer-layer resistance to deformation caused by the underlying material during bending load tests.

Another shortcoming of the bending technique is that when plastic yielding occurs, stresses in the member cannot be readily calculated. Even in tests performed in the elastic range, minute localized plastic deformation may change the outer fiber stress.

There is a greater chance of failure from minor surface defects in bending than in axial loading. These defects may also create larger scatter with a limited number of specimens.

In calculating stress, the simple moment formula can be used only on specimens free from holes, grooves, and outline or surface discontinuities, such as weld beads. Therefore, to evaluate the bending fatigue of welded specimens, it would be more desirable to machine the weld bead flush. However, this would detract from the validity of the joint information because it eliminates stress concentrations.

The proposed material applications in cryogenic booster and space vehicles under conditions of cyclic loading suggest that alternating tension/compression stresses may more closely simulate the service history of the structure.

Because of the superiority of the axial-loading technique and its ability to simulate anticipated structural loads, this method has been selected for this program. The axial-loading machines used employ a rotating mass to apply a controlled dynamic load sinusoidally about a static-load level.

Tension/compression tests of sheet materials under axial loading are not often performed, for these tests are normally restricted to bar materials. Fortunately, the sheet gage selected by NASA presented the opportunity to attempt complete reversal of stresses without having to resort to the bending technique. The success of such an approach depends on the flatness of the sheet products available. The aluminum alloys used for this research were sufficiently flat to permit fully reversed stressing. Unfortunately, the heat-treated titanium sheet materials were rather warped and could not be tested safely under compressive loads. Tension/tension loads were therefore used for both the annealed and heat-treated titanium alloys.

Testing at liquid hydrogen temperature was conducted at the Denver laboratories. All equipment was designed and constructed at this location. Evaluation of fatigue properties at 70 and -320°F was conducted at the Baltimore laboratories.

II. MATERIALS

The materials selected for evaluation in this program include those that are being considered for structural service at cryogenic temperatures. Several of the materials selected by NASA were mutually recognized as exhibiting poor behavior at these temperatures. However, they were retained to show the comparison between various compositions.

Material condition was selected to give the highest strength level for each alloy. Weldable alloys were evaluated in both the parent metal and as-welded conditions.

Parent-metal specimens of the eight alloys listed in Table I were evaluated.

Table I List of Materials* Selected for Experimental Program

Alloy Base	Designation	Temper	Thickness Nominal, in.	Vendor	Heat No.
Aluminum	2014	-T6	0.100	Reynolds	-
Aluminum	2219	-T87	0.100	Alcoa	-
Aluminum	2020	-T6	0.090	Unknown*	-
Aluminum	5456	-H343	0.100	Alcoa	-
Aluminum	7075	-T6	0.100	Reynolds	-
Titanium	Ti-5Al-2.5Sn	Annealed	0.100	Titanium Metals Corporation	D-3272
Titanium	Ti-6Al-4V	Solution-Treated and Aged (1660F/ 5 min, WQ; 1000F/ 4 hr, AC)	0.100	Titanium Metals Corporation	D-2488
Titanium	Ti-13V-11Cr-3Al	Solution-Treated and Aged (1450F/ 20 min, AC; 900F/ 24 hr AC)	0.100	Titanium Metals	D-1639

*Material supplied by National Aeronautics and Space Administration.

Four of the five aluminum alloys were readily available. The fifth composition, 2020-T6, was commercially available only if a mill run (2000 lb) would be purchased. Fortunately, sufficient sheet material was available from NASA to perform the required testing.

The alpha (Ti-5Al-2.5Sn) and alpha-beta (Ti-6Al-4V) alloys were purchased as extra-low interstitial grade to assure maximum toughness at cryogenic temperatures. No attempt was made to procure low interstitial beta (Ti-13V-11Cr-3Al) alloy because of its well-known brittle behavior, independent of impurities, below -100°F.

Much difficulty was experienced in the procurement of solution-treated and aged Ti-13V-11Cr-3Al alloy. The first sheet received was rejected by Martin Company because of its very poor flatness. A second sheet, heat-treated to Martin's requirement, was rejected by the vendor for poor flatness control. A third sheet, however, was accepted by Martin even though flatness was still poor. The solution-treated and aged Ti-6Al-4V sheet was also poor, but was within specification limits. Only the alpha titanium and aluminum alloys exhibited good flatness characteristics.

Procurement of welding wire for the titanium alloys was very difficult. The only company prepared to offer low interstitial Ti-5Al-2.5Sn and Ti-6Al-4V and normal interstitial Ti-13V-11Cr-3Al wire was the R & D Metals Corporation of Kidron, Ohio, and it experienced great difficulty in fabricating the wire. Martin Company's order for the wire was placed in May 1962, and delivery was promised for July 1962. However, only the Ti-6Al-4V arrived on schedule, for trouble was experienced in drawing the remaining two alloys below 0.060-in. diameter. Finally, in November these items were shipped. Unfortunately, the Ti-13V-11Cr-3Al was claimed to have been lost in transit. To prevent further delays, a search was conducted at the Martin Company for Ti-13V-11Cr-3Al wire in a similar size for the required welding. A sufficient amount was located at the Baltimore Division.

Aluminum and titanium alloys were welded with the tungsten inert gas (TIG) process and automatic welding heads. Tables II and III list details of the procedure used for each material.

All weld panels were radiographically inspected. The aluminum panels were found to exceed the Class II requirements of MSFC drawing No. 10509310. Weld quality approximated the requirements displayed in the NASA specifications for Class I welds. Similarly, the titanium alloys were of high quality. Very minor porosity was noted in several areas of the Ti-13V-11Cr-3Al.

Particular emphasis was placed on procurement of low-interstitial titanium sheet and welding wire and on prevention of contamination during welding to maintain low interstitial content. Interstitial analyses reported in the certification of test provided by the vendors for the sheet and wire were confirmed by vacuum fusion analyses for oxygen, nitrogen, and hydrogen performed by Titanium Metals Corporation of America on the sheet metal, welding wire, and weld beads. These results, listed in Table IV, show excellent agreement between the certification analyses and the check analyses. The low levels of oxygen and nitrogen in the weld beads are proof of satisfactory inert gas protection during the welding process.

Table II Details of Welding Procedure for Aluminum Alloys

Alloy	Filler Wire	Wire Diameter, in.	Voltage, v	Current, amp	Speed, in./min
2014-T6	2319	3/32	11	160	11
2219-T87	2319	3/32	11	170	12
5456-H343	5556	3/32	11	170	11
TIG-welded with Airco D head; argon protective gas; AC.					

Table III Details of Welding Procedure for Titanium Alloys

Alloy	Wire Diameter, in.	Voltage, v	Current, amp	Speed, in./min
Ti-5Al-2.5Sn	0.030	10.5	215	13
Ti-6Al-4V	0.030	11	215	13
Ti-13V-11Cr-3Al	0.045	11	215	13
TIG-welded with Airco D head and 300A. P & H power supply; DC, straight polarity; helium-argon backup and trailing gas protection; parent-metal filler wire.				

Table IV Chemical Analyses of Titanium Alloy Sheet, Wire, and Weld Bead

Material	Composition, Weight Percent*								
	Al	V	Sn	Cr	Fe	C	O	N	H
Ti-5Al-2.5Sn Parent Metal	5.1	-	2.5	-	0.08	0.022	0.06 (0.07)	0.014 (0.016)	0.017 (0.013)
Ti-5Al-2.5Sn Welding Wire	5.5	-	2.5	-	0.20	0.033	0.10 (0.07)	0.012 (0.118)	0.005 (0.003)
Ti-5Al-2.5Sn Weld Bead	-	-	-	-	-	-	(0.07)	(0.020)	(0.007)
Ti-6Al-4V Parent Metal	6.0	4.1	-	-	0.09	0.019	0.09 (0.12)	0.016 (0.020)	0.006 (0.006)
Ti-6Al-4V Welding Wire	6.1	4.0	-	-	0.20	0.03	0.12 (0.14)	0.010 (0.012)	0.0038 (0.003)
Ti-6Al-4V Weld Bead	-	-	-	-	-	-	(0.12)	(0.017)	(0.007)
Ti-13V-11Cr-3Al Parent Metal	3.1	13.4	-	11.4	0.17	0.027	0.14	0.027	0.008

*Analyses from vendor's certification of test; values in parentheses are checks performed by Titanium Metals Corporation of America.

III. SPECIMENS

Tensile specimens were machined to the specifications shown in Fig. 1. These specimens were designed specifically for use with the multiple-linkage systems described by Keys (Ref. 1).

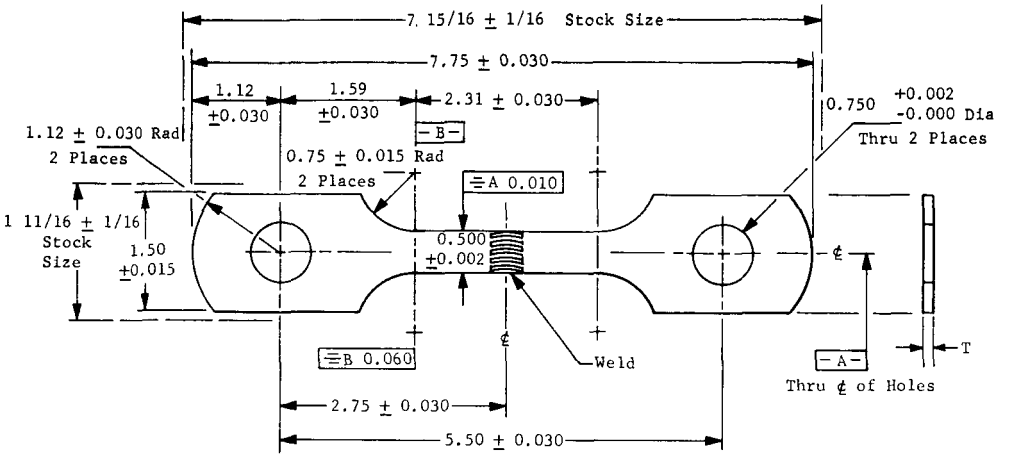

Fig. 1 Specifications for Tensile Specimen

Fatigue specimens were machined according to the sketch in Fig. 2. Aluminum specimens were machined to the 0.375-in. gage width A dimension; titanium material, to a gage width of 0.200-in. In contrast to the usual fatigue specimen shapes, the specimen design incorporates a straight-column test-gage section. A constant-width test section was selected to permit proper evaluation of weld bead and heat-affected zone in a short column length.

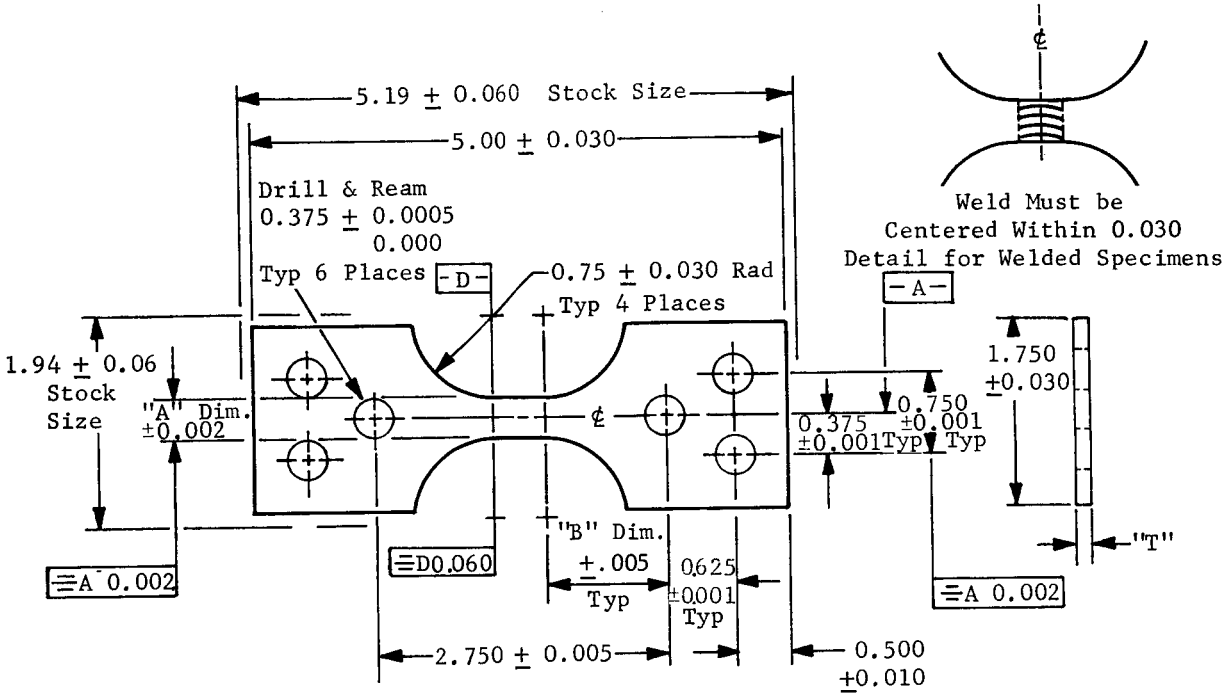

Note: When "A" = 0.200, "B" = 1.250.
When "A" = 0.375, "B" = 1.125.

Fig. 2 Specifications for Fatigue Specimen

Column analysis revealed that the specimen exhibited a high margin of safety from column buckling if properly aligned. An additional analysis was performed to show the relationship between the degree of misalignment and applied axial loads for various alloys. Figure 3 shows this relationship for a typical aluminum alloy composition (5456-H343) at -423°F. As shown in the diagram, to permit axial loads in the 1500 to 2000-lb range, alignment must be maintained at better than 0.001 in.

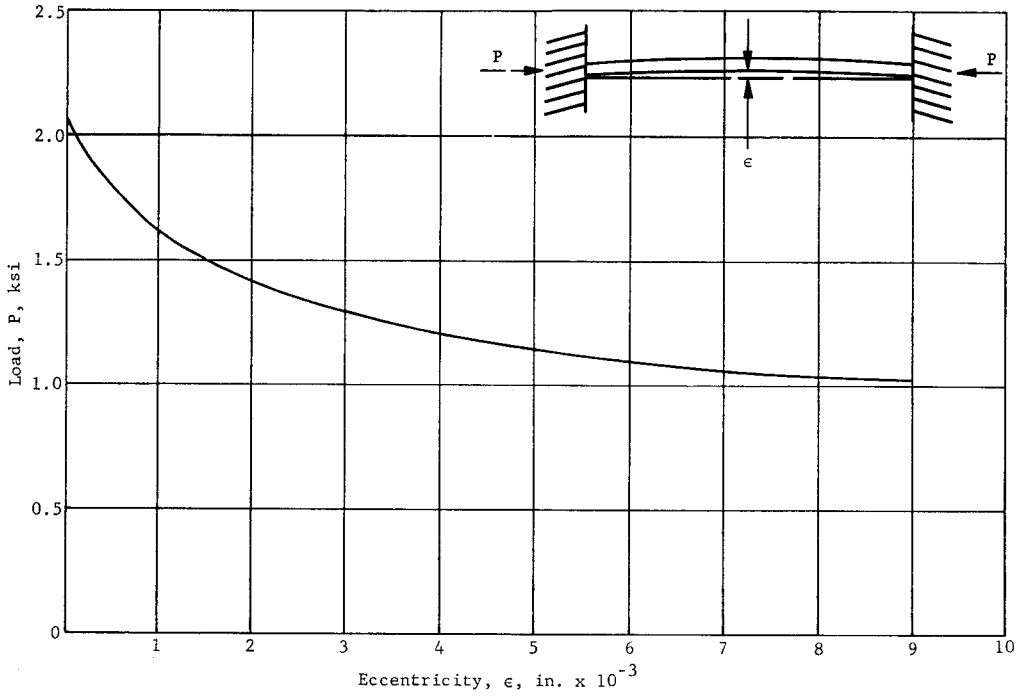

Fig. 3 Effect of Misalignment on the Applied Axial Load of 5456-H343 Aluminum Alloy at -423°F

IV. TEST APPARATUS AND FACILITIES

The fatigue-test apparatus (Fig. 4) was designed for use with Sonntag SF 10 U fatigue-testing machines. These machines have a reciprocating platen located in the center of the test bed. Load is applied between this platen and the head frame anchored to the test bed. Such machines have a capacity of 5000 lb dynamic load and $\pm$5000 lb static load. Therefore the test apparatus was designed to match this capacity.

The principal requirements for this system were:

1) Ability to operate at -320 and -423°F;

2) Good thermal efficiency;

3) Ease of specimen change;

4) Precise alignment;

5) Automation of temperature-control system.

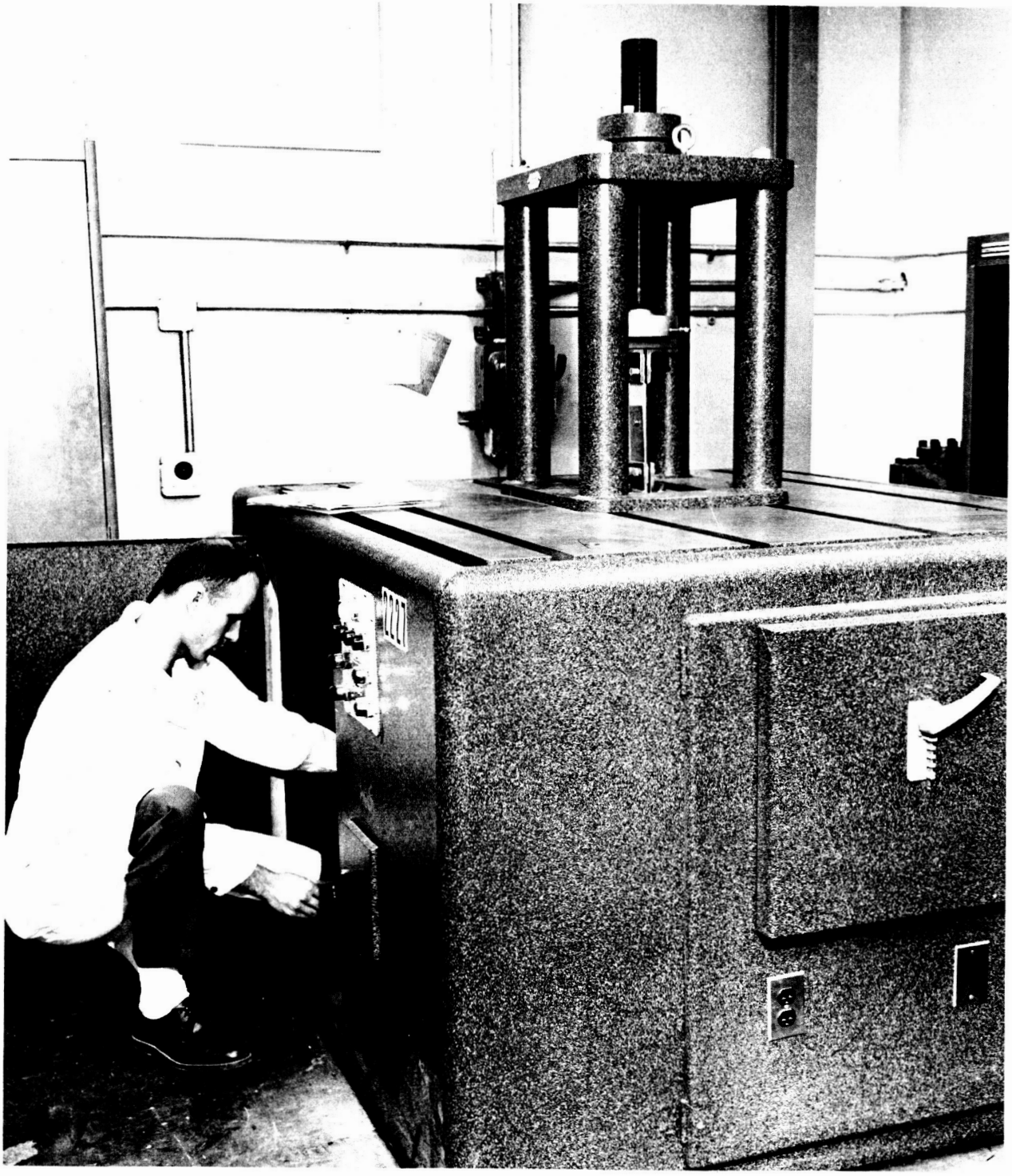

Fig. 4 SF 10U Fatigue-Testing Machine

A. CRYOSTAT

Based on the described requirements, a test cryostat was designed (see Appendix A for detailed drawings of the components). Figure 5 shows a cutaway view of the liquid hydrogen cryostat assembly mounted in the test machine. The design incorporates a vacuum-insulated, double-walled, stainless steel container with a tubular loading stem that passes through its central axis. Another tubular loading stem passes through the cryostat lid. The test specimen is gripped between these two stems. The cryostat mounts on the reciprocating platen of the test machine and moves with the platen while the lid, with the liquid supply line, vent line, and instrumentation support attached, remains fixed to the machine head frame. By using this system, the test cryostat would have to withstand long-term forces of approximately 2 g, and after fracture of the test specimen, forces exceeding 36-g acceleration as well as impact from the broken ends of the specimen hammering together.

The tubular loading stems were machined to a diameter of approximately 2 in. and a wall thickness of 0.070 in. The ends were threaded to receive the specimen grips and anchor into base blocks. Richards-type vacuum valves were recessed into the stem bases to avoid accidental damage and freezeout during test. The double-walled body was made by welding cylindrical sections to spun dome pieces that in turn were welded to small flanges on the stems. An unusual feature of the cryostats was the use of ready-formed, stainless steel, spun domes. These domes were cookingware items (soup tureens and flour scoops) purchased from a local restaurant supply store. Figure 6 shows the cryostat components before assembly.

The liquid hydrogen cryostat lid was made so that a vacuum-insulated liquid-fill line and a vent line with a concentric liquid dump line within it were welded into the lid unit. The dump line served as a support for the liquid-level sensor elements. The seal between the lid and the cryostat was a conductive neoprene bellows. An O-ring was used to seal the lid against the upper stem. Figure 7 shows the lid assembly.

All cryogenic structural parts were made from 300 series stainless steels. Two cryostats were constructed: one for use at -423°F, and one for -320°F service. The two units were identical except for the absence of liquid nitrogen cooling of the lower stem in the nitrogen cryostat and a less-sophisticated lid assembly for nitrogen service.

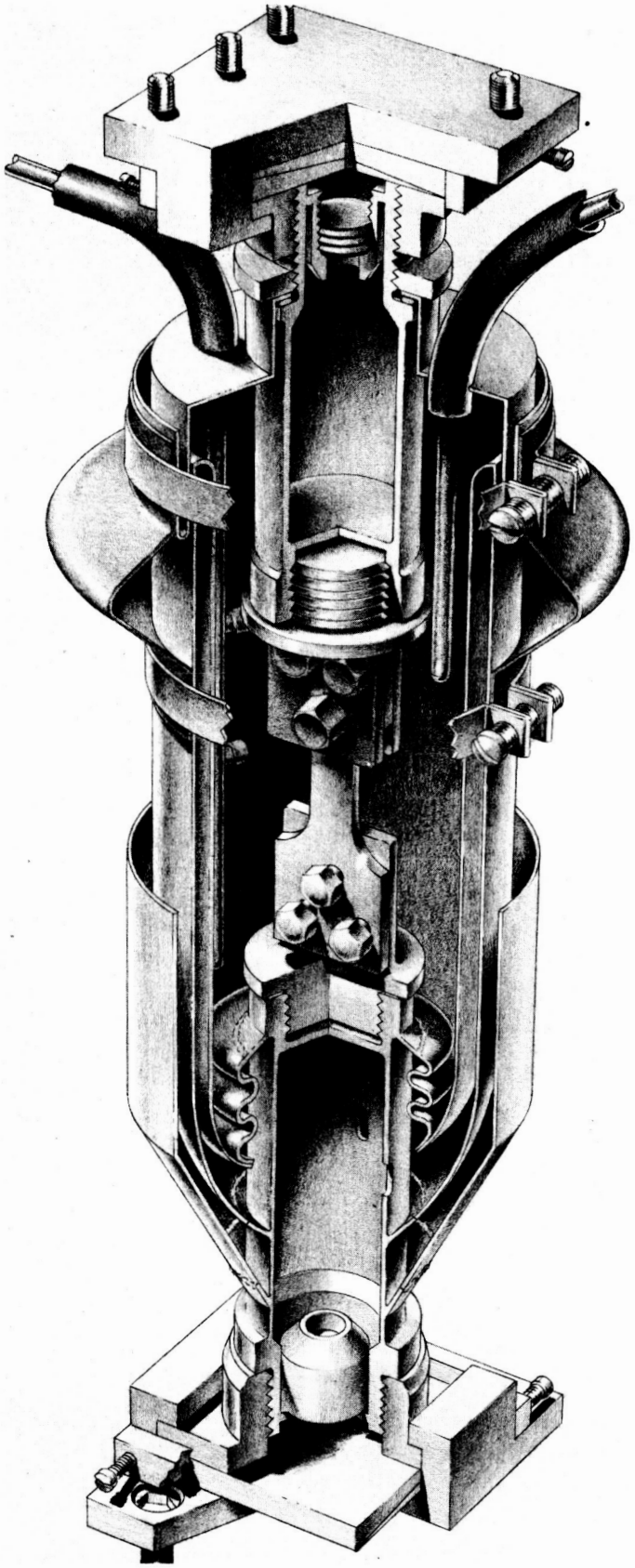

Fig. 5 Cutaway View of Cryostat Assembly Mounted in Fatigue-Testing Machine

Fig. 6 Cryostat Components before Assembly

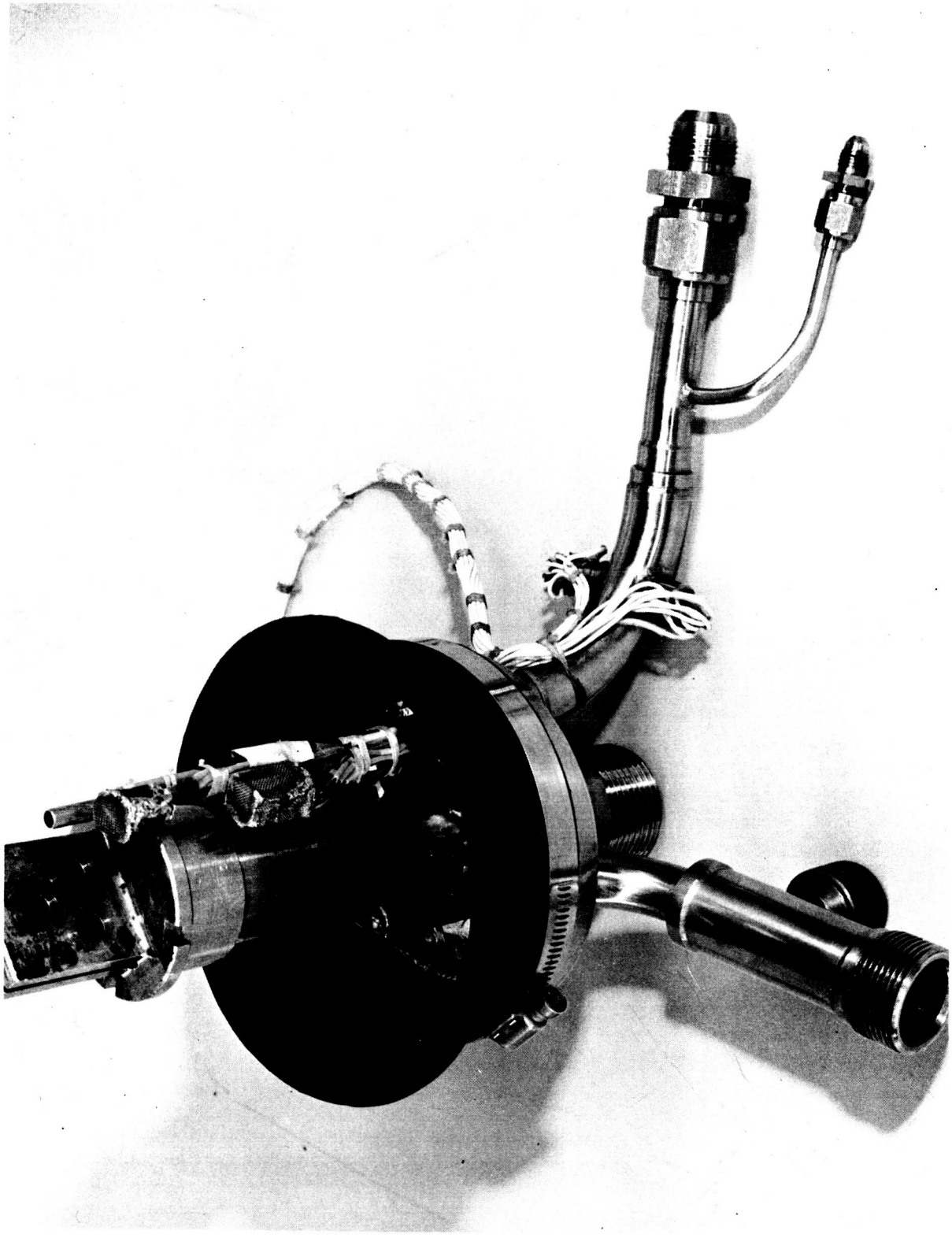

Fig. 7 Liquid Hydrogen Cryostat Lid Assembly

B. ALIGNMENT AND ASSEMBLY

Because test alignment is critical, the specimens were designed to align themselves axially by three close-tolerance fastener holes in each end. Lateral alignment was provided by confining the specimen between polished guide shoulders extending well into the fillet sections. Allowance was made in the design of the grip slots for up to 0.005-in. variation in specimen thickness. The grips were made by furnace-brazing premachined grip halves and then finish-machining the assembly for precise alignment. The bases of the grips are threaded for ease of installation in the loading stems. A slotted alignment shoulder permits the grip to be wrench-tightened.

A thermal locking action was used to obtain tight joints within the grips. When aluminum specimens are used, they contract tightly against the steel-mounted fastener pins, producing locking. Conversely, with titanium specimens, the grips contract to tighten the bolt group against the specimen. A thermal lock is also achieved by using titanium washers between the threaded grip bases and the loading stems.

The loaded cryostat assembly inserts into the fatigue-testing machine by a unique mounting system that provides rapid installation and precise alignment. This mounting system uses tee-slotted retainer plates fixed to the test machine heads; matched tee-shaped blocks, tapped out to accept the loading stems, are mounted on the cryostat assembly. When these blocks are inserted in the retainer plates, they provide a precise fit of the entire assembly. The mounting system is locked by using paired wedge plates located inside the retainer plates. Figure 8 shows the retainer plate (A), tee-block (B), and wedge plates (C). Alignment of each component of the system is necessary for testing of sheet materials, and each component must be installed in its indexed position for each test. The tee blocks and their retainers were hand-fitted for precise alignment. The entire system was also given a final precise alignment after assembly by using a strain-gaged alignment cell. Alignment was achieved by adjusting the head frame and retainer plates.

To illustrate the effect of column alignment, high-speed motion pictures were made of both an aligned and an intentionally misaligned (7075-T6 aluminum alloy) specimen tested at 70°F. Figure 9 shows the effect of misalignment. Column buckling is clearly shown under compressive load; this column buckling is shown to

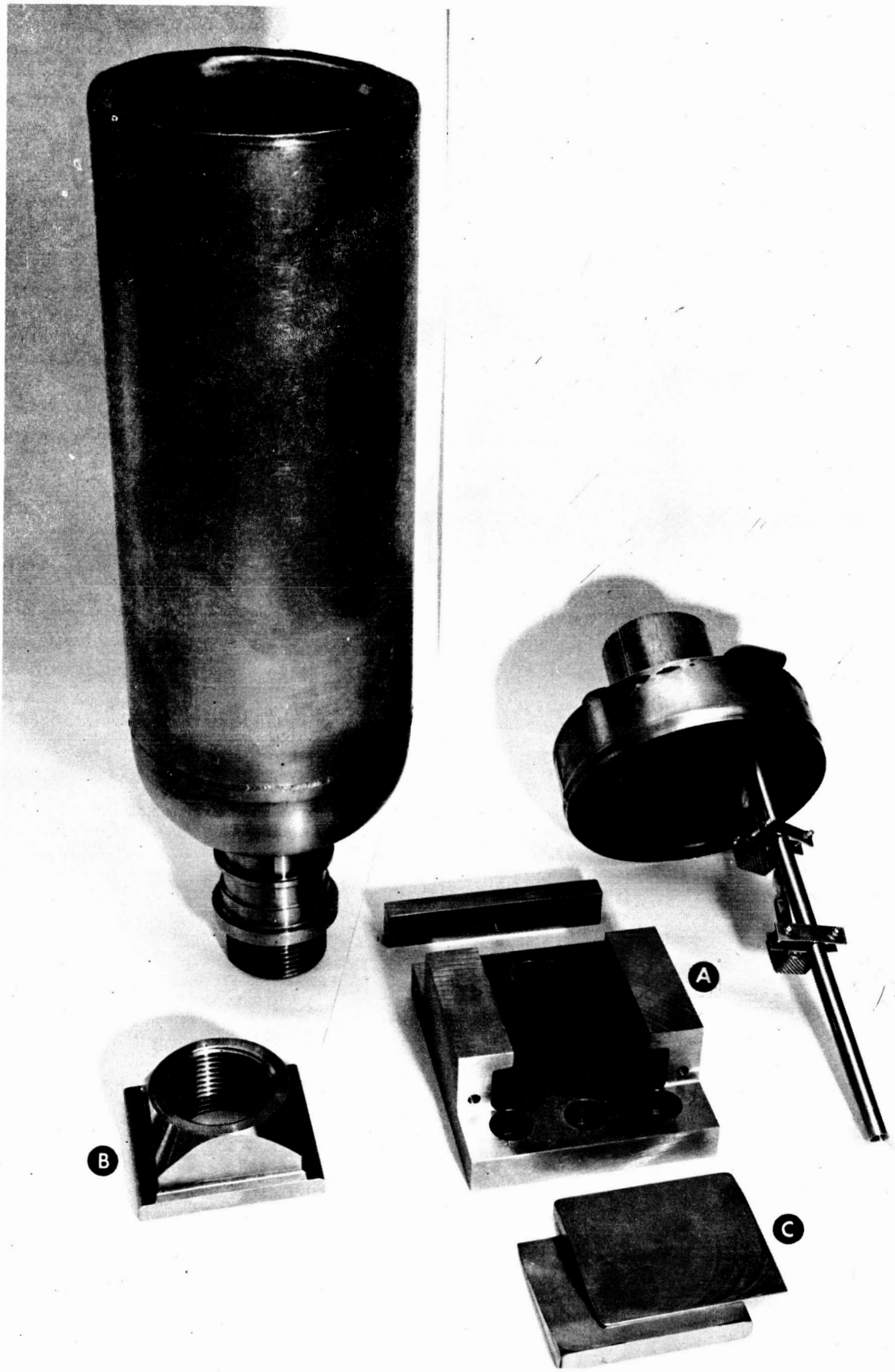

Fig. 8 View of Cryostat and Mounting Hardware

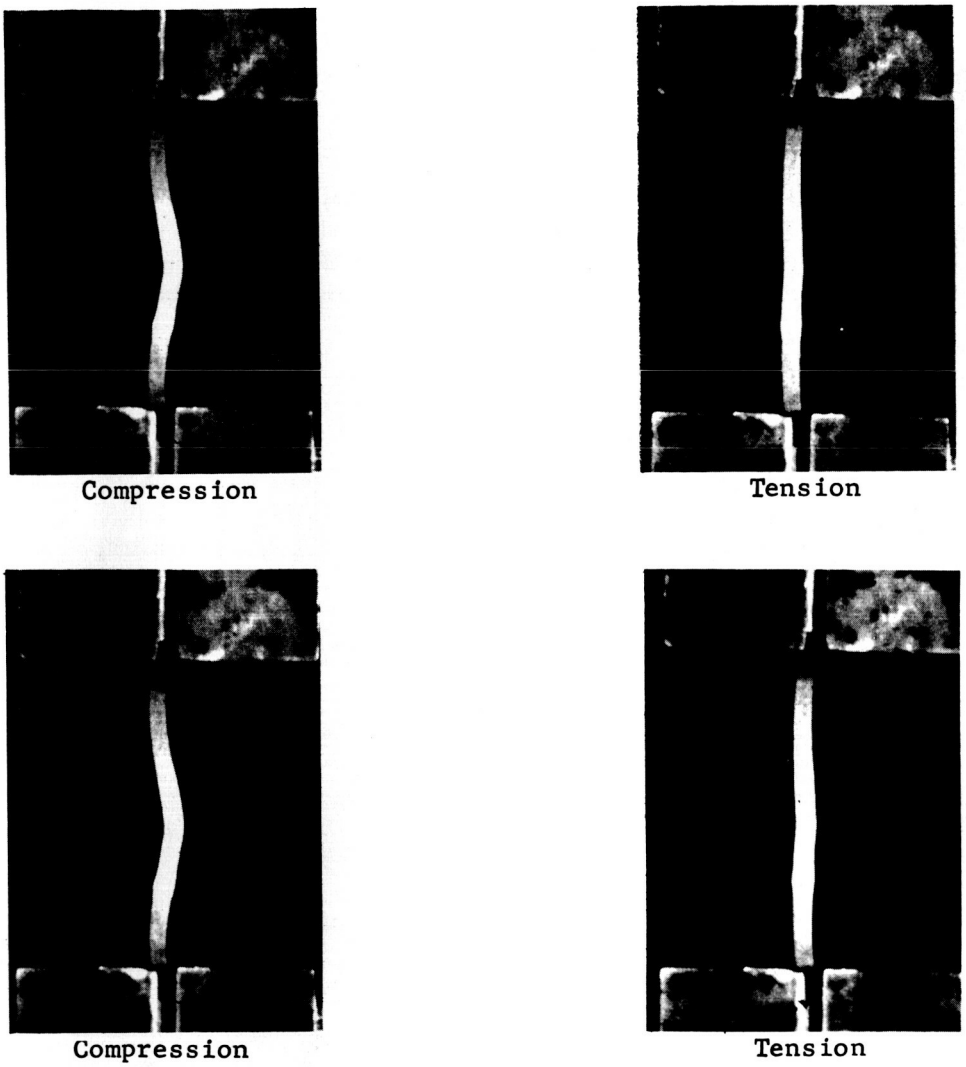

(a) Views before Failure (two complete cycles)

(b) Views at Failure (adjacent frames)

Fig. 9 Frames from High-Speed Motion Pictures of Misaligned 7075-T6 Aluminum Alloy Fatigue Test

cause failure. A properly aligned 7075-T6 specimen was tested at three stress levels (20,000, 63,000, and 75,000 psi). The latter stress level was above the yield strength for this material. Figure 10 shows no evidence of column buckling under compressive loads. Failure occurred in the tension portion of the cycle.

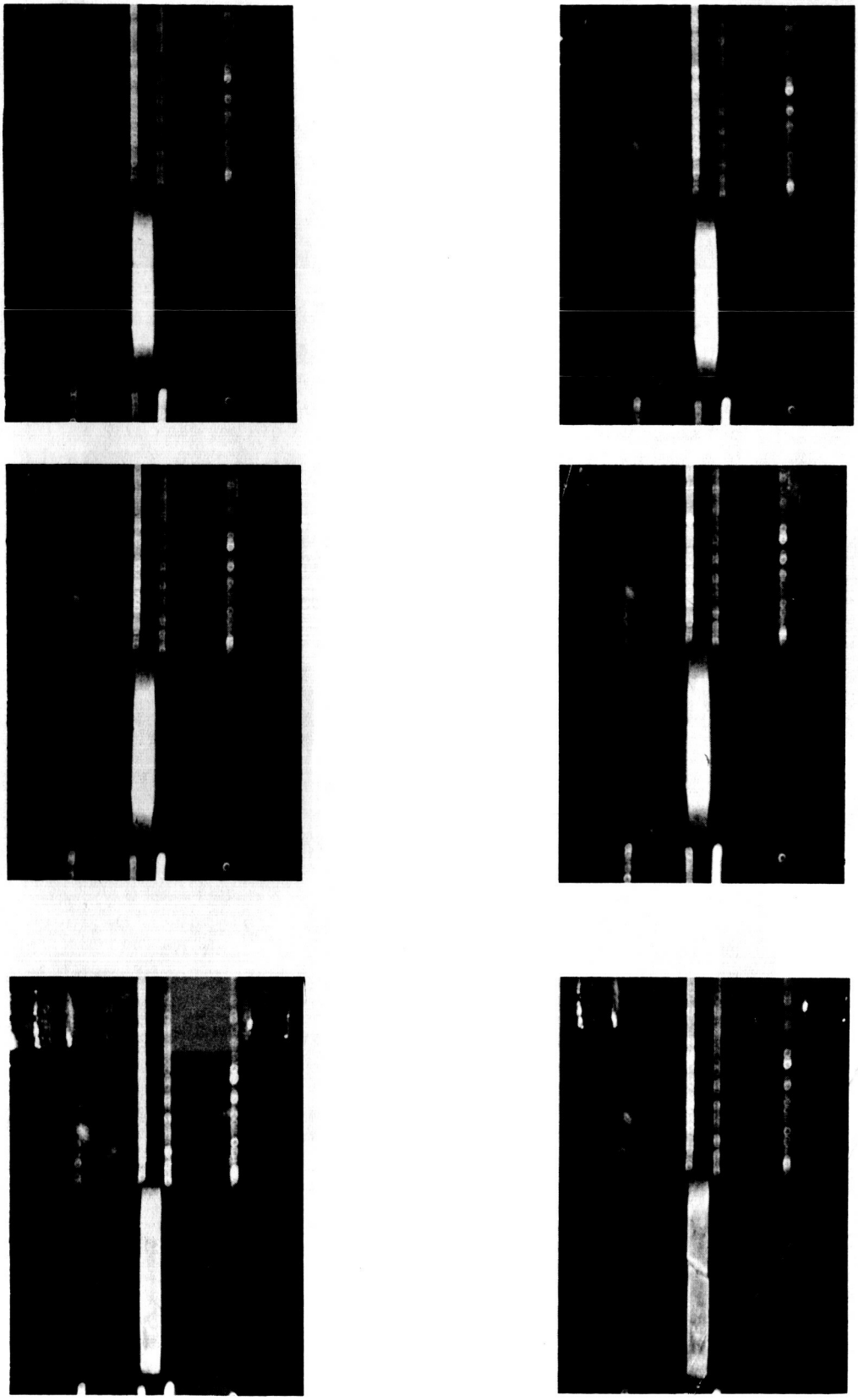

(b) Views at Failure (adjacent frames)

Fig. 10 Frames from High-Speed Motion Picture of Properly Aligned 7075-T6 Aluminum Alloy Fatigue Test

C. AUTOMATION

The systems used for both -320 and -423°F operation were constructed so that testing could be performed automatically, with only periodic monitoring required. Automatic level sensor/fill controllers were constructed for each system. These sensors use a Martin-developed circuit that incorporates a small-diameter platinum wire (0.0005-in.) approximately 3/8-in. long as the sensing element. A sharp resistance change of the heated platinum wire occurs as the element is cycled from the liquid to the vapor phases. A transistorized relay-control circuit is used to detect the resistance changes of the wire. Point sensors located approximately 2 in. apart in the cryostat are used to maintain liquid level between the sensors. Fill is automatic through a solenoid-operated valve that permits liquid fill until the upper sensor is immersed. Fill is then discontinued until the lower sensor becomes exposed because of boiloff. The fill process is then repeated. Tests at -320°F (LN_2) for 46 hr (5.00×10^6 cycles) and at -423°F (LH_2) for 14 hr (1.50×10^6 cycles) have been routinely conducted using these automated systems. Figures 11 and 12 show the liquid nitrogen and liquid hydrogen controllers, respectively.

For safety, a thermistor in the lid of the liquid hydrogen cryostat serves as an overfill sensor. In case of overfill, the fill valve closes, and the fatigue machine is stopped. This action also occurs if the facility power fails.

For additional safety, the control panel includes remote controls to start and stop the fatigue machine. It is therefore unnecessary for the operator to enter the test cell after the cryostat is installed in the fatigue machine. An intercom system provides audible monitoring of the test, both in the control room and at various laboratory locations.

A schematic diagram for the liquid hydrogen flow system is given in Fig. 13. A self-pressurizing, 1000-ℓ, mobile storage Dewar is used to provide liquid hydrogen. Fill is controlled by a Martin-designed and -constructed cryogenic valve, which is operated by a solenoid-gas actuator combination. All liquid transfer lines are vacuum-insulated. Nitrogen and helium gas are supplied to the system to sweep-purge the cryostat, fill line, and vent system. The entire system is normally purged for 5 min before filling. The vent system has been designed to permit hydrogen testing under all weather conditions. The necessity for this approach results from

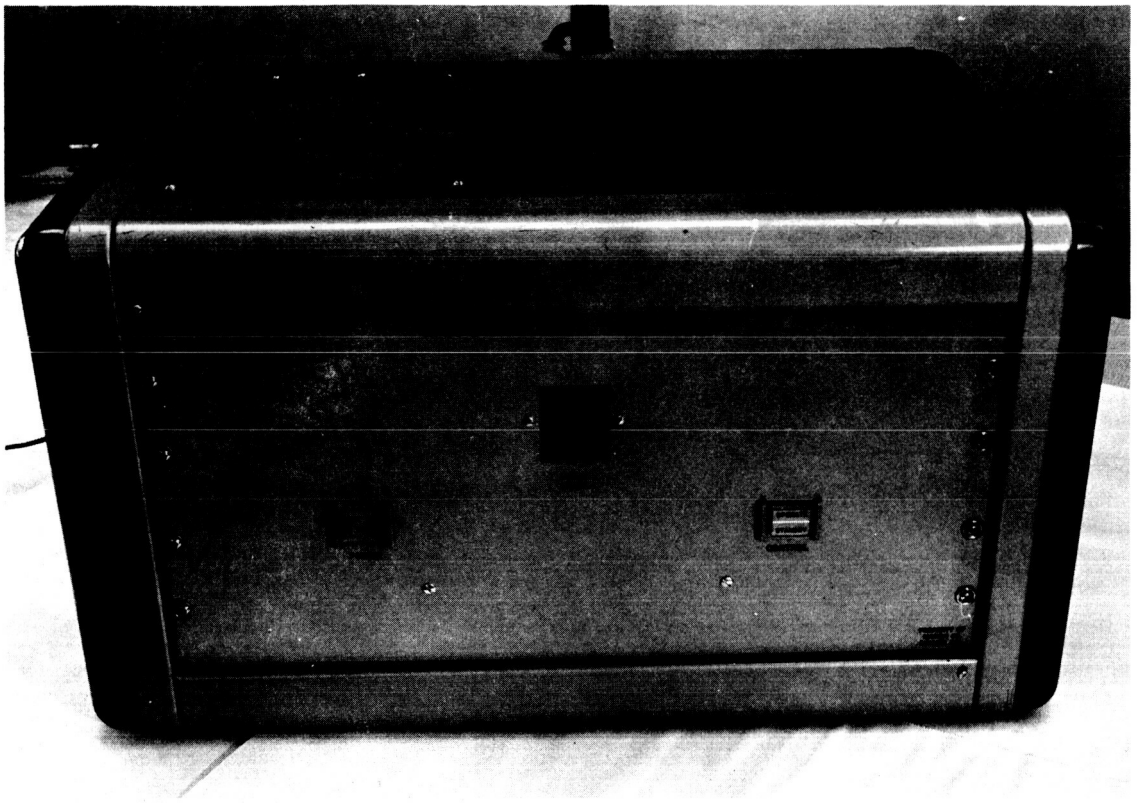

Fig. 11 Liquid Nitrogen Fill Controller

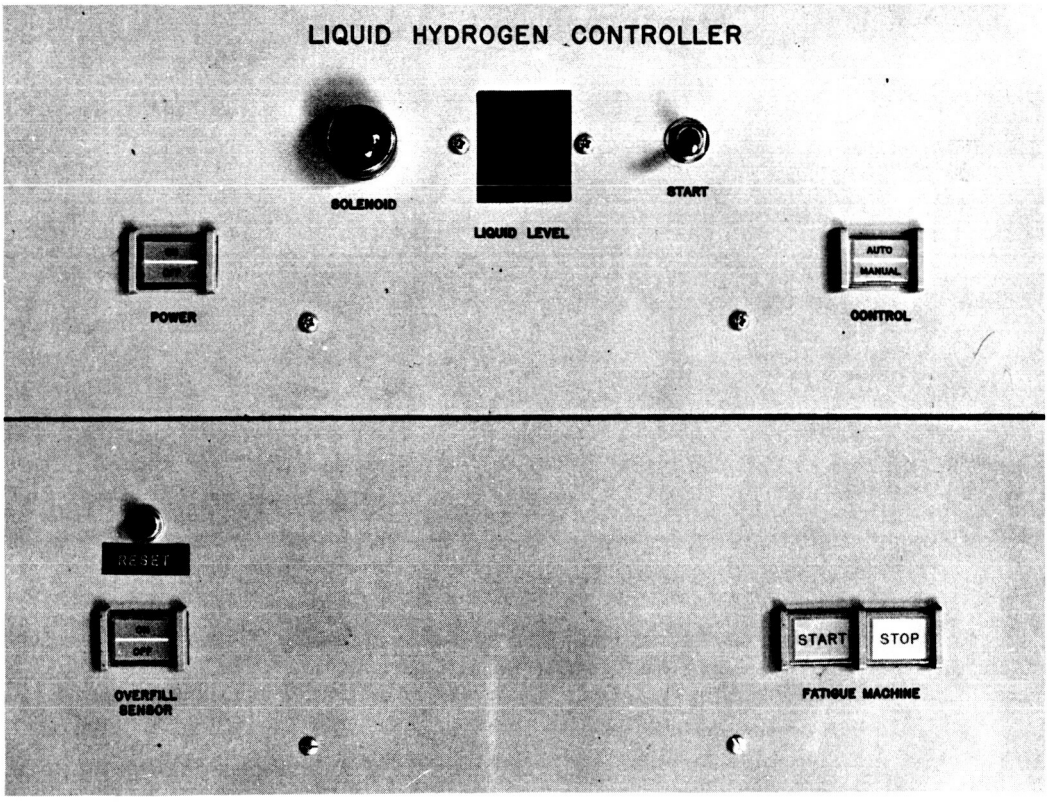

Fig. 12 Liquid Hydrogen Fill Controller

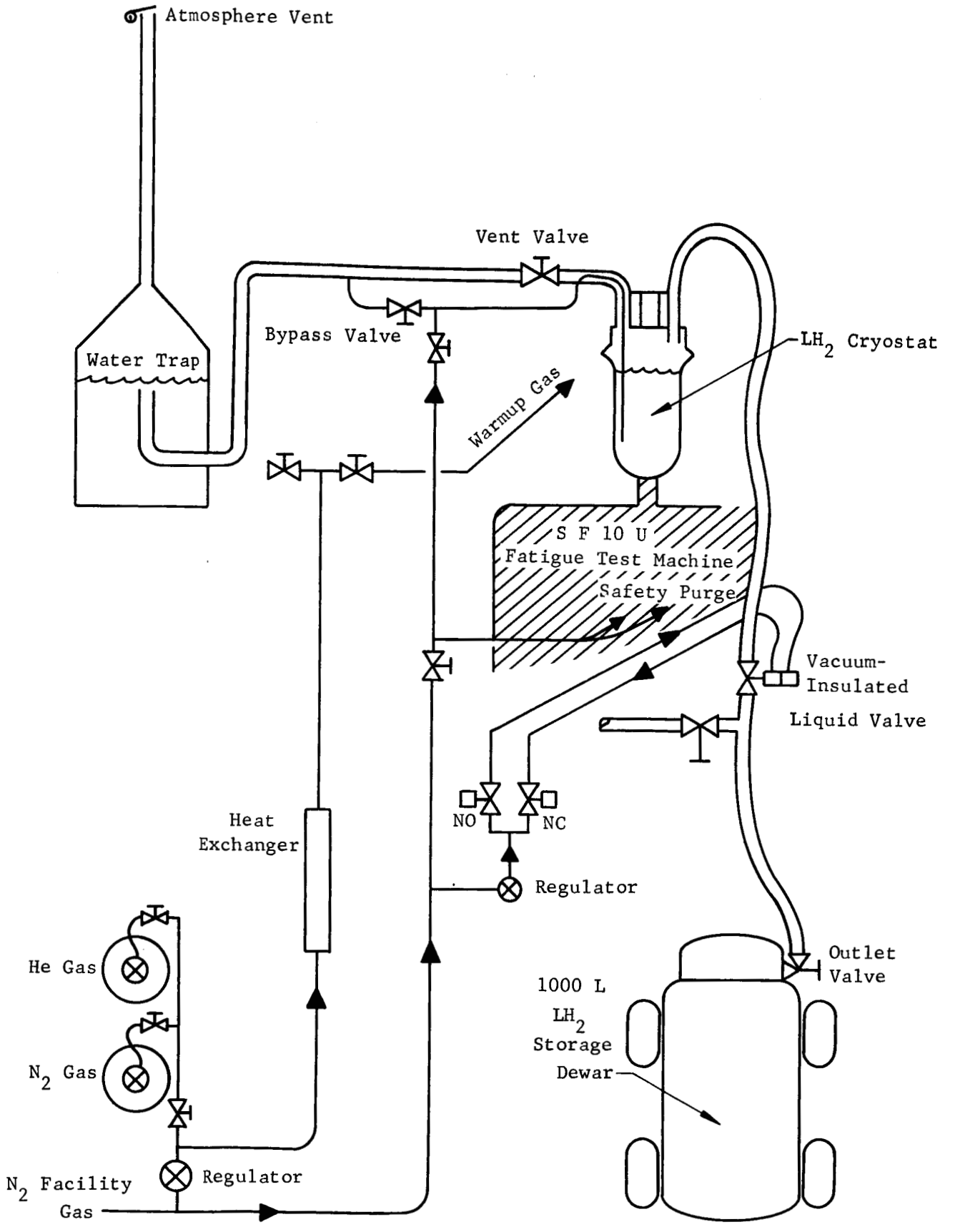

Fig. 13 Schematic Diagram of Liquid Hydrogen Flow System

a potential gradient to ground that is developed through the atmosphere during certain weather conditions. This potential is often sufficient to ignite a hydrogen-oxygen mixture at the vent stack outlet. The vent system includes a water valve to preclude ignition back to the cryostat and possible explosion. The water valve consists of a 30-gal. drum containing a bell jar. The inlet to the bell jar is below liquid level; the outlet above. A goose-neck trap is used to prevent water from backing into the vent.

D. FACILITY

To perform the liquid hydrogen testing in a safe location, it was necessary to move an SF 10 U fatigue-testing machine from the Denver Materials Engineering Laboratory to the Denver Hydrogen Research Laboratory, where liquid hydrogen can be handled safely. It was necessary to construct a test cell for this machine. A concrete slab base, 12x14 ft, and blowout-type test room were prepared, the latter adjoining the existing tensile test cell. It is constructed of welded steel, with a heavy plate blast wall separating the two cells and a similar blast wall between the cell and Dewar parking area. The remaining two sides are covered with fiberglas attached to the frames with screws so that the wall can readily blow out in the event of an explosion. A sketch (A) and a photograph (B) of the liquid hydrogen fatigue-testing facility are shown in Fig. 14.

The liquid nitrogen facility is shown in Fig. 15.

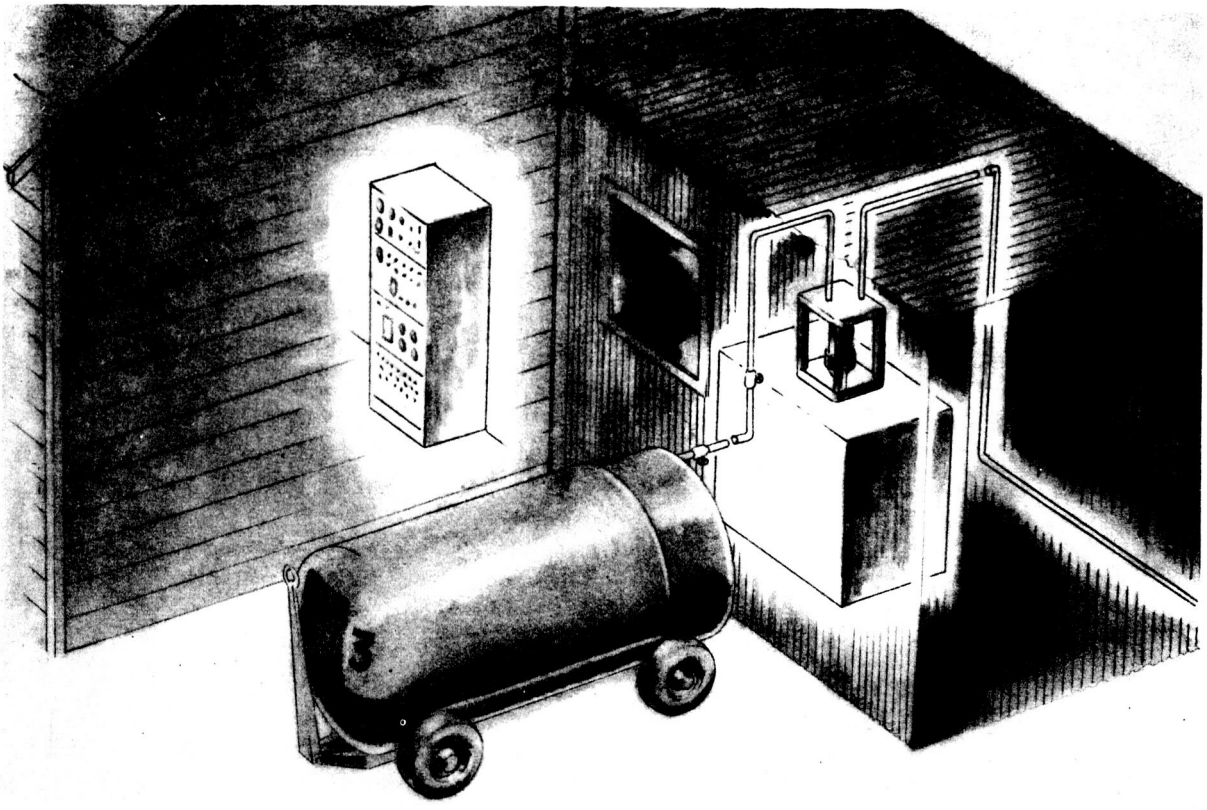

(A)

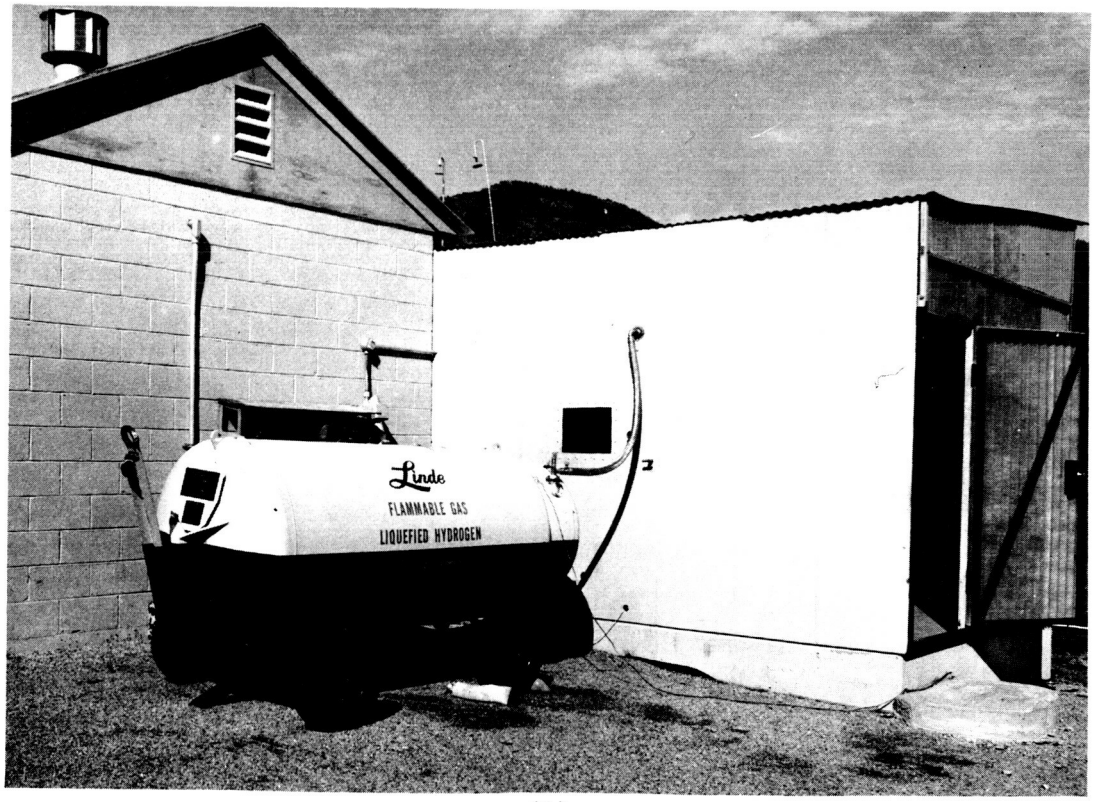

(B)

Fig. 14 Liquid Hydrogen Fatigue-Testing Facility

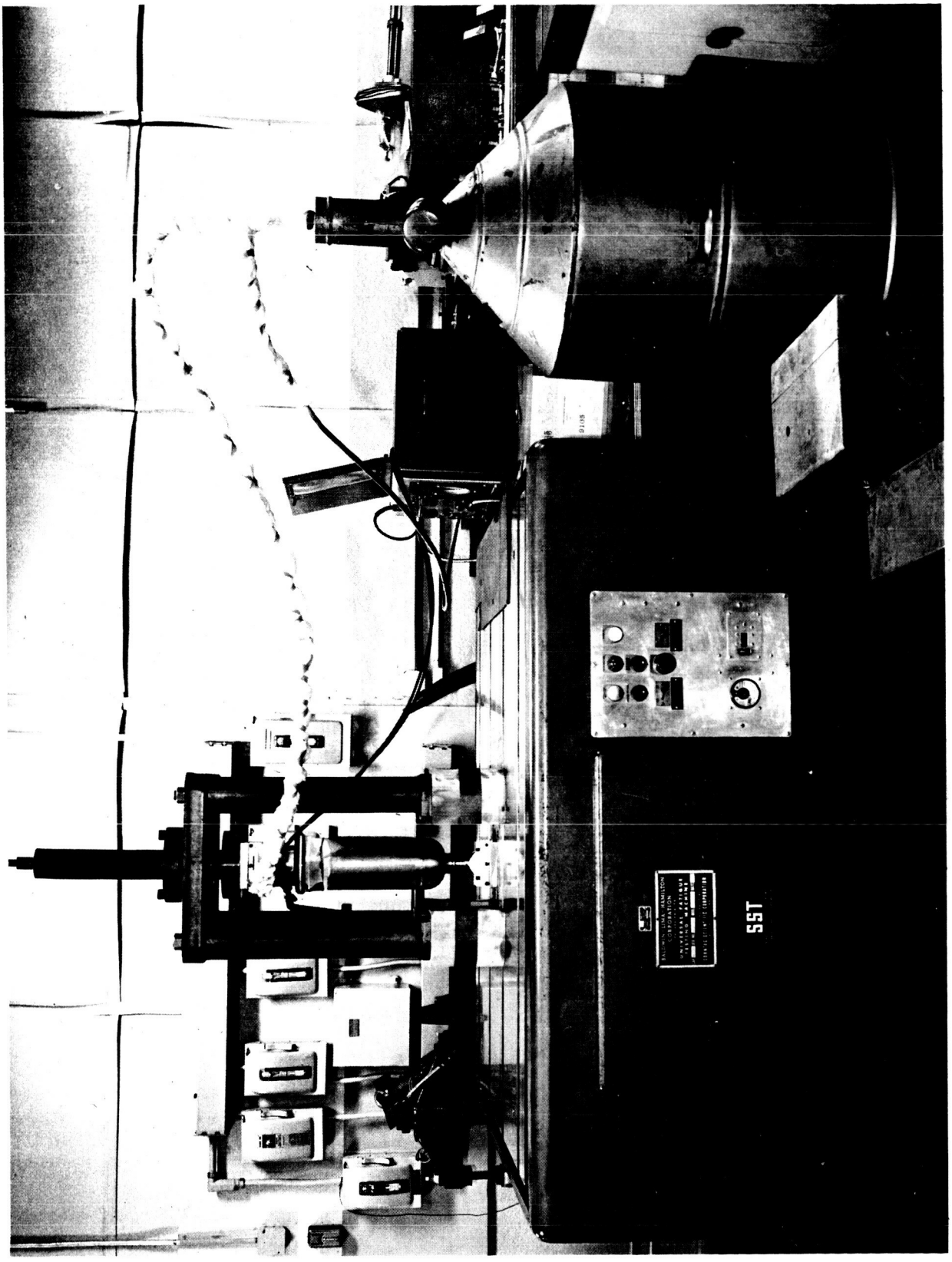

Fig. 15 Liquid Nitrogen Fatigue-Testing Facility

E. PERFORMANCE

Thermal performance of the cryostat and system has been very satisfactory. Original calculations indicated a liquid hydrogen boiloff rate of 3.5 ℓ per test hour for the cryostat alone, using a liquid nitrogen-filled outer jacket to minimize hydrogen loss. In actual practice, the liquid nitrogen fill was discontinued since the total system boiloff of the cryostat, 7 ft of transfer line, six coupling joints, a liquid shutoff valve, and a storage Dewar outlet system averaged only 7 ℓ/hr.

Although the fill controllers performed very satisfactorily for many months, frequent failures of the platinum elements and the transistors occurred during the latter months of this program, causing considerable loss of time. As a last resort, a breadboard circuit with thermistors was prepared to provide control for the remaining liquid nitrogen tests. It is planned to construct new controllers for both liquid nitrogen and liquid hydrogen testing during the second year of the program.

The performance of the fatigue machines was surprisingly poor. Numerous failures in the balance meter circuit and static load controller resulted in a significant loss of testing time. New equipment has been obtained to replace the defective components.

V. TEST PROCEDURE

Specimens were tested at three temperatures: 70, -320, and -423°F. Cryogenic temperatures were achieved by constant-temperature liquid baths: liquid nitrogen for -320°F and liquid hydrogen for -423°F.

A. TENSION

Parent metal aluminum specimens were tested at constant test machine platen speed corresponding to an approximate strain rate of 0.010 in./in./min in the elastic range. After the specimen yielded, platen speed was increased tenfold. Welded specimens were tested to failure at a constant platen speed equivalent to 0.010 in./in./min. Titanium specimens were similarly evaluated except that the test speed was one half that used for aluminum specimens.

The equipment and techniques used for tensile evaluation are similar to those described in the literature.[1,2] Type AB-3 Bakelite resistance strain gages bonded with EPY 400 cement were used for strain measurement on tensile specimens. Specimens were single-gaged except for one specimen of each type that was double-gaged for modulus determination. To establish accurate modulus data, the specimen was strained in the elastic range at least three times. The same specimen was used at each of the three temperatures. Strain gages were calibrated using a tapered cantilever beam device to indicate strain sensitivity (or gage factor) at each temperature so that modulus data could be properly converted to correct for temperature effects.

B. FATIGUE

Specimens for fatigue-testing were hand-polished on their edges to remove all evidence of machining marks. All specimens were prepared with the as-received surfaces intact. Afterwards, the specimens were carefully measured and then installed in the cryostat. The cryostat was inserted into the fatigue machine and the entire unit flushed with inert gas for a minimum of 5 min before the liquid hydrogen fill process. After testing, the

cryostat was thoroughly flushed with warmed nitrogen gas before opening.

Except for the cryogenic aspects, testing was performed in a routine manner. To obtain extra data at liquid hydrogen temperature, some of the discontinued specimens were re-run at high stresses to produce low cycle failures. Results obtained from re-run specimens compared favorably with data obtained from previously untested specimens.

VI. EXPERIMENTAL RESULTS

Tension-testing at all temperatures and liquid hydrogen fatigue-testing were performed at the Denver facility. Fatigue-testing at room and at liquid nitrogen temperatures was performed at the Baltimore division.

A. TENSION TESTS

Tension tests were performed at 70, -320, and -423°F to provide data on:

Ultimate strength;

Yield strength;

Elongation;

Modulus of elasticity.

Triplicate tests were performed for each condition. Results of these tests are shown graphically in Fig. 16 thru 23. Detailed test data are given in Appendix B, Tables B-I thru B-VIII.

B. FATIGUE TESTS

Fatigue tests were performed to provide S/N curves at 70, -320, and -423°F. A stress ratio (R) of -1 was used for all aluminum specimens. The titanium specimens were not sufficiently flat to permit fully reversed stressing and were tested under tension/tension loading at a stress ratio of 0.01. Based on the brittle behavior of the Ti-13V-11Cr-3Al in the tension tests it was assumed that it might not be possible to fatigue test the beta titanium alloy satisfactorily at cryogenic temperatures. Therefore, the welded panels of this alloy were not machined into specimen form. Evaluation of the parent metal fatigue specimens showed that data could be generated. Unfortunately, time did not permit machining and testing of the welded specimens during the contract period. This portion of the work will be completed during the second year's effort.

Fatigue test results are illustrated in Fig. 24 thru 36. Detailed tabular presentations of these data are given in Appendix C, Tables C-I thru C-XIII.

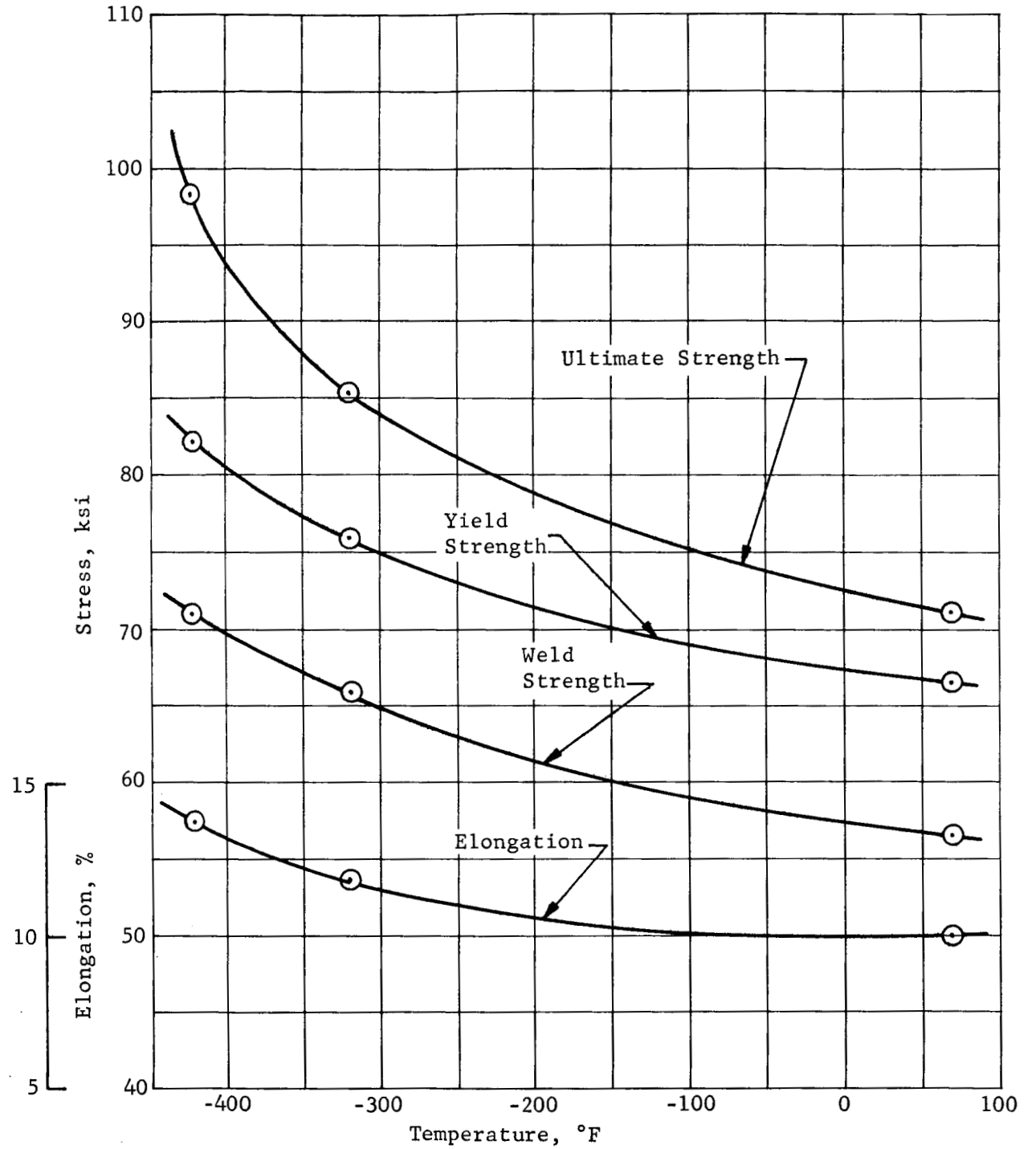

Fig. 16 Tensile Properties of 2014-T6 Aluminum Alloy at Cryogenic Temperatures

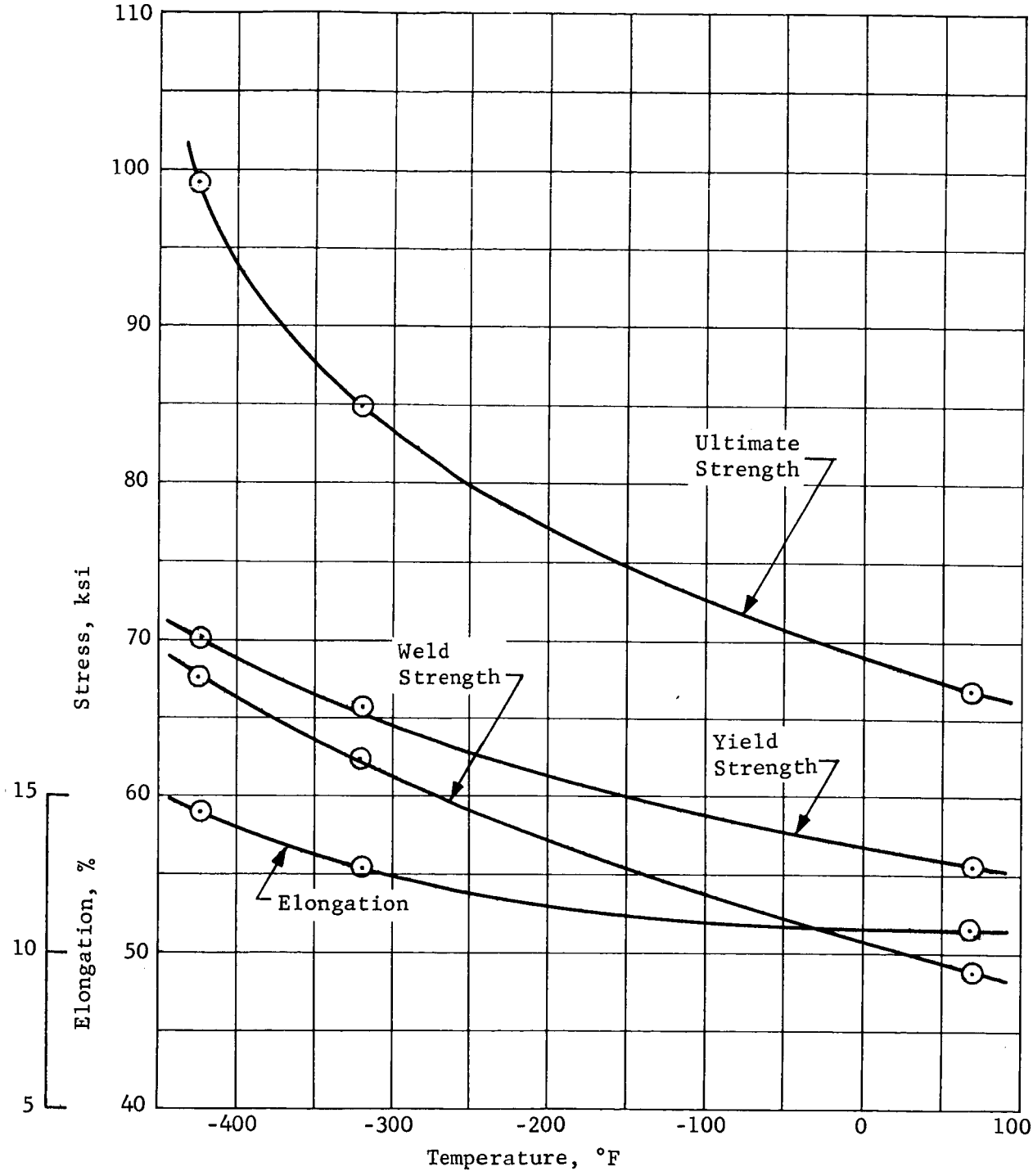

Fig. 17 Tensile Properties of 2219-T87 Aluminum Alloy at Cryogenic Temperatures

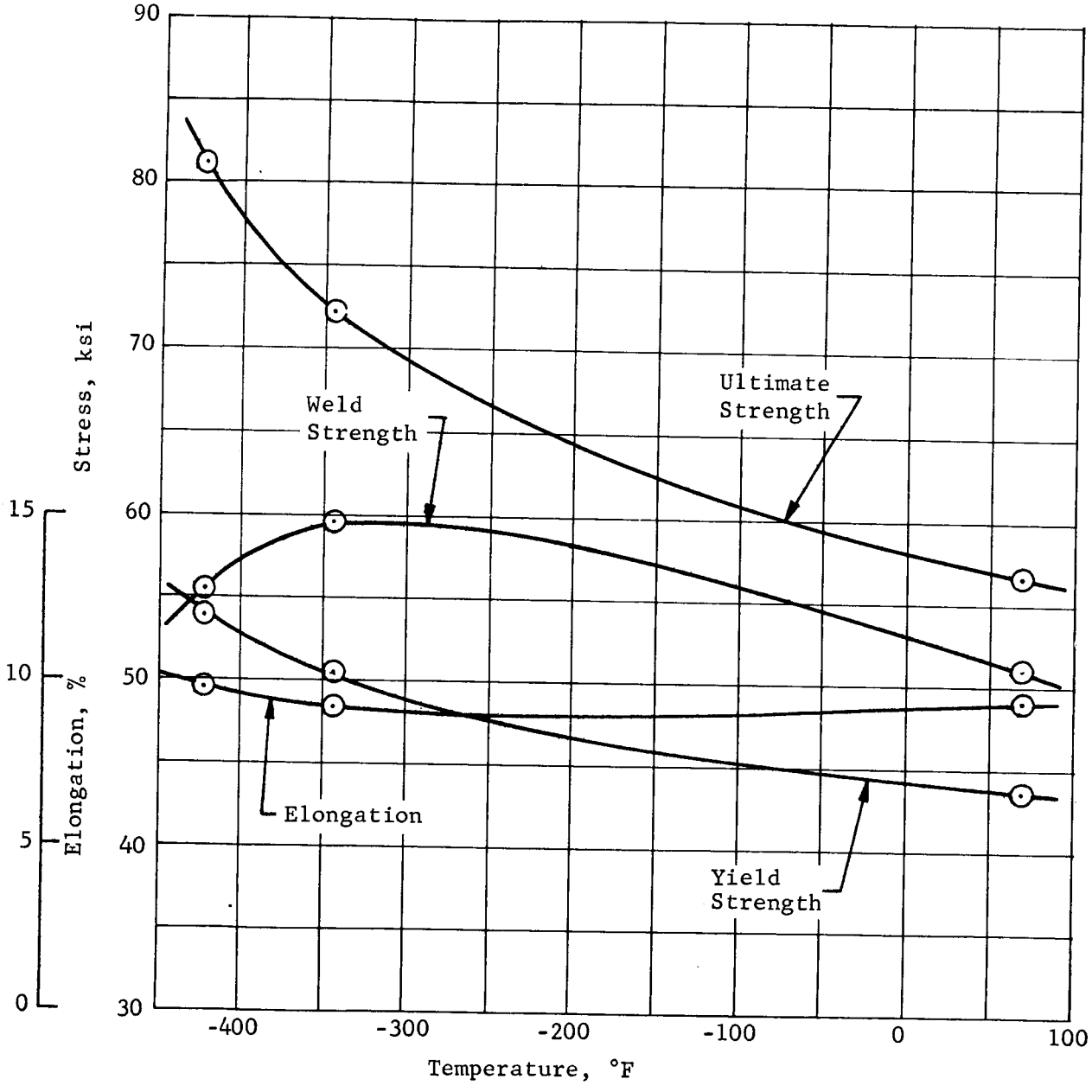

Fig. 18 Tensile Properties of 5456-H343 Aluminum Alloy at Cryogenic Temperatures

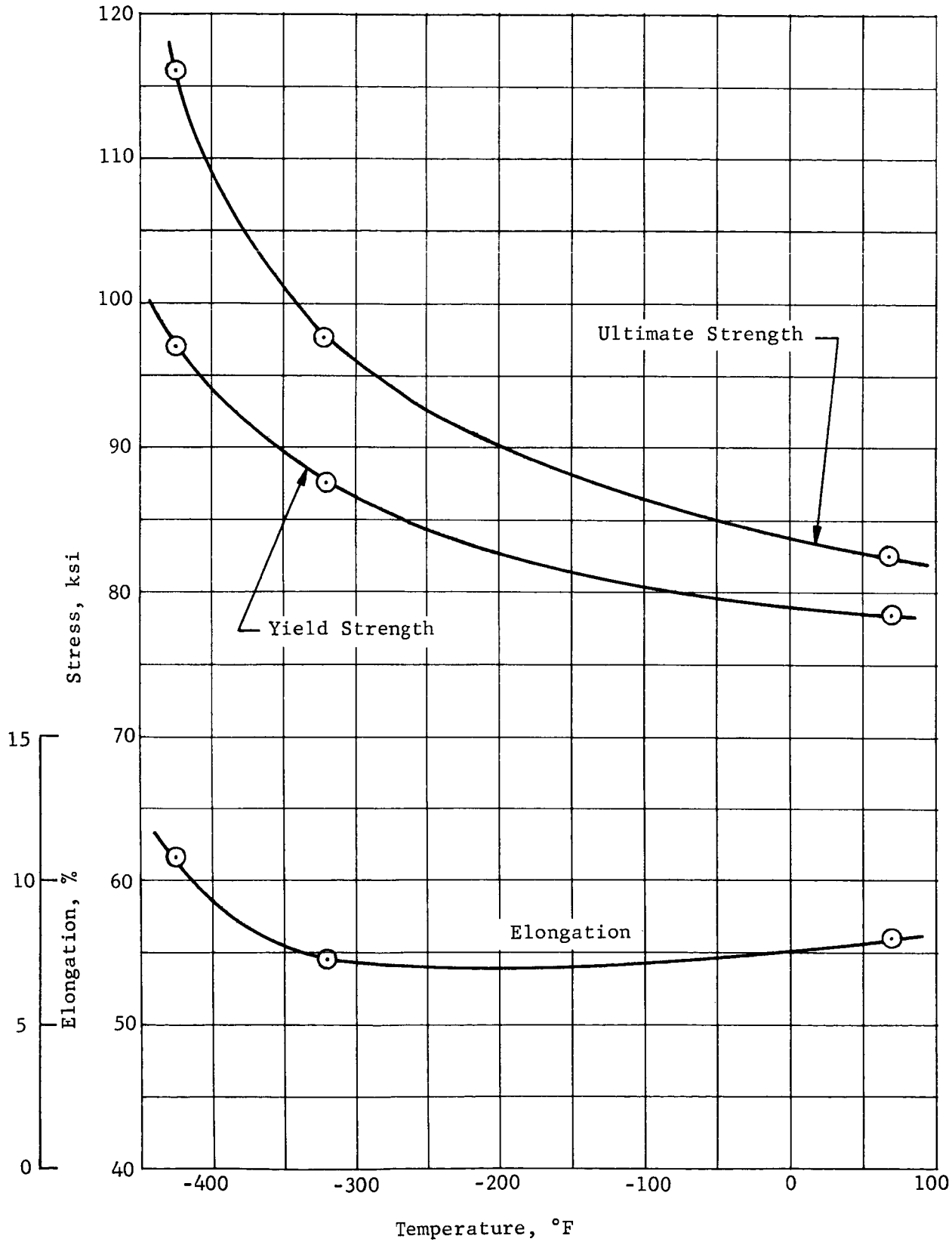

Fig. 19 Tensile Properties of 2020-T6 Aluminum Alloy at Cryogenic Temperatures

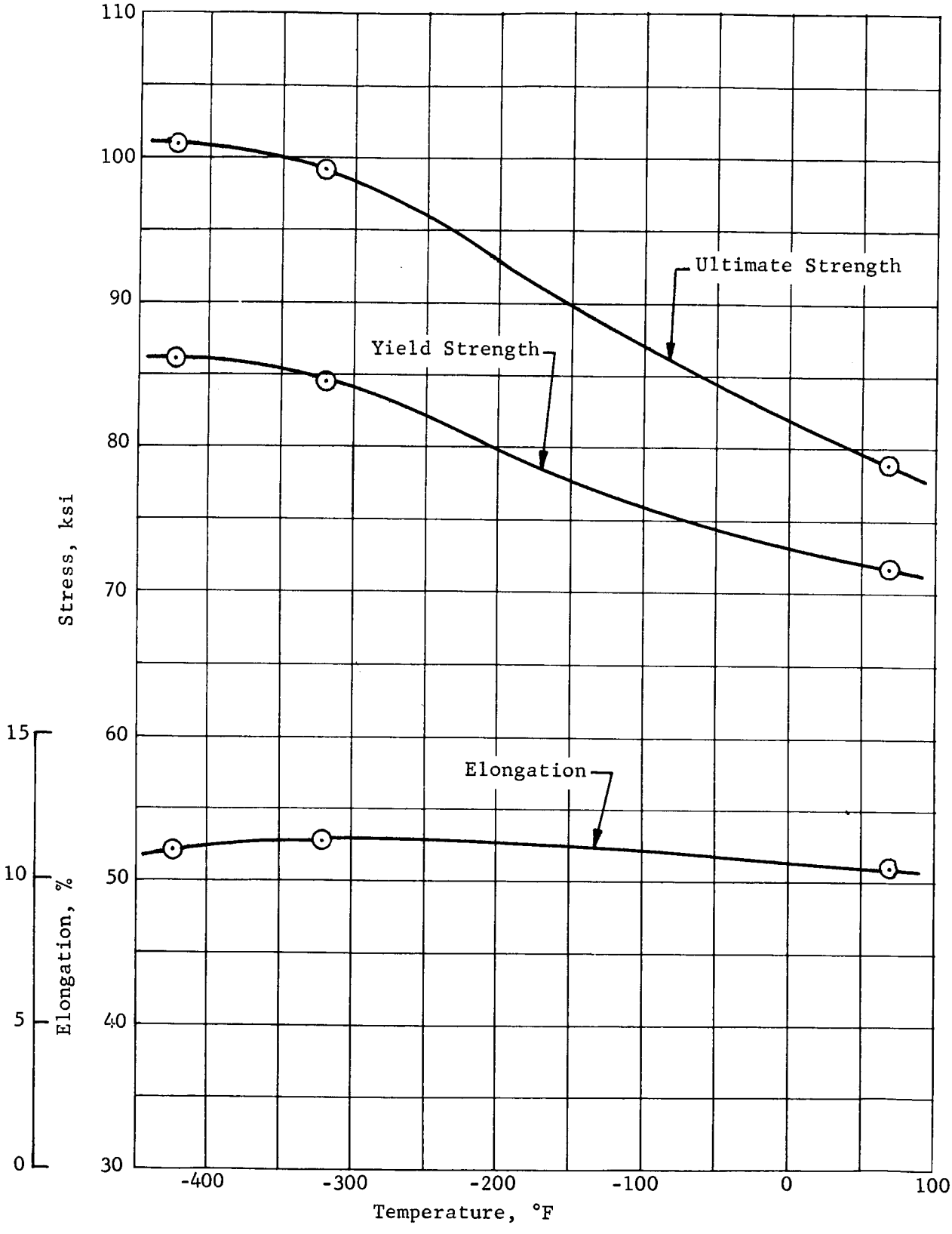

Fig. 20 Tensile Properties of 7075-T6 Aluminum Alloy at Cryogenic Temperatures

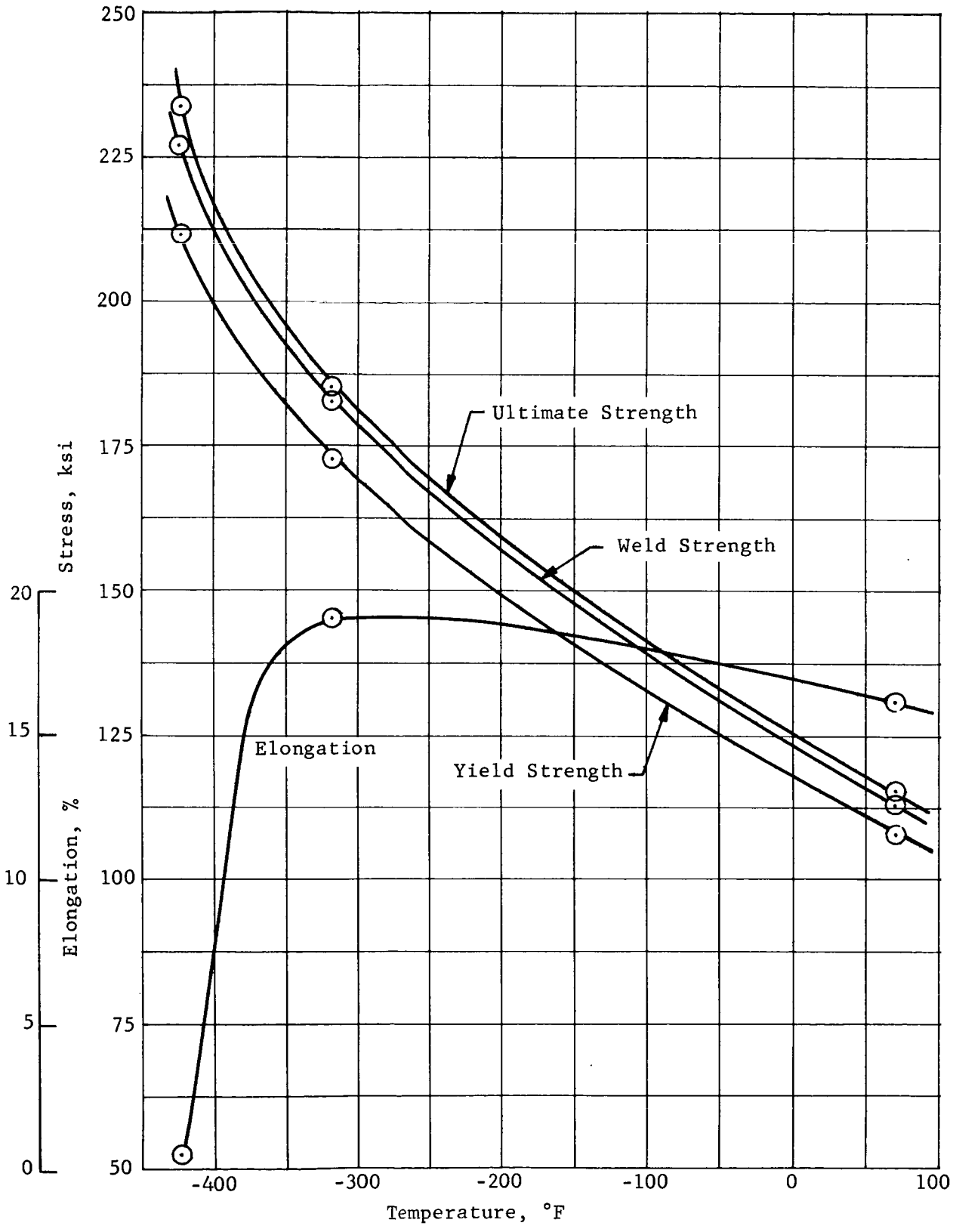

Fig. 21 Tensile Properties of 5Al-2.5Sn Titanium Alloy at Cryogenic Temperatures

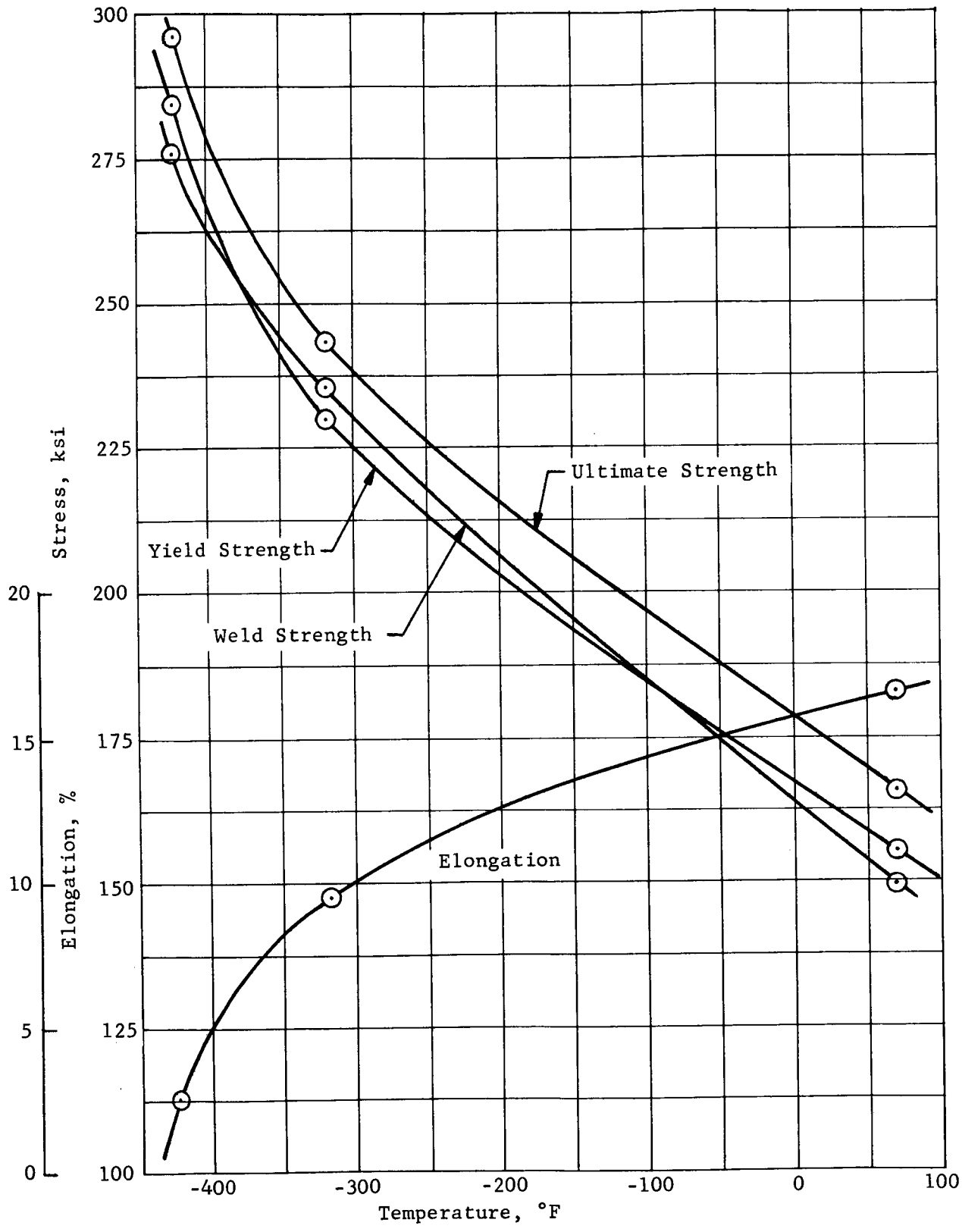

Fig. 22 Tensile Properties of 6Al-4V Titanium Alloy at Cryogenic Temperatures

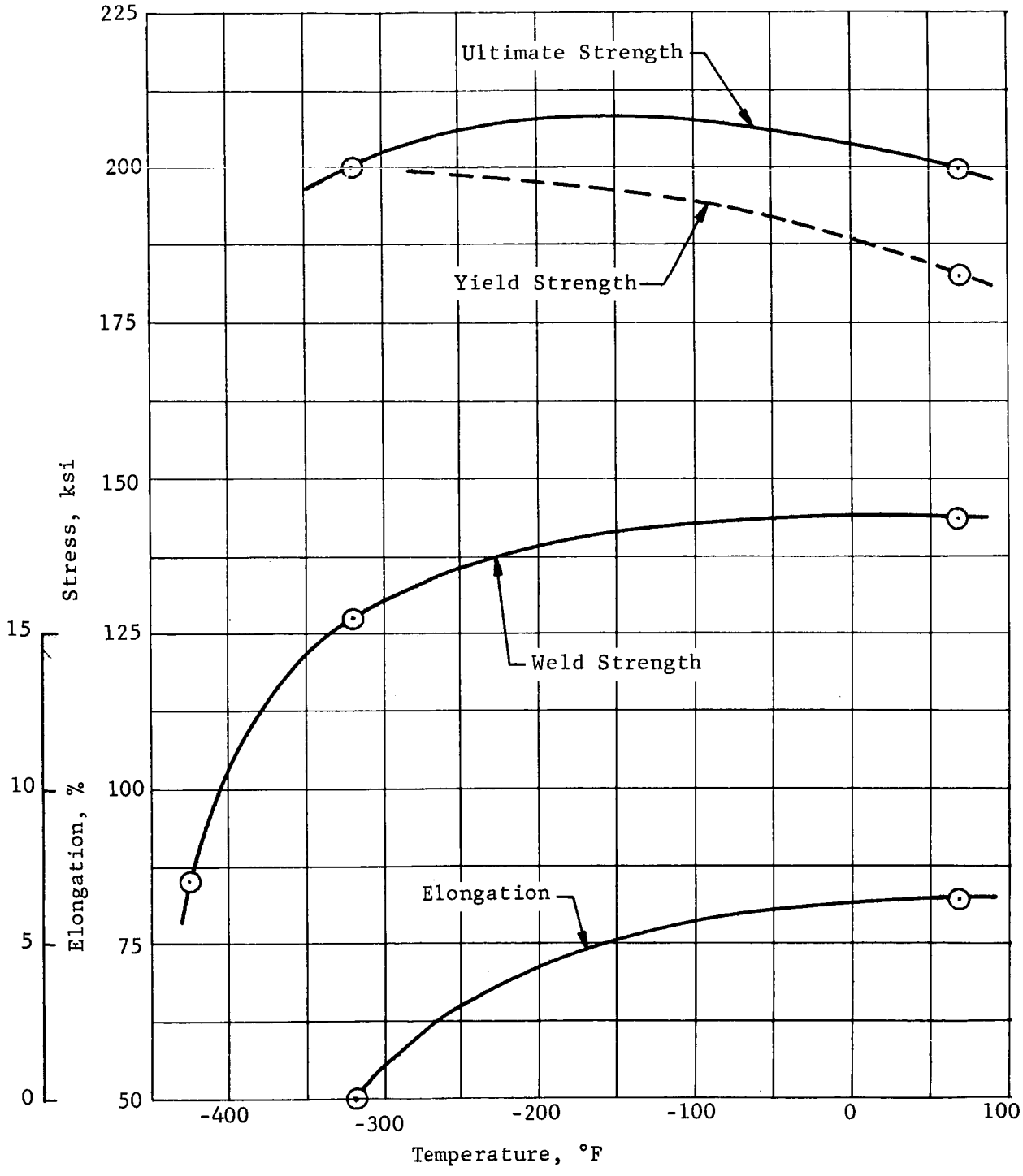

Fig. 23 Tensile Properties of 13V-11Cr-3Al Titanium Alloy at Cryogenic Temperatures

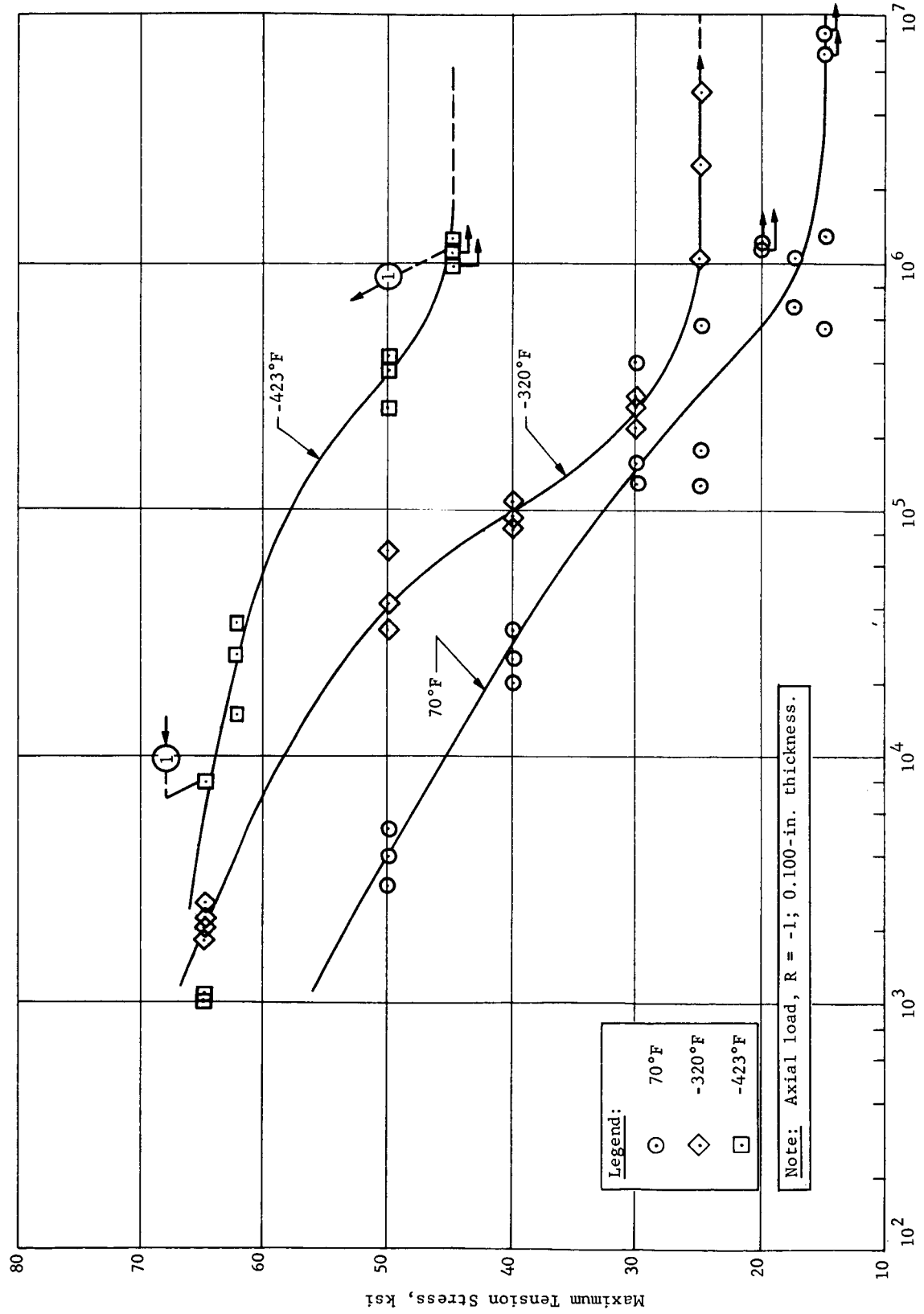

Fig. 24 Fatigue Properties of Parent Metal 2014-T6 Aluminum Alloy

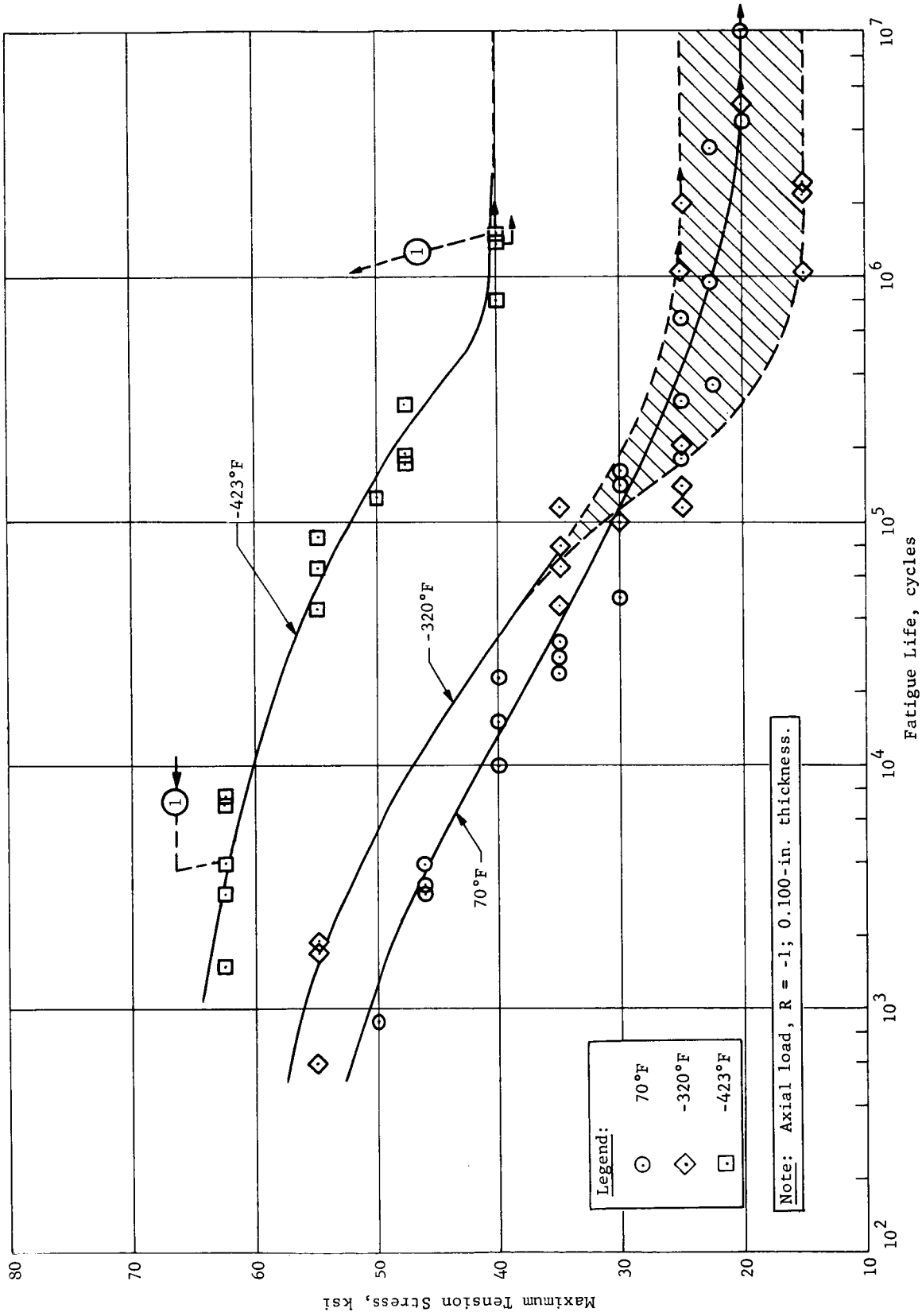

Fig. 25 Fatigue Properties of Parent Metal 2219-T87 Aluminum Alloy

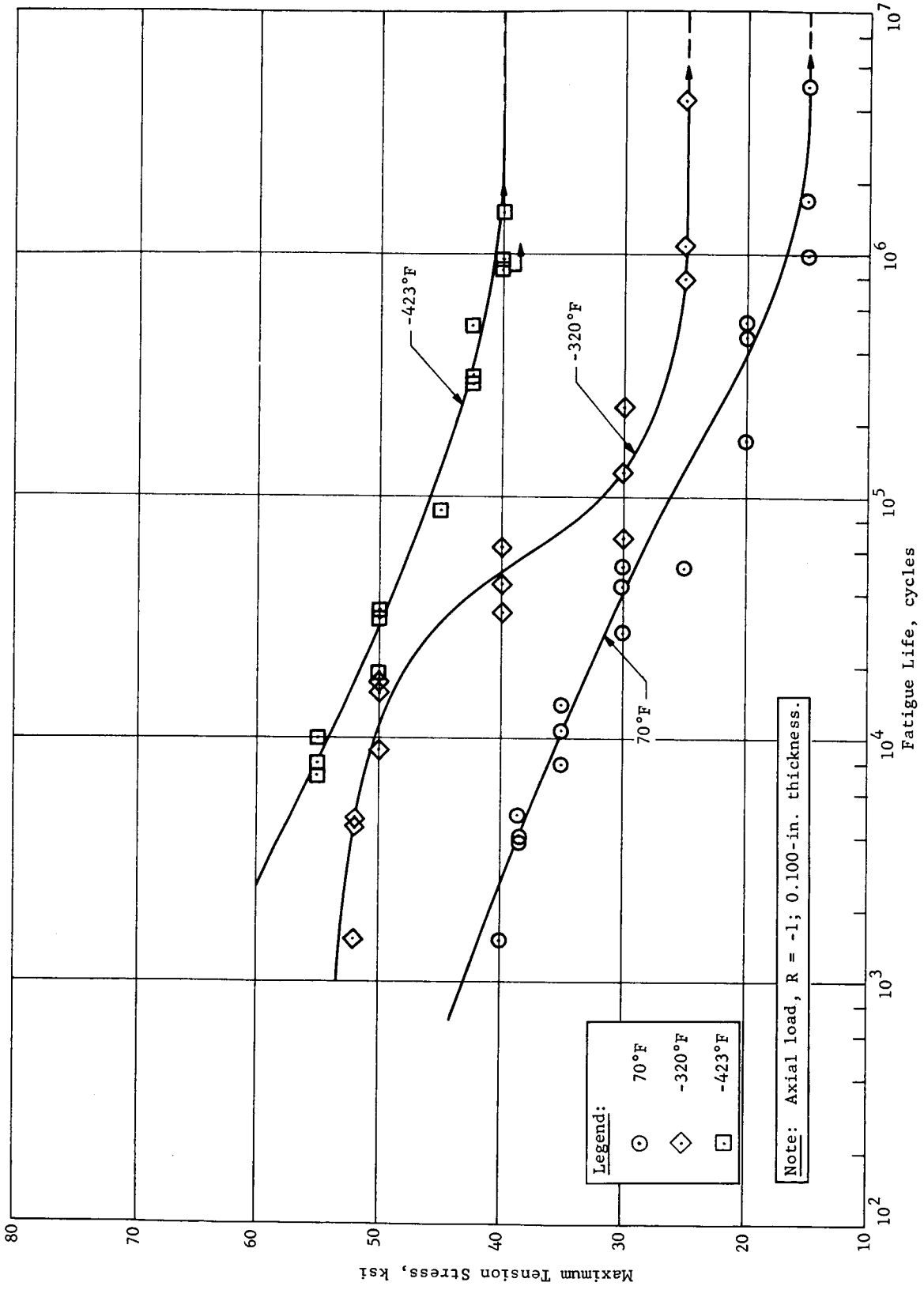

Fig. 26 Fatigue Properties of Parent Metal 5456-H343 Aluminum Alloy

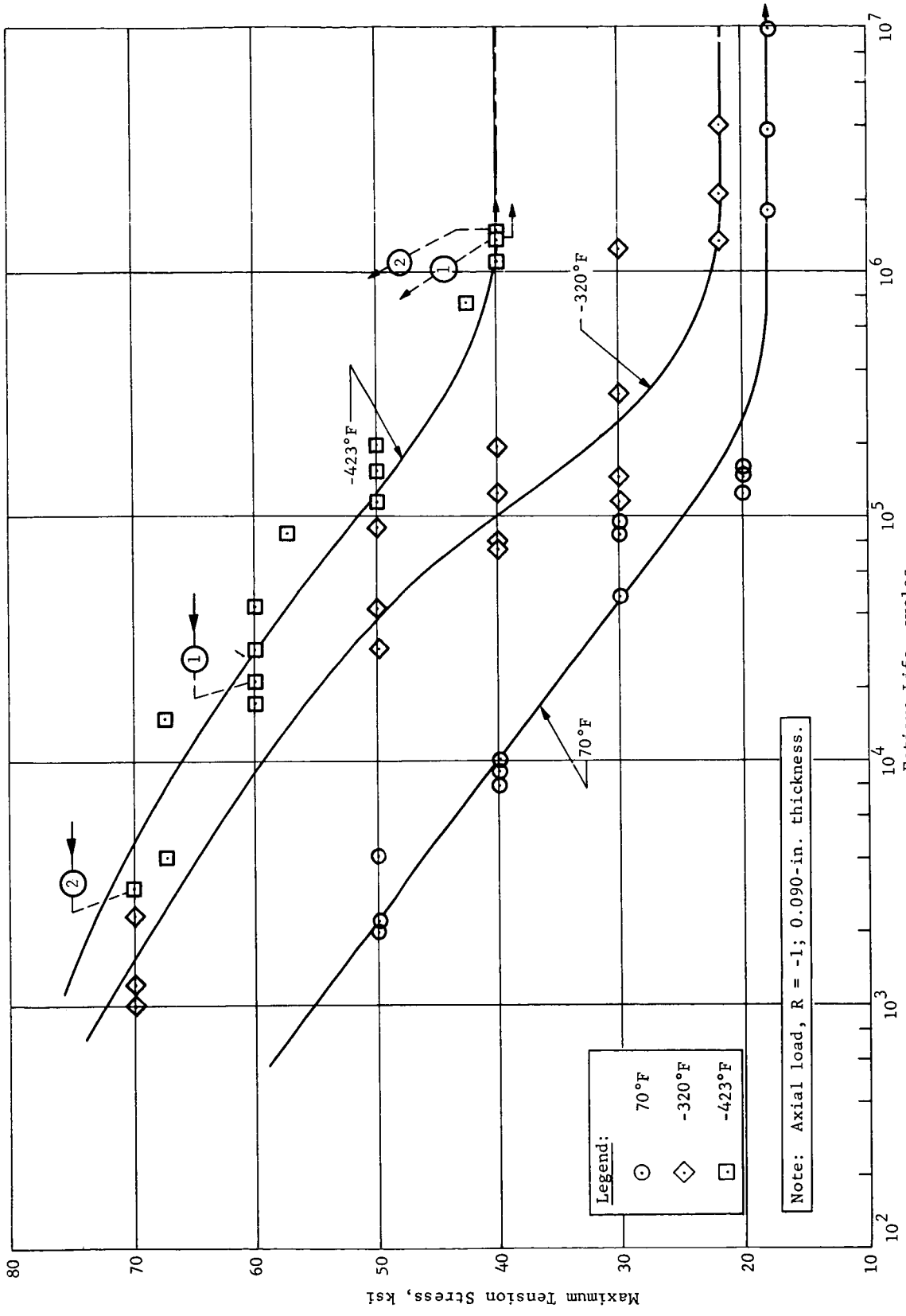

Fig. 27 Fatigue Properties of Parent Metal 2020-T6 Aluminum Alloy

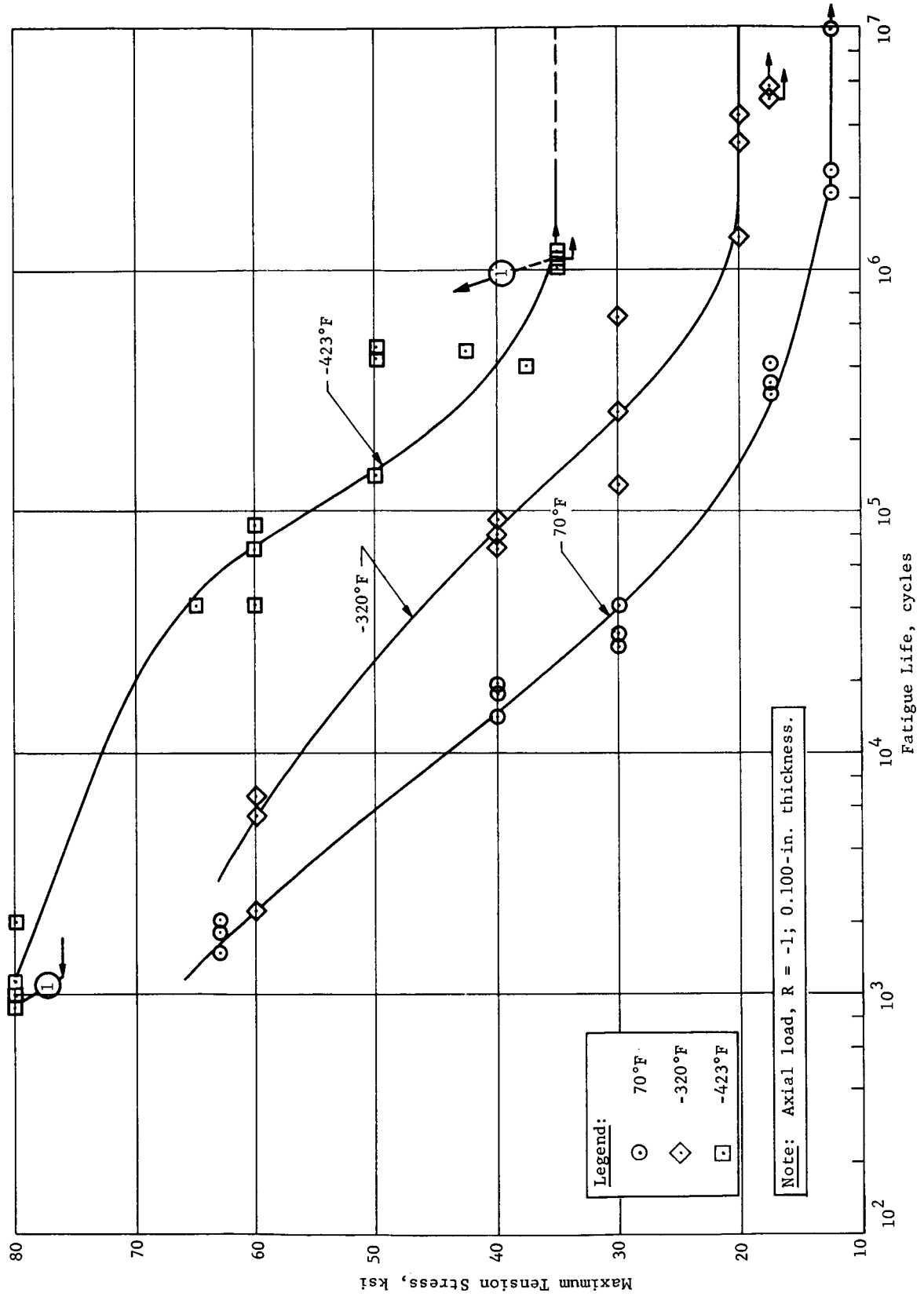

Fig. 28 Fatigue Properties of Parent Metal 7075-T6 Aluminum Alloy

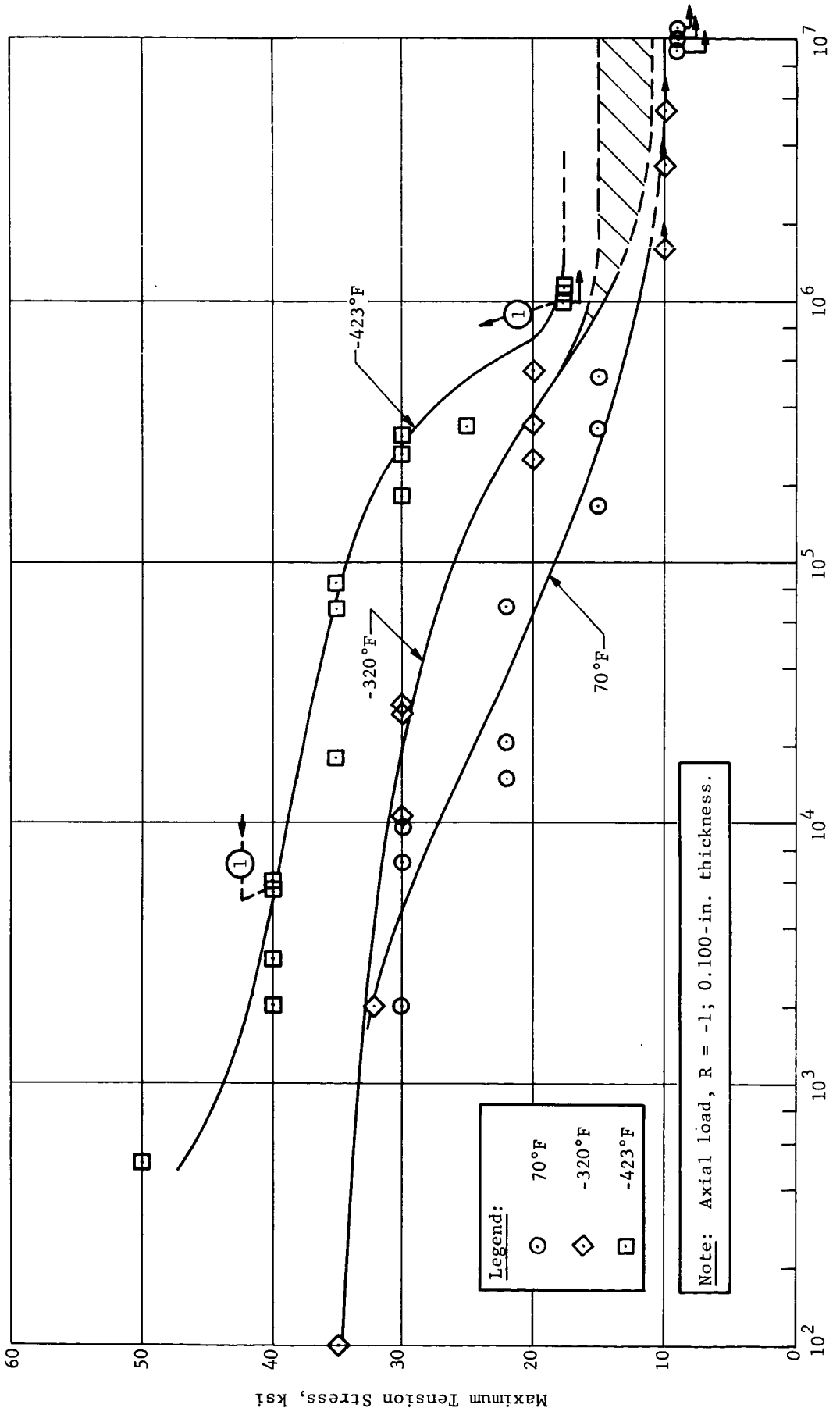

Fig. 29 Fatigue Properties of Welded 2014-T6 Aluminum Alloy

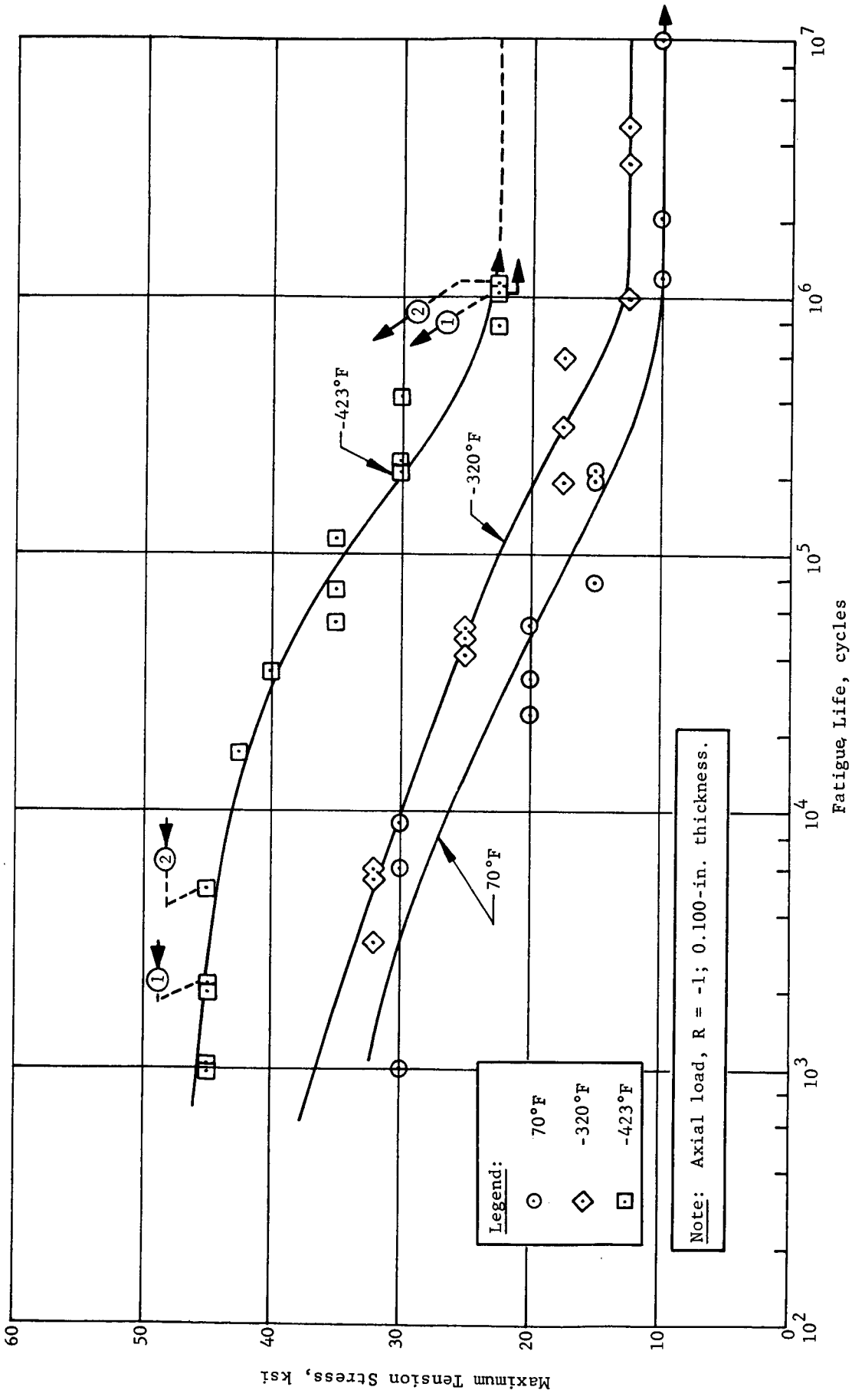

Fig. 30 Fatigue Properties of Welded 2219-T87 Aluminum Alloy

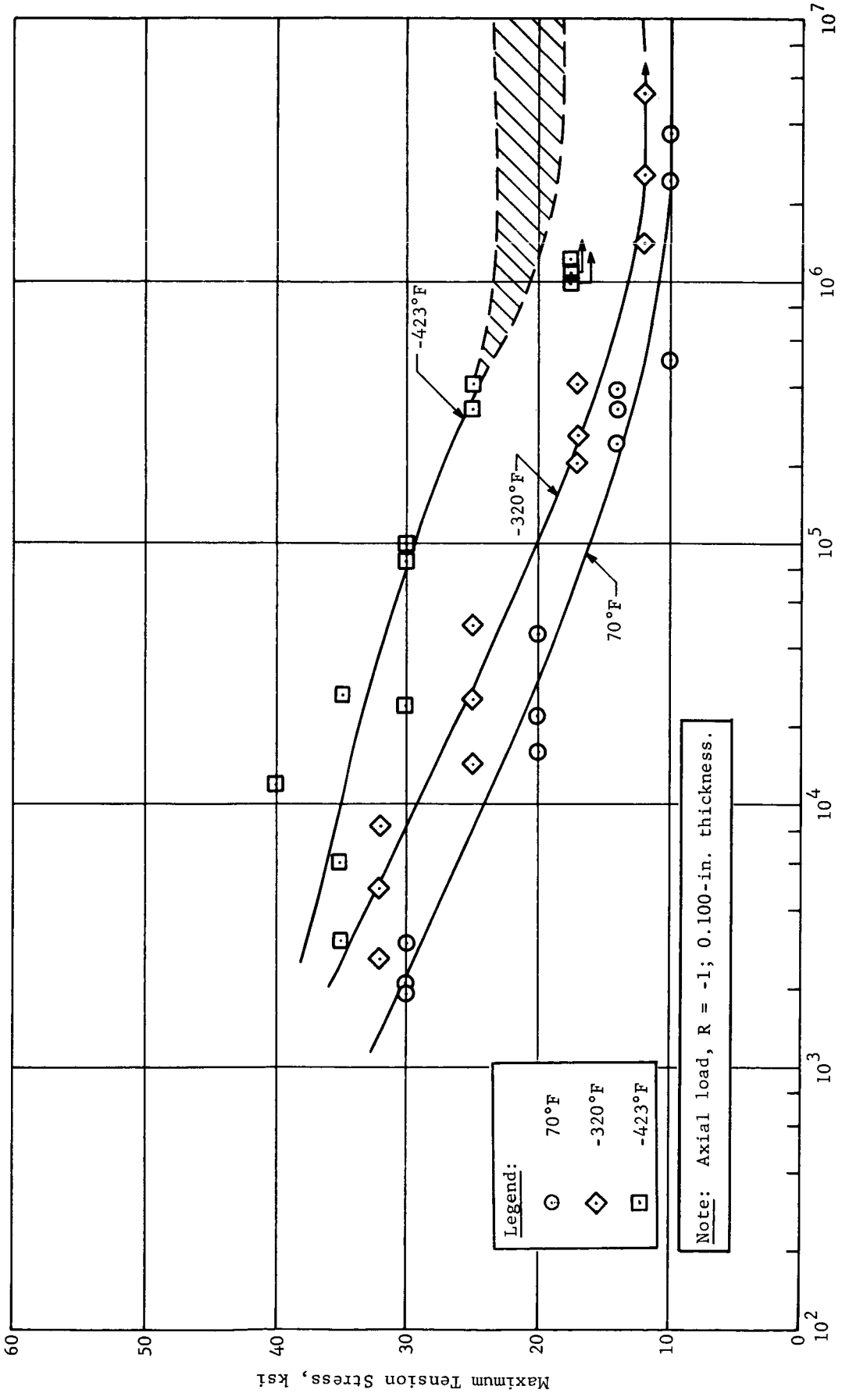

Fig. 31 Fatigue Properties of Welded 5456-H343 Aluminum Alloy

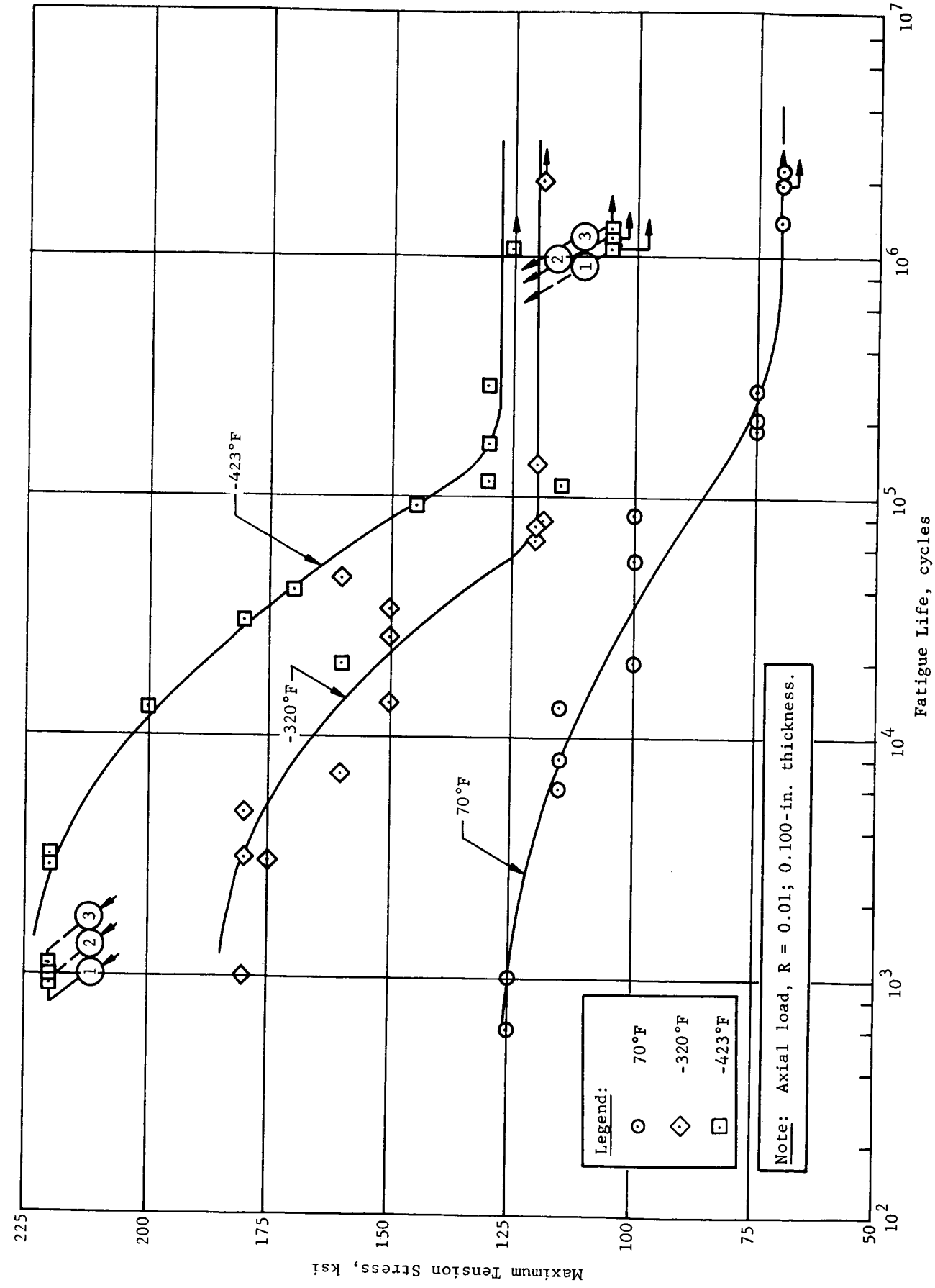

Fig. 32 Fatigue Properties of Annealed Parent Metal 5Al-2.5Sn Titanium Alloy

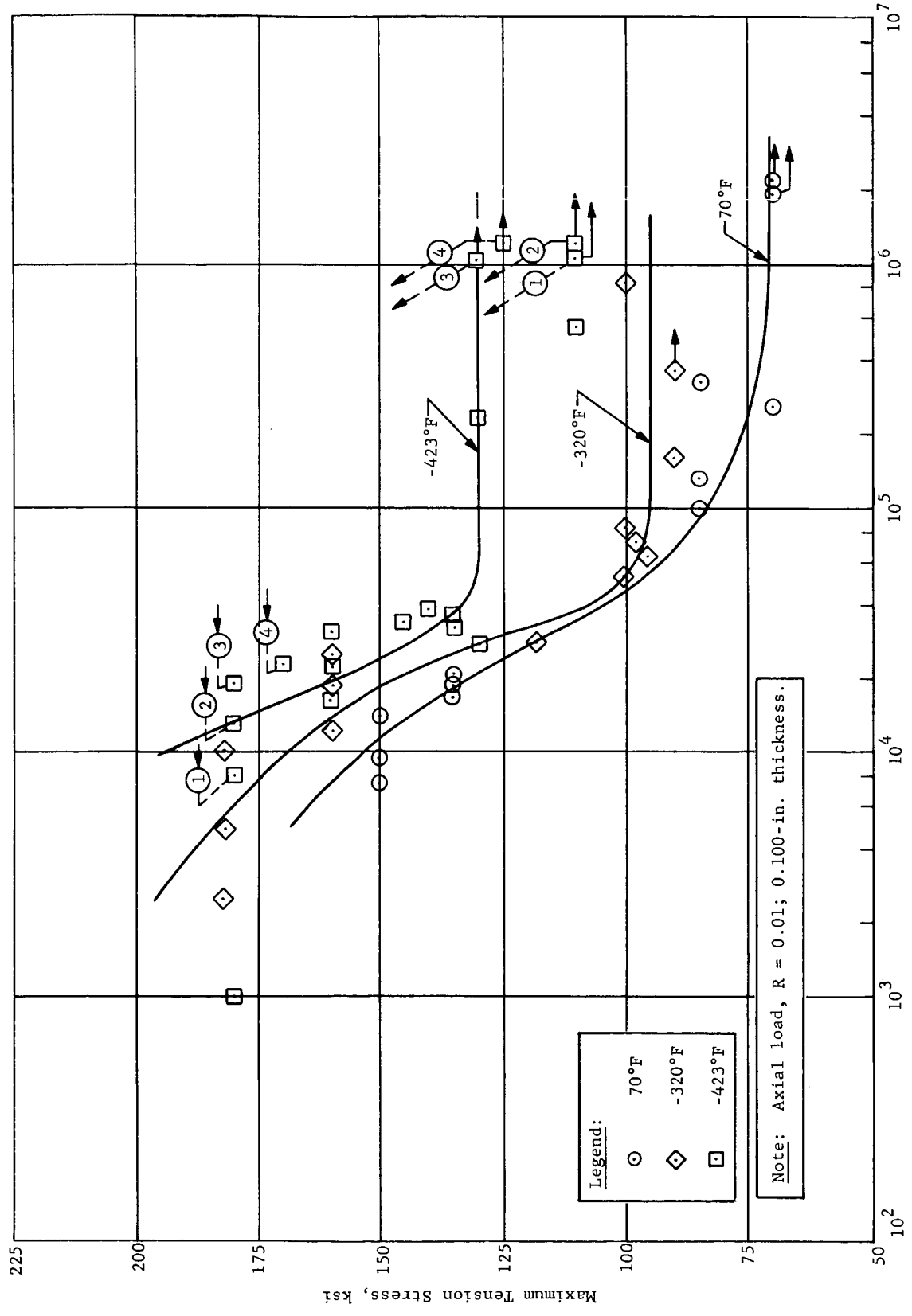

Fig. 33 Fatigue Properties of Solution-Treated and Aged Parent Metal 6Al-4V Titanium Alloy

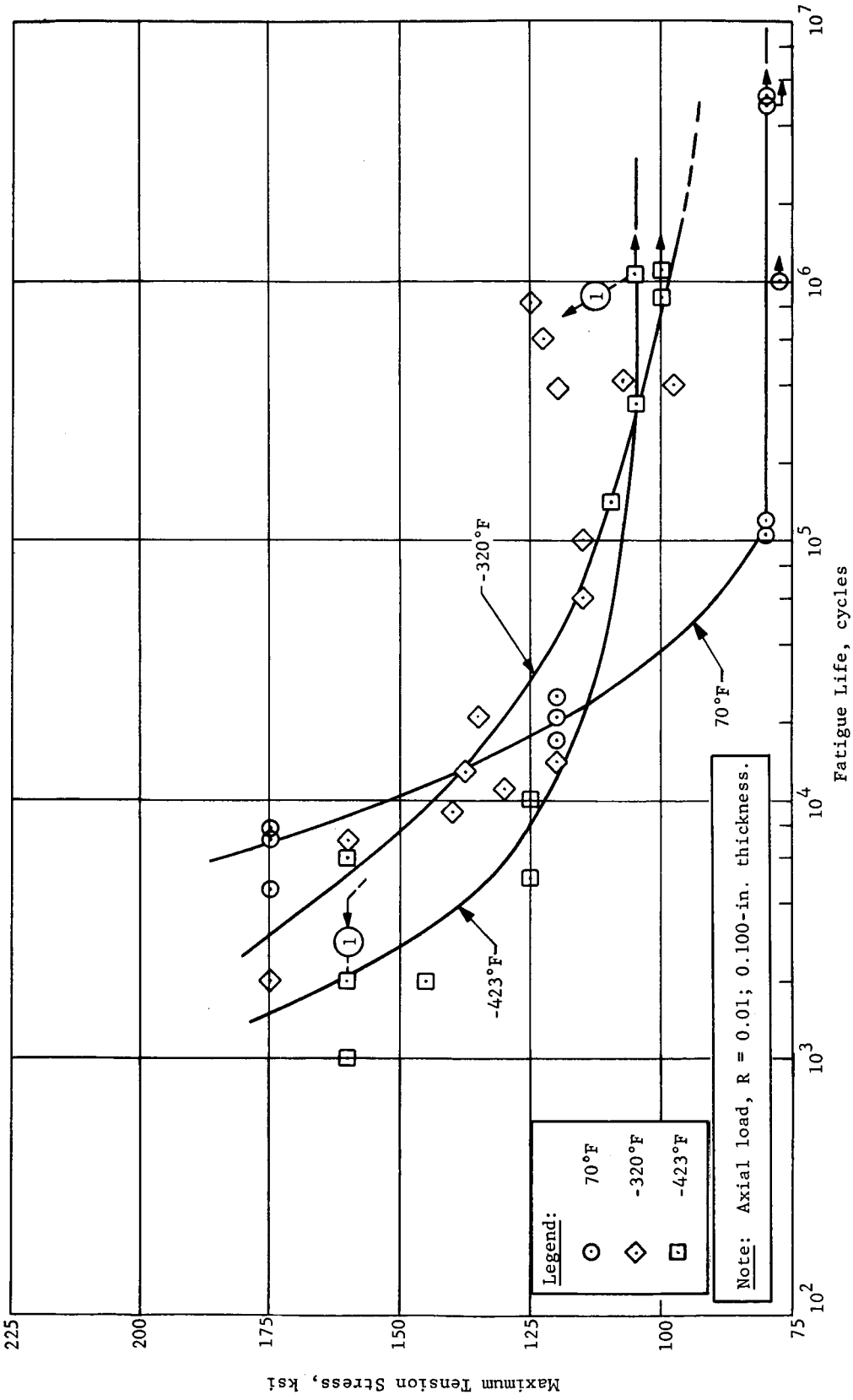

Fig. 34 Fatigue Properties of Solution-Treated and Aged Parent Metal 13V-11Cr-3Al Titanium Alloy

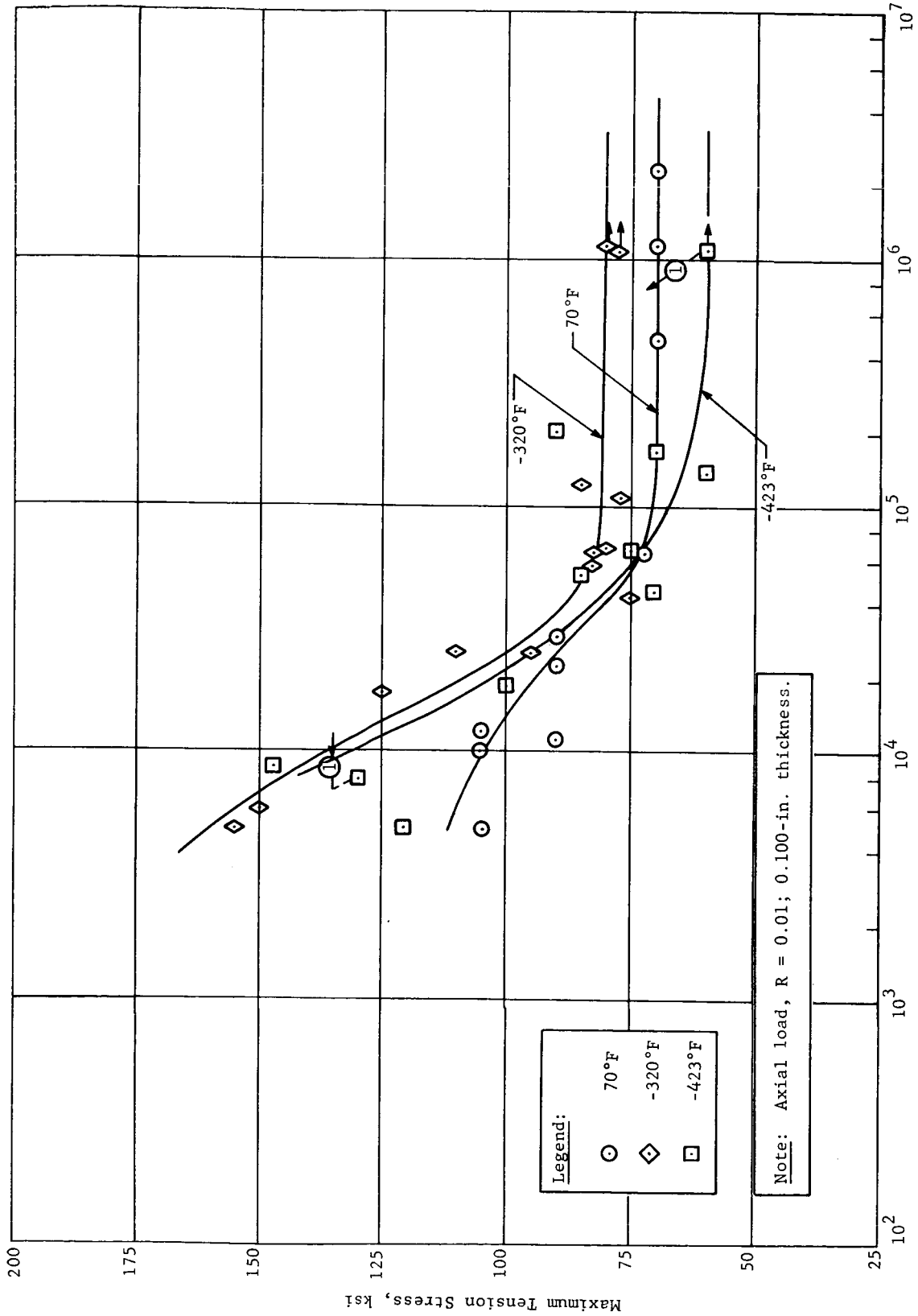

Fig. 35 Fatigue Properties of Annealed, Welded 5Al-2.5Sn Titanium Alloy

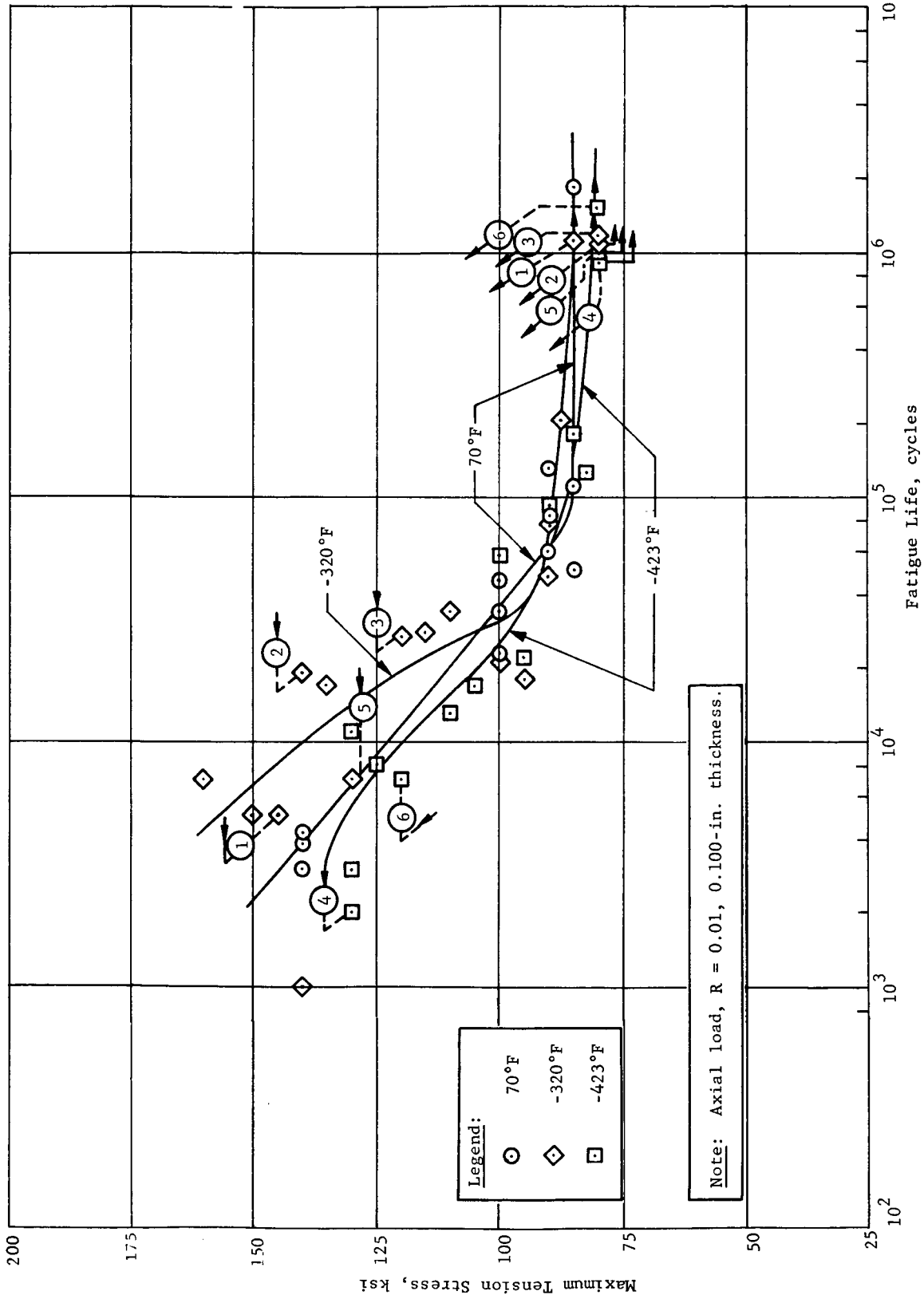

Fig. 36 Fatigue Properties of Solution-Treated and Aged Welded 6Al-4V Titanium Alloy

VII. DISCUSSION OF RESULTS

Test results for the aluminum and titanium alloys are discussed in this chapter.

A. ALUMINUM ALLOYS

Of the five aluminum compositions employed in this study, three are being used or have been considered for cryogenic service. These alloys are 2014, 2219, and 5456. The other two compositions, 2020 and 7075, have not been contenders for cryogenic service primarily because they are nonweldable grades. In addition, the 7075 is known to exhibit poor toughness characteristics at cryogenic temperatures. However, these latter compositions were included in the study for comparative purposes.

1. Tension Properties

The mechanical properties of the 2014-T6 and 2219-T87 alloys (Fig. 16 and 17, respectively) are very similar and in substantial agreement with the data of others.[3,4] These alloys are characterized by a greater temperature dependence of strength from -320 to -423°F than from 70 to -320°F. Yield and weld strengths show a relatively constant rate of increase with decreasing temperature. Elognation increases approximately 50% from 70 to -423°F. The principal difference in properties of these alloys is the significantly lower yield strength in the 2219-T87 alloy.

The 5456-H343 alloy (Fig. 18) exhibits approximately 20% lower ultimate strength than the 2014-2219 alloys. The ratio of yield/ultimate strength is rather low. Elongation is relatively independent of temperature. At 70 to -320°F, weld strength increases, but then decreases with further temperature reduction. This decrease in weld strength and flat ductility curve is suggestive of loss of toughness at low temperatures. The results of other studies (Ref 3 and 5) have shown lower toughness for this alloy at -423°F than for the 2000 series alloys.

The 2020-T6 alloy (Fig. 19) shows very high strength properties. Room temperature ultimate strength is equal to the strength of 5456-H343 at -423°F. Although this composition is expected to exhibit poor toughness at cryogenic temperatures, the limited evaluation performed is not sufficient to detect such behavior. Tensile ductility increases to approximately 10% at -423°F.

The 7075-T6 material (Fig. 20) shows evidence of the onset of brittle action at -423°F. Ultimate and yield strengths flatten out between -320 and -423°F. Elongation is relatively independent of temperature. Although no notch tests were performed in this study, data obtained by Christian and Watson (Ref 6) show a significant loss of toughness for this alloy at low temperatures.

Modulus data for the five alloys are given in Fig. 37. Room-temperature results are slightly lower but agree within 2% with data obtained from the Aluminum Association and from producers. Published data are compared with the experimental data below:

	Modulus of Elasticity, 10^6 psi	
Alloy	Experimental	Published
2014-T6	10.6	10.6
2219-T87	10.5	10.6
5456-H343	10.2	10.3
2020-T6	11.1	11.3
7075-T6	10.2	10.4

The highest modulus material is the 2020 composition. When introduced, this composition was reported to exhibit a 10% improvement over existing alloys. However, subsequent study showed it to be approximately 5%. Nevertheless, this level is still higher than almost all other aluminum alloys.

There is insufficient reliable data in the literature to confirm the cryogenic modulus data.

2. Fatigue Properties

Fatigue data for the aluminum alloys are presented in the following figures and tables.

Material	Figure	Table
2014-T6 Parent Metal	24	C-I
2219-T87 Parent Metal	25	C-II
5456-H343 Parent Metal	26	C-III
2020-T6 Parent Metal	27	C-IV
7075-T6 Parent Metal	28	C-V
2014-T6 Welded	29	C-VI
2219-T87 Welded	30	C-VII
5456-H343 Welded	31	C-VIII

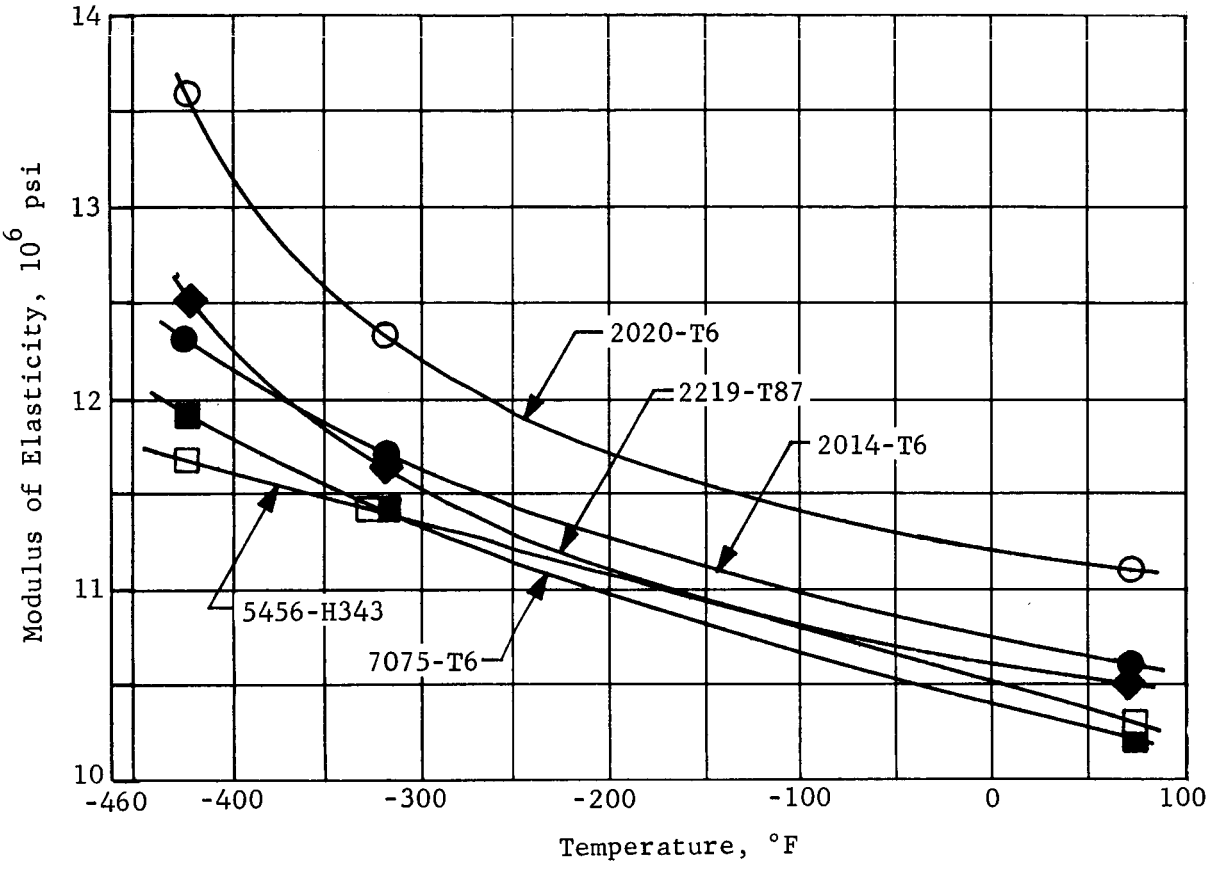

Fig. 37 Modulus of Elasticity of Five Aluminum Alloys at Cryogenic Temperatures

S/N (stress vs number of cycles to failure) curves for all materials were generally good. Reproducibility of fatigue life for multiple tests performed at a constant stress level was surprisingly good considering the alignment problems and sheet gages evaluated. In several cases, the tests performed in the 10^6 cycle range were at a stress sufficiently lower than the 10^5 cycle tests so that the endurance limit stress could not be selected with great accuracy. In these few cases, the spread for the endurance limit is presented. However, the spread does not exceed 5000 psi. In only one case were the data difficult to interpret. This was in the case of the 2219-T87 parent metal at -320°F. These data are discussed in detail later in this section.

The parent metal S/N curves for 2014-T6 and 5456-H343 were similar except for lower short-time strength properties for the latter alloy. In both cases the 70 and -423°F curves were flatter than the -320°F curve, which showed a slight knee. Endurance limit values are given in Table V.

Table V Endurance Limits for Aluminum Alloys

Alloy	Temperature, °F	Endurance Limit, ksi	
		Parent Metal	Welded
2014-T6	70	15	10
	-320	25	10 to 15
	-423	45	18
2219-T87	70	20	10
	-320	15 to 25	12
	-423	40	22
5456-H343	70	15	10
	-320	25	12
	-423	40	18 to 23
2020-T6	70	18	
	-320	22	
	-423	40	
7075-T6	70	12	
	-320	20	
	-423	35	

The behavior of the 2219-T87 parent metal was similar to that of the former alloys except that the liquid nitrogen curve appears to be flatter in the low cycle range. The endurance limit portion of the curve is presented as a spread band that crosses the room temperature curve. Conflicting data points require that this technique be used. Although the upper line of the band gives

the expected behavior, the data points at 15,000 psi cannot be ignored. The duplicate tests performed at 25,000 psi produced failures through the pinholes. No reason for this type of failure is apparent.

The nonweldable alloys, 2020-T6 and 7075-T6, exhibited steeper S/N curves than the weldable grades. The 2020-T6 curve at 70°F flattened out after a relatively short number of cycles. The 7075-T6 composition showed a very low room temperature endurance limit. The liquid hydrogen curve was quite steep.

Fracture surfaces of the parent metal fatigue specimens showed typical transgranular fatigue failures, and the 5456-H343 and 7075-T6 specimens showed a laminated appearance. This behavior is typical for the strain hardened 5456 alloy even in static tension failures, but is not observed for the 7075 composition in tension.

Fatigue curves for the three welded alloys exhibited very similar shape and strength properties. Endurance limit values varied little.

A review of techniques proposed for curve fitting suggested that insufficient data were available for use with these methods.

In an attempt to compare data obtained for the various alloys, the fatigue properties were reduced to ratios of fatigue strength/tensile strength and fatigue strength/yield strength. This approach permits a comparison of behavior under dynamic conditions with that under static conditions. Table VI presents the data for fatigue strength properties at 10^4, 10^5, and 10^6 cycles and for the endurance limit compared to tensile properties. Table VII gives a similar comparison for yield data. Figures 38 and 39 present graphically these comparisons at the three test temperatures for the endurance limit condition. The data clearly show the poor behavior of 7075-T6 at all temperatures. The 2020-T6 is similarly lower than the remaining alloys. The three remaining alloys (parent metal condition) are similar at 70°F, with 2219 exhibiting slightly higher properties. At the cryogenic temperatures, 5456-H343 shows the highest dynamic/static strength ratio. A comparison of the weld properties shows very similar results for the three alloys at room temperature. At cryogenic temperatures, the 5456 appears to be superior. The results of this analysis can be compared with notch toughness properties to determine whether any trends become apparent. Table VIII compares the fatigue strength to tensile and yield strength ratios with the notch/unnotch strength ratio at various temperatures. The table shows that the 5456-H343 alloy that exhibits an outstanding fatigue strength ratio is rather poor in notch toughness and that the 7075-T6 alloy is poor in both categories.

Table VI Fatigue Strength/Ultimate Strength Ratio for Aluminum Alloys

Material	Temperature, °F	Ultimate Strength, ksi	Fatigue Strength (ksi) and Fatigue Strength/Ultimate Strength Ratio (in parenthesis) for Indicated Life (cycles)			
			10^4	10^5	10^6	Endurance Limit
2014-T6 Parent Metal	70	71	45 (0.63)	33 (0.46)	17 (0.24)	15 (0.21)
	-320	85	58 (0.68)	40 (0.47)	25 (0.29)	25 (0.29)
	-423	98	64 (0.65)	58 (0.59)	46 (0.47)	45 (0.46)
2219-T87 Parent Metal	70	67	41 (0.61)	30 (0.45)	22 (0.32)	20 (0.30)
	-320	85	47 (0.55)	32 (0.38)	15 to 25 (0.18 to 0.29)	15 to 25 (0.18 to 0.29)
	-423	99	60 (0.61)	52 (0.53)	41 (0.41)	40 (0.40)
5456-H343 Parent Metal	70	57	35 (0.61)	26 (0.46)	17 (0.30)	15 (0.26)
	-320	72	50 (0.69)	32 (0.44)	25 (0.35)	25 (0.35)
	-423	81	54 (0.67)	46 (0.57)	41 (0.51)	40 (0.49)
2020-T6 Parent Metal	70	83	40 (0.48)	25 (0.30)	18 (0.22)	18 (0.22)
	-320	98	59 (0.60)	40 (0.41)	23 (0.23)	22 (0.22)
	-423	101	66 (0.65)	52 (0.51)	41 (0.40)	40 (0.39)
7075-T6 Parent Metal	70	79	45 (0.57)	23 (0.29)	14 (0.18)	12 (0.15)
	-320	99	56 (0.57)	39 (0.39)	21 (0.21)	20 (0.20)
	-423	116	73 (0.63)	56 (0.48)	36 (0.31)	35 (0.30)
2014-T6 Welded	70	57	27 (0.47)	18 (0.32)	12 (0.21)	10 (0.18)
	-320	66	31 (0.47)	26 (0.39)	15 (0.23)	10 to 15 (0.15 to 0.23)
	-423	71	39 (0.55)	34 (0.48)	18 (0.25)	18 (0.25)
2219-T87 Welded	70	49	26 (0.53)	17 (0.35)	10 (0.20)	10 (0.20)
	-320	62	30 (0.48)	22 (0.35)	13 (0.21)	12 (0.19)
	-423	68	43 (0.63)	34 (0.50)	22 (0.32)	22 (0.32)
5456-H343 Welded	70	51	24 (0.47)	16 (0.31)	11 (0.22)	10 (0.20)
	-320	59	29 (0.49)	20 (0.34)	13 (0.22)	12 (0.20)
	-423	55	35 (0.64)	30 (0.54)	21 to 23 (0.38 to 0.42)	18 to 23 (0.33 to 0.42)

Table VII Fatigue Strength/Yield Strength Ratio for Parent Metal Aluminum Alloys

Material	Temperature, °F	Yield Strength, ksi	Fatigue Strength (ksi) and Fatigue Strength/Yield Strength Ratio (in parenthesis) for Indicated Life (cycles)			
			10^4	10^5	10^6	Endurance Limit
2014-T6	70	67	45 (0.67)	33 (0.49)	17 (0.25)	15 (0.22)
	-320	76	58 (0.76)	40 (0.52)	25 (0.32)	25 (0.32)
	-423	82	64 (0.78)	58 (0.70)	46 (0.56)	45 (0.54)
2219-T87	70	55	41 (0.74)	30 (0.54)	22 (0.40)	20 (0.36)
	-320	66	47 (0.71)	32 (0.48)	15 to 25 (0.22 to 0.37)	15 to 25 (0.22 to 0.37)
	-423	70	60 (0.85)	52 (0.74)	41 (0.58)	40 (0.57)
5456-H343	70	44	35 (0.79)	26 (0.59)	17 (0.38)	15 (0.34)
	-320	51	50 (0.98)	32 (0.62)	25 (0.49)	25 (0.49)
	-423	54	54 (1.00)	46 (0.85)	41 (0.75)	40 (0.74)
2020-T6	70	79	40 (0.50)	25 (0.31)	18 (0.22)	18 (0.22)
	-320	87	59 (0.67)	40 (0.45)	23 (0.26)	22 (0.25)
	-423	97	66 (0.68)	52 (0.53)	41 (0.42)	40 (0.41)
7075-T6	70	72	45 (0.62)	23 (0.31)	14 (0.19)	12 (0.16)
	-320	85	56 (0.65)	39 (0.45)	21 (0.24)	20 (0.23)
	-423	86	73 (0.84)	56 (0.65)	36 (0.41)	35 (0.40)

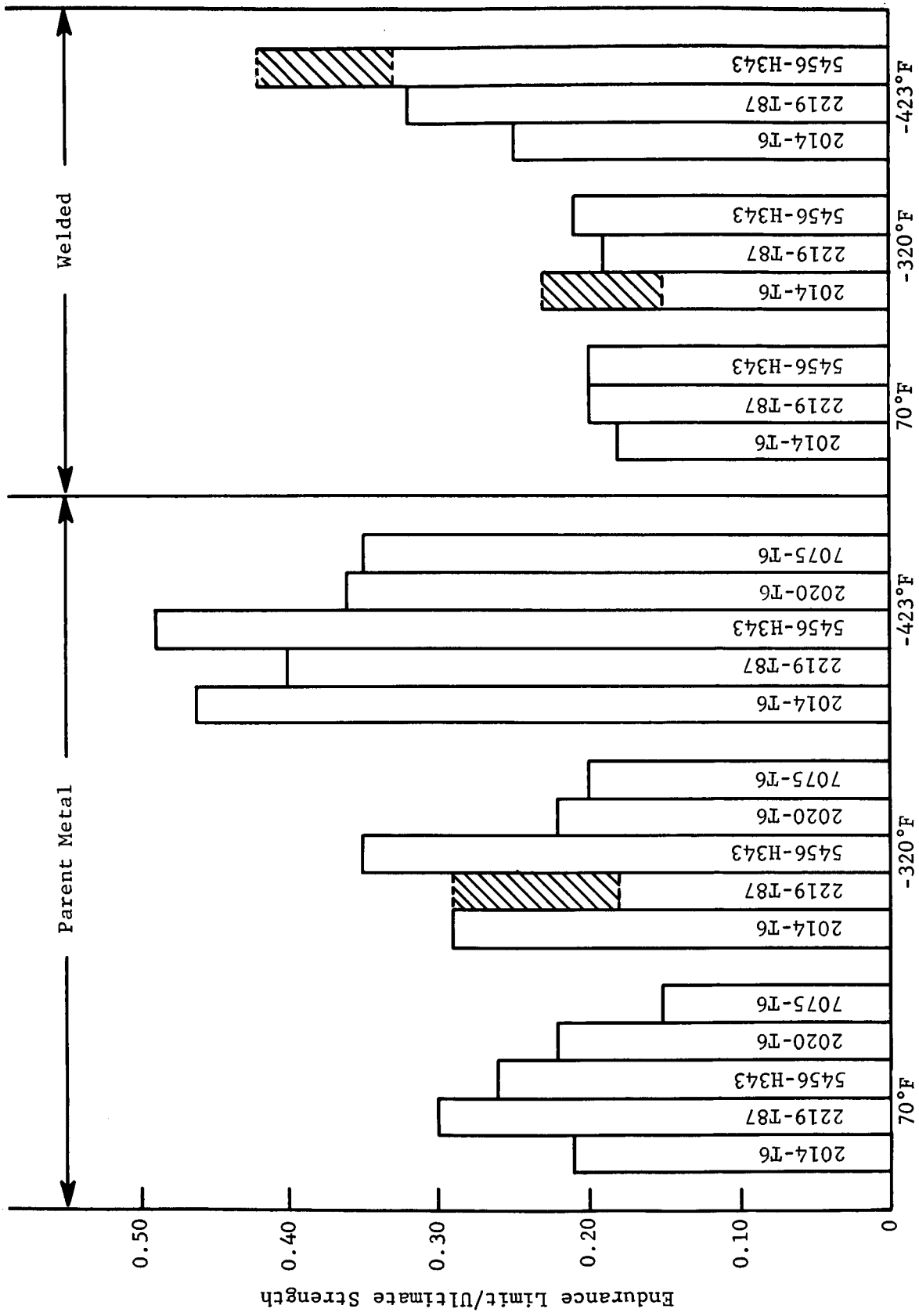

Fig. 38 Fatigue Strength/Ultimate Strength Ratio for Five Aluminum Alloys

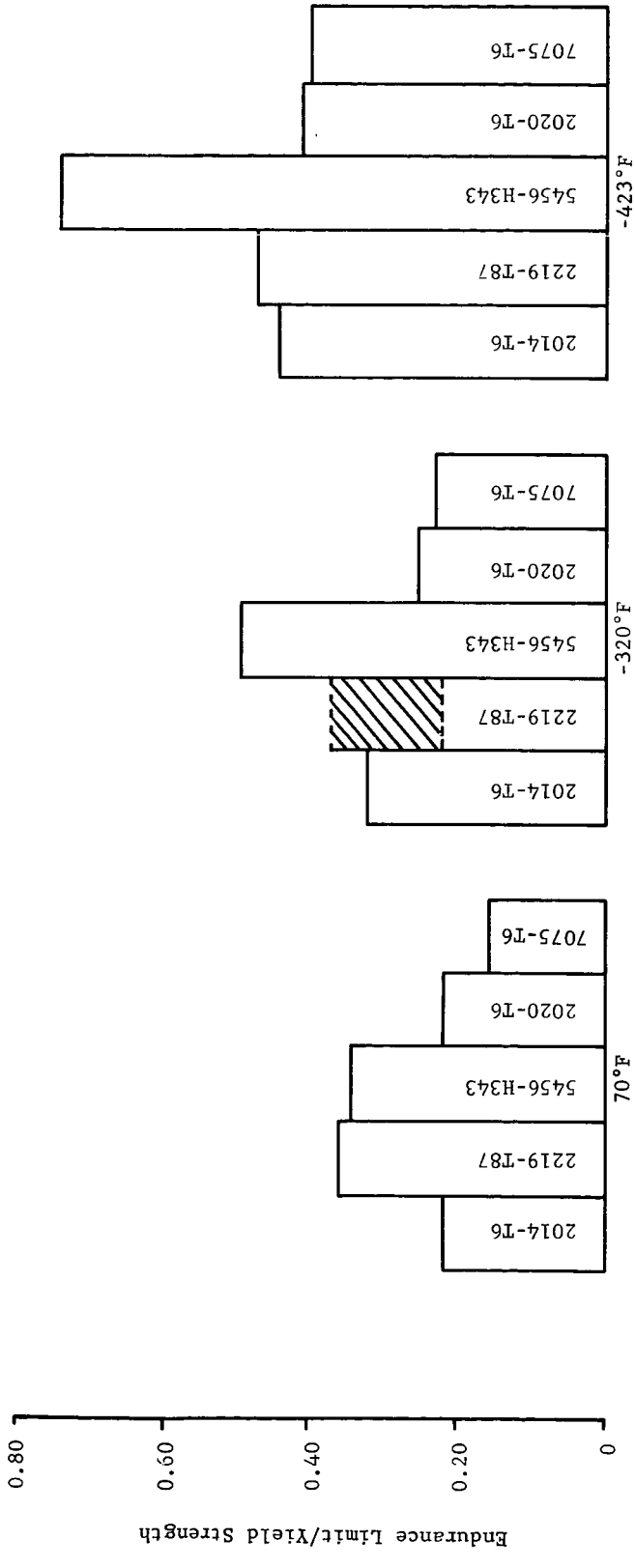

Fig. 39 Fatigue Strength/Yield Strength Ratio for Five Parent Metal Aluminum Alloys

Table VIII Comparison of Fatigue Strength Ratios with Notch Strength Ratios for Aluminum Alloys

Alloy	Temperature, °F	Fatigue/Yield Ratio	Fatigue/Ultimate Ratio	Notch/Unnotch Ratio*
2014-T6 (Ref 4)	70	0.22	0.21	1.06
	-320	0.32	0.29	0.92
	-423	0.54	0.49	0.84
2219-T87 (Ref 3)	70	0.36	0.30	0.99
	-320	0.22 to 0.37	0.18 to 0.29	0.97
	-423	0.57	0.40	0.92
5456-H343 (Ref 3)	70	0.34	0.26	0.92
	-320	0.49	0.35	0.68
	-423	0.74	0.49	0.66
7075-T6 (Ref 6)	70	0.16	0.15	1.02
	-320	0.23	0.20	0.78
	-423	0.40	0.30	0.73

*K_t = 7.3 to 8.0.

The results of two tests performed under tension/tension loading show the effect of stress ratio on fatigue properties. Although insufficient data are presented for a quantitative analysis of the effect, the marked increase in life is apparent. Figure 40 compares 2219-T87 parent metal and 2014-T6 welded properties tested at R = -1 with points obtained for R = 0 at -423°F.

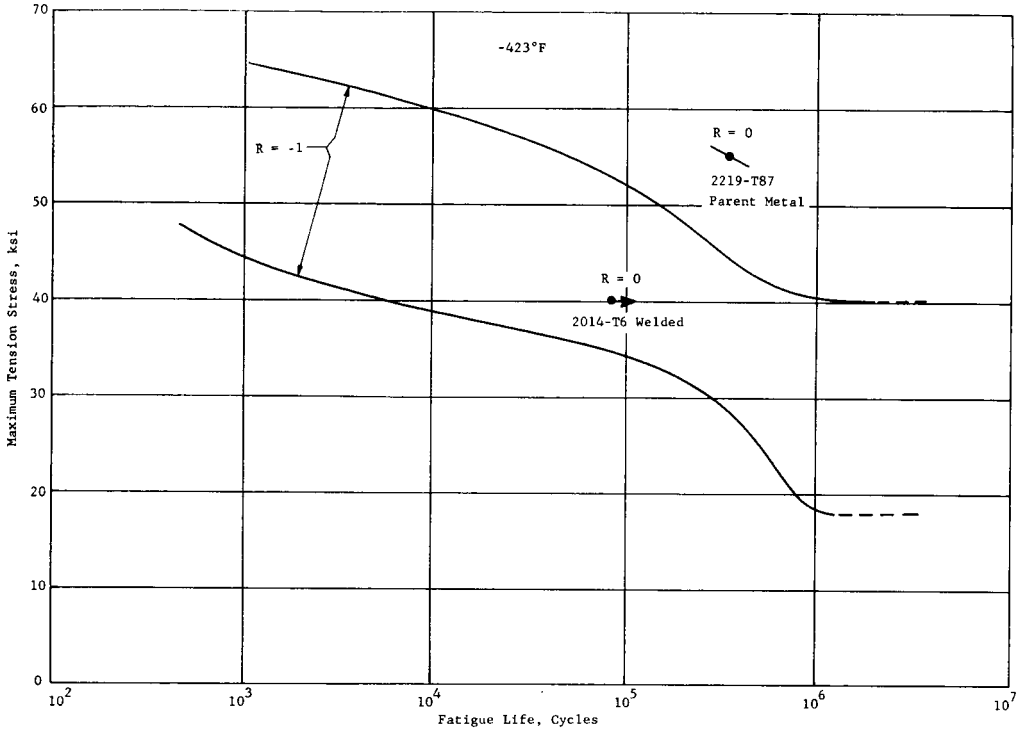

Fig. 40 Effect of Stress Ratio on the Fatigue Properties of Two Aluminum Alloys at -423°F

B. TITANIUM ALLOYS

The titanium alloys evaluated in this program represent each system used commercially: (a) alpha; (b) beta, and (c) alpha-beta. The Ti-5Al-2.5Sn crystallizes in the hexagonal-close-packed structure (alpha) and is characterized by good retention of properties down to very low temperatures. The Ti-13V-11Cr-3Al alloy is a beta type crystallizing in the body-centered-cubic structure. Body-centered-cubic materials are typified by ductile-brittle transition behavior and consequently are not suited for cryogenic

service. The Ti-6Al-4V alloy represents the alpha-beta type and combines hexagonal and body-centered-cubic phases. Due to the relatively low percentage of beta phase in this particular composition, toughness and ductility can be retained to moderately low temperatures. However, below -320°F there is a marked decrease in mechanical properties. Hence, alpha alloys, such as Ti-5Al-2.5Sn, are clearly the best titanium selection for most applications down to -423°F.

1. Tension Properties

The mechanical properties of the Ti-5Al-2.5Sn alloy are shown in Fig. 21. Strength properties increase almost 100% from 70 to -423°F. Weld joint efficiency is very close to 100%. Elongation increases slightly from room temperature to -320°F, but decreases sharply to 1.8% at -423°F. This behavior would be expected for normal interstitial Ti-5Al-2.5Sn but not for low-interstitial grade. A study of the chemical analysis shows both iron and interstitial elements to be quite low. No explanation for this unusual behavior can be found. Plotting the interstitial content of this material with the data previously reported by Schwartzberg and Keys (Ref 7) on interstitial effects in Ti-5Al-2.5Sn shows that the ultimate strength falls slightly above the curve (Fig. 41). Data of Espey et al. (Ref 8) and Christian (Ref 9) at higher oxygen equivalent contents showed satisfactory ductility.

The behavior of the solution-treated and aged Ti-6Al-4V alloy is shown in Figure 22. Strength increased from 165,000 psi at 70°F to almost 300,000 psi at -423°F. As expected for this composition in the fully heat-treated condition, ductility decreased continuously below room temperature. Weld joint efficiency was very good.

Figure 23 presents tensile data for the Ti-13V-11Cr-3Al alloy. As expected, brittle behavior was observed below room temperature. At room temperature, a strength level of 200,000 psi was achieved while maintaining 6.5% elongation. At -320°F, brittle failures occurred through the pinholes or specimen fillet. No attempt was made to test specimens at -423°F.

Modulus data obtained at 70, -110, and -320°F are presented in Fig. 42. Data obtained at -423°F were not satisfactory and are not presented.

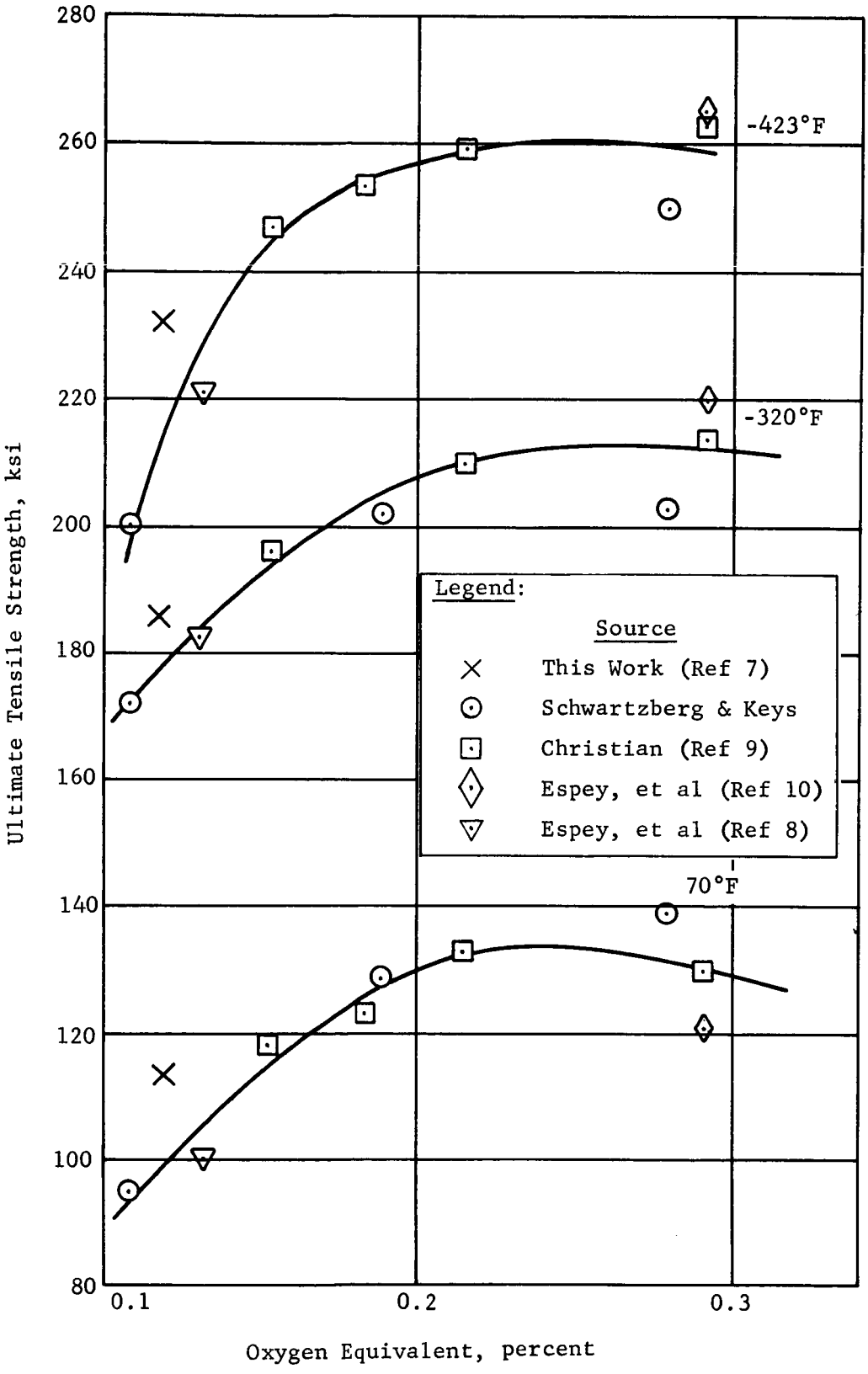

Fig. 41 Effect of Interstitial Content on the Unnotch Tensile Strength of Ti-5Al-2.5Sn

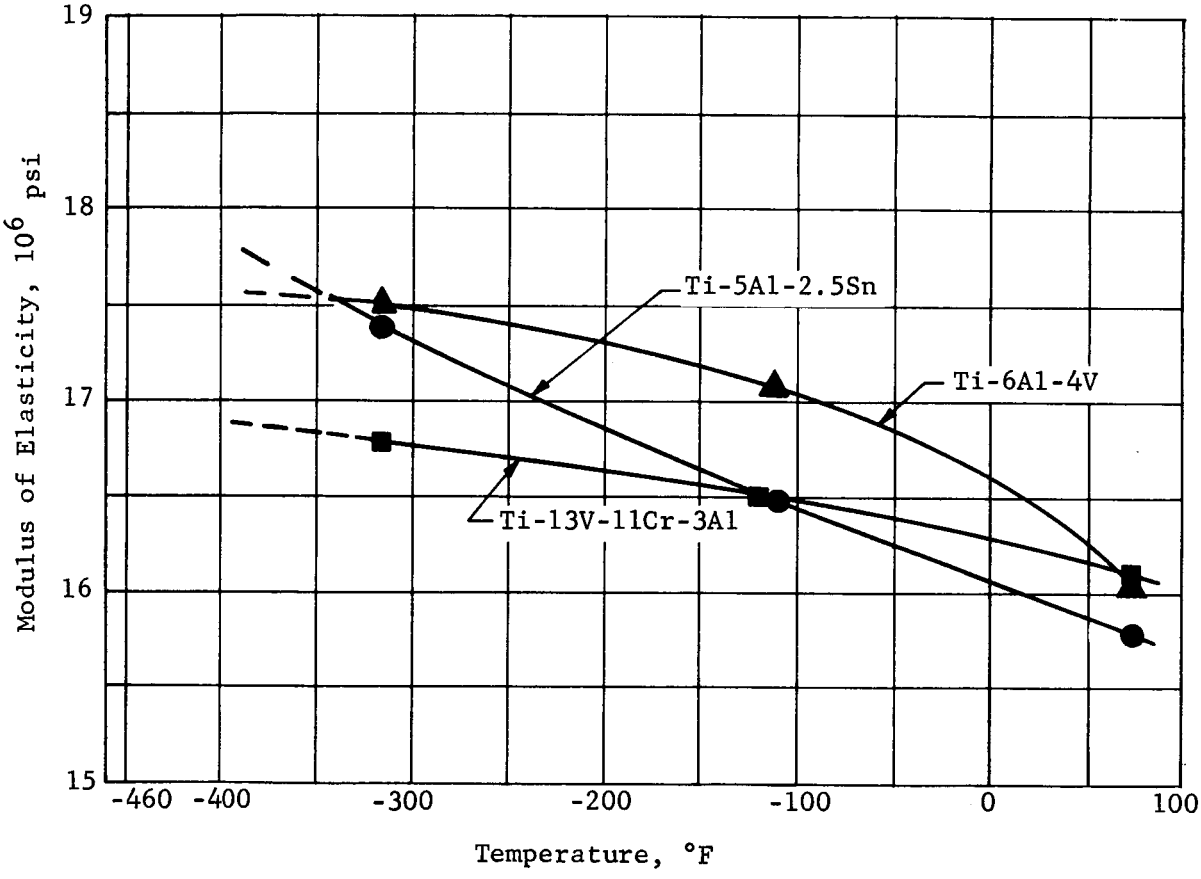

Fig. 42 Modulus of Elasticity of Three Titanium Alloys at Cryogenic Temperatures

2. Fatigue Properties

Fatigue data for the following titanium alloys are presented in the figures and tables tabulated below.

Material	Figure	Table
Ti-5Al-2.5Sn, Parent Metal	32	C-IX
Ti-6Al-4V, Parent Metal	33	C-X
Ti-13V-11Cr-3Al, Parent Metal	34	C-XI
Ti-5Al-2.5Sn, Welded	35	C-XII
Ti-6Al-4V, Welded	36	C-XIII

The parent metal curves for the titanium alloys are characterized by a general sharp transition from high strength to the level of the endurance limit and rather flat behavior above 10^5 cycles. The aluminum alloy curves do not flatten out until 10^6 cycles are reached.

The Ti-5Al-2.5Sn alloy exhibits a wide variation in low cycle fatigue strength as a function of temperature. However, at the endurance limit the cryogenic properties at -320 and -423°F do not differ widely. Endurance limit stresses for the three temperatures shown are listed in Table IX.

Table IX Endurance Limits for Titanium Alloys

Alloy	Temperature, °F	Endurance Limit, ksi	
		Parent Metal	Welded
Ti-5Al-2.5Sn	70	70	70
	-320	120	80
	-423	128	60
Ti-6Al-4V	70	70	85
	-320	95	85
	-423	130	80
Ti-13V-11Cr-3Al	70	80	
	-320	90	
	-423	105	

For the Ti-6Al-4V alloy there is a smaller difference in strength properties at the low cycle end of the curve than for the Ti-5Al-2.5Sn. However, at cryogenic temperatures a wider spread between -320 and -423°F endurance limits is observed. Endurance limit data are given in Table VIII. The behavior of the Ti-13V-11Cr-3Al alloy is unusual. At the low cycle portion of

the curve, strength properties are shown to decrease with decreasing temperature, contrary to the normal behavior. However, the 70°F curve is quite steep and crosses the cryogenic S/N curves. The -423°F curve decreases sharply initially and then levels off to give the highest endurance limit for the three temperatures. The -320°F results show a more gradual decrease with reduction in temperature. Endurance limit values are given in Table IX.

Evaluation of welded Ti-5Al-2.5Sn and Ti-6Al-4V showed that the -423°F endurance limit was lower than that obtained at 70 and -320°F. In the Ti-5Al.2.5Sn material, the 70°F endurance limit lies between the -320°F and -423°F results. The Ti-6Al-4V alloy exhibited identical endurance limits at 70 and -320°F, only slightly above the -423°F result.

Presentation of test results in terms of fatigue strength/tensile and yield strength ratios are presented in Tables X and XI and in Fig. 43 and 44, respectively.

The results clearly show the excellent behavior of the Ti-5Al-2.5Sn alloy in the parent metal condition. In the welded condition, the Ti-5Al-2.5Sn and Ti-6Al-4V show similar behavior. The fatigue strength ratios obtained for titanium alloys are significantly higher than those obtained for aluminum alloys.

Table X Fatigue Strength/Ultimate Strength Ratio of Titanium Alloys

Material	Temperature, °F	Ultimate Strength, ksi	Fatigue Strength (ksi) and Fatigue Strength/ Ultimate Strength Ratio (in parenthesis) for Indicated Life (cycles)			
			10^4	10^5	10^6	Endurance Limit
Ti-5Al-2.5Sn Parent Metal	70	116	113 (0.97)	85 (0.73)	70 (0.060)	70 (0.60)
	-320	186	165 (0.89)	120 (0.65)	120 (0.065)	120 (0.65)
	-423	234	202 (0.86)	140 (0.60)	128 (0.55)	128 (0.55)
Ti-6Al-4V Parent Metal	70	165	153 (0.93)	85 (0.52)	70 (0.52)	70 (0.42)
	-320	243	170 (0.70)	95 (0.39)	95 (0.39)	95 (0.39)
	-423	297	195 (0.66)	130 (0.44)	130 (0.44)	130 (0.44)
Ti-13V-11Cr-3Al Parent Metal	70	200	150 (0.75)	82 (0.41)	80 (0.40)	80 (0.40)
	-320	200	143 (0.71)	112 (0.50)	98 (0.49)	90 (0.45)
Ti-5Al-2.5Sn Welded	70	113	105 (0.93)	70 (0.62)	70 (0.62)	70 (0.62)
	-320	182	138 (0.76)	81 (0.45)	80 (0.44)	80 (0.44)
	-423	227	132 (0.58)	68 (0.30)	60 (0.26)	60 (0.26)
Ti-6Al-4V Welded	70	149	122 (0.82)	85 (0.57)	85 (0.57)	85 (0.57)
	-320	234	140 (0.60)	89 (0.38)	85 (0.36)	85 (0.36)
	-423	275	120 (0.44)	86 (0.31)	82 (0.30)	80 (0.29)

Table XI Fatigue Strength/Yield Strength Ratio of Parent Metal Titanium Alloys

Material	Temperature, °F	Yield Strength, ksi	Fatigue Strength (ksi) and Fatigue Strength/ Yield Strength Ratio (in parenthesis) for Indicated Life (cycles)			
			10^4	10^5	10^6	Endurance Limit
Ti-5Al-2.5Sn	70	108	113 (1.05)	85 (0.78)	70 (0.65)	70 (0.65)
	-320	173	165 (0.95)	120 (0.69)	120 (0.69)	120 (0.69)
	-423	211	202 (0.95)	140 (0.66)	128 (0.60)	128 (0.60)
Ti-6Al-4V	70	154	153 (0.99)	85 (0.55)	70 (0.45)	70 (0.45)
	-320	229	170 (0.74)	95 (0.44)	95 (0.41)	95 (0.41)
	-423	284	195 (0.68)	130 (0.45)	130 (0.45)	130 (0.45)
Ti-13V-11Cr-3Al	70	200	150 (0.75)	82 (0.41)	80 (0.41)	80 (0.41)
	-320	201	143 (0.71)	112 (0.55)	98 (0.48)	90 (0.44)

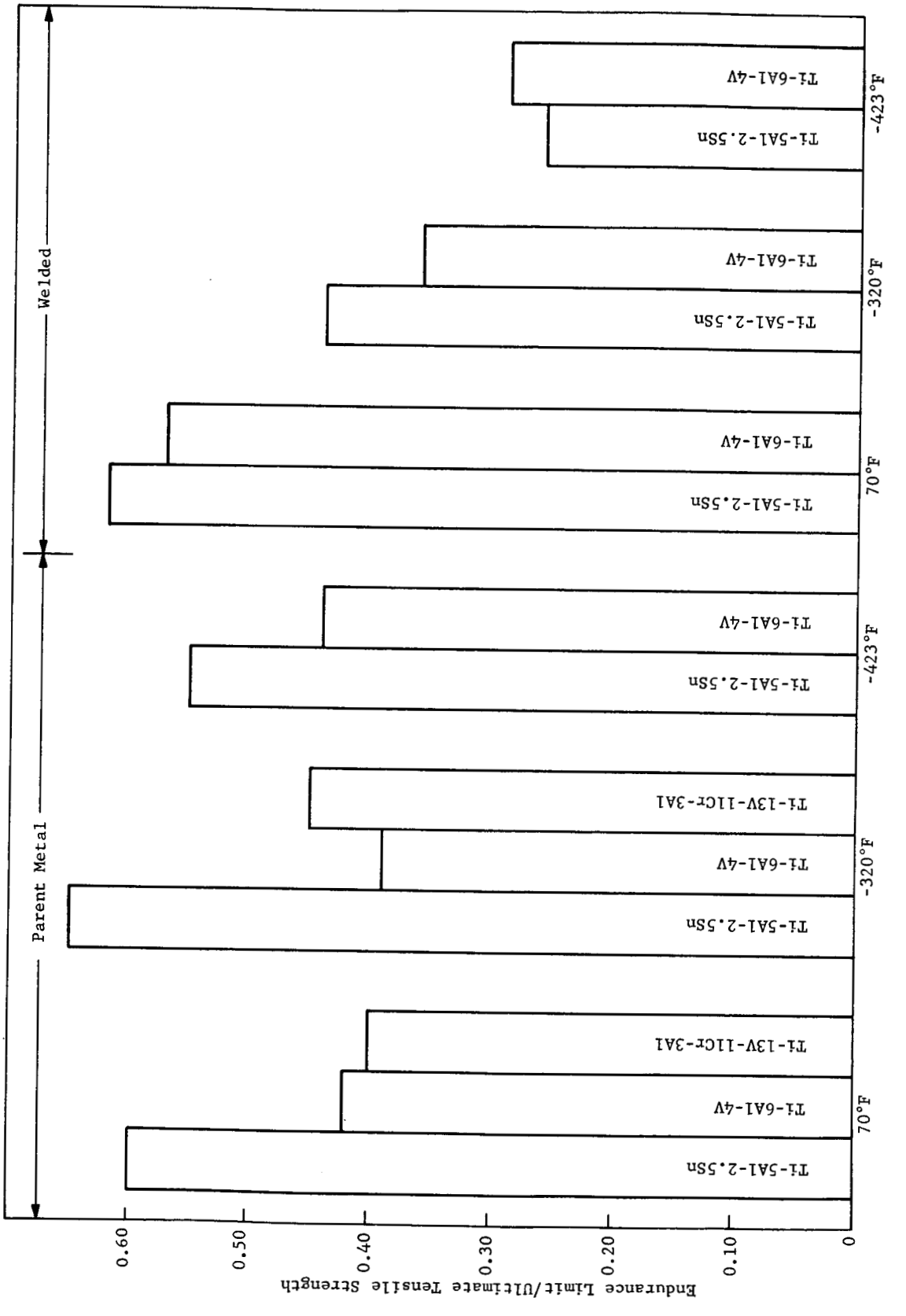

Fig. 43 Fatigue Strength/Tensile Strength Ratio for Three Titanium Alloys

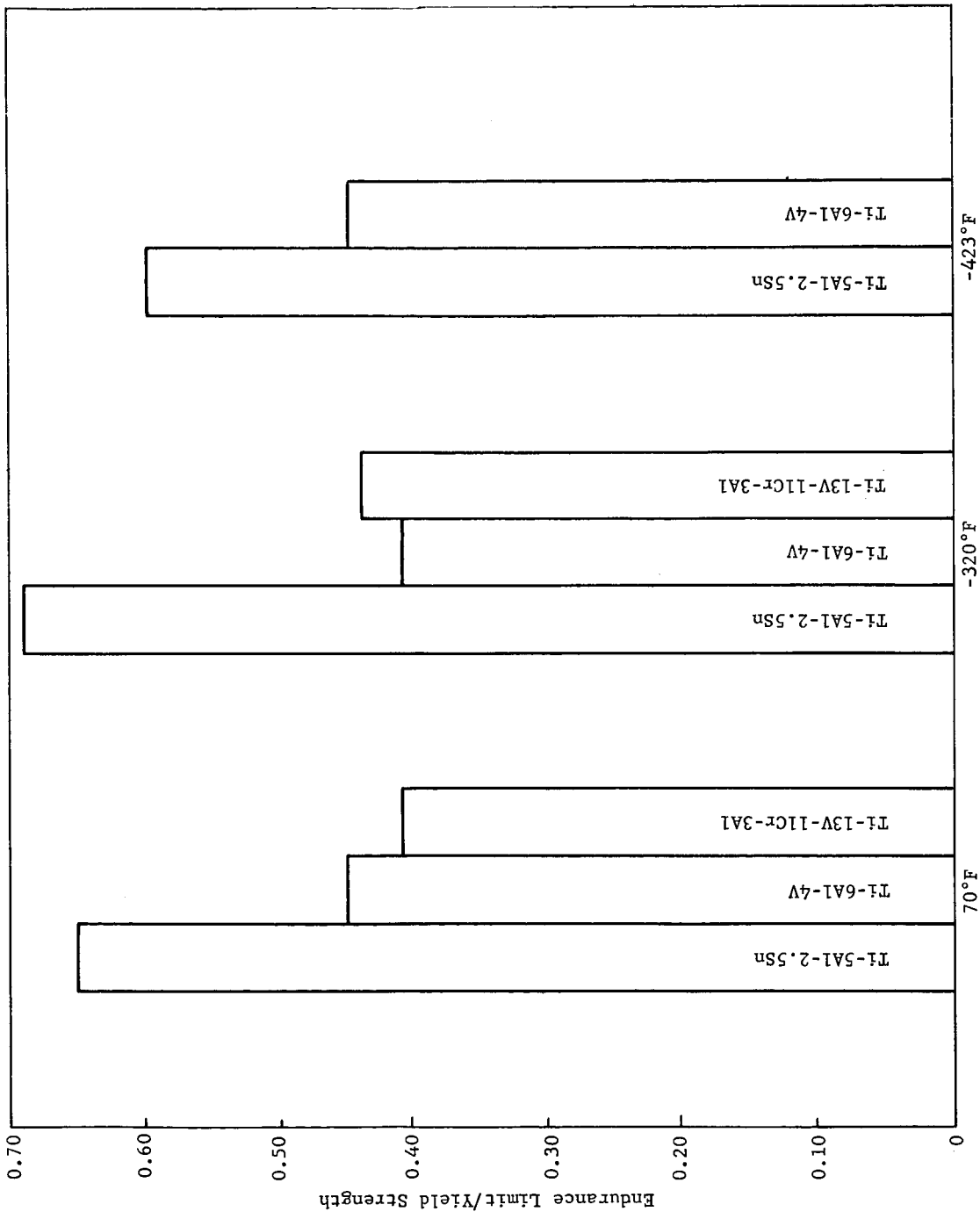

Fig. 44 Fatigue Strength/Yield Strength Ratio for Three Parent Metal Titanium Alloys

VIII. CONCLUSIONS

This program has demonstrated that tension/compression fatigue properties could be obtained under axial loading for flat sheet materials at temperatures down to -423°F. Furthermore, it has been demonstrated that tests at liquid hydrogen temperature could be performed for long periods with automatic fill control.

The data generated for aluminum alloys show that the three weldable grades 2014-T6, 2219-T87, and 5456-H343 behave satisfactorily under cyclic loads down to -423°F. The 5456 grade exhibits the highest properties of all of the aluminum alloys on a basis of fatigue strength/tensile strength ratio. The 2020-T6 and 7075-T6 alloys show poorer fatigue properties. The welded fatigue properties of the three weldable grades were similar.

The titanium alloys Ti-5Al-2.5Sn and Ti-6Al-4V show superior fatigue behavior at cryogenic temperatures compared to the beta alloy, Ti-13V-11Cr-3Al. On the basis of fatigue strength ratio, parent metal Ti-5Al-2.5Sn is clearly superior to the Ti-6Al-4V. Welded material also showed the superiority of Ti-5Al-2.5Sn on the basis of fatigue strength ratio.

The fatigue strength ratios of the titanium alloys exceeded those obtained for aluminum alloys.

REFERENCES

1. R. D. Keys: "A Multiple Tensile Specimen Test Device for Use in Liquid Hydrogen," in Advances in Cryogenic Engineering, Vol 7, Plenum Press, New York, 1962.

2. R. Markovich and F. R. Schwartzberg: Testing Techniques and Evaluation of Materials for Use at Liquid Hydrogen Temperature. R-61-4. The Martin Company, Denver, Colorado, February 1961. Also, ASTM STP 302, ASTM, Philadelphia, Pennsylvania, 1961.

3. J. L. Christian: Mechanical Properties of Aluminum Alloys at Cryogenic Temperatures. MRG-190. Convair-Astronautics, 2 December 1960.

4. F. R. Schwartzberg and R. D. Keys: Mechanical Properties of 2000 Series Aluminum Alloys at Cryogenic Temperatures. R-61-32. The Martin Company, Denver, Colorado, October 1961.

5. Martin Company unpublished data.

6. J. L. Christian and J. F. Watson: "Properties of 7000 Series Aluminum Alloys at Cryogenic Temperatures," in Advances in Cryogenic Engineering, Vol 6, Plenum Press, New York, 1961.

7. F. R. Schwartzberg and R. D. Keys: Mechanical Properties of an Alpha Titanium Alloy at Cryogenic Temperatures. Paper Presented at Annual ASTM Meeting, 23-29 June 1962.

8. G. B. Espey, M. H. Jones, and W. F. Brown, Jr: Some Factors Influencing the Fracture Toughness of Sheet Alloys for Use in Lightweight Cryogenic Tankage. ASTM STP 302, ASTM, Philadelphia, Pennsylvania, 1961.

9. J. L. Christian: Mechanical Properties of Titanium and Titanium Alloys at Cryogenic Temperatures. MRG-189, Convair-Astronautics, 14 October 1960.

10. G. B. Espey, M. H. Jones, and W. F. Brown, Jr: Sharp-Edge-Notch Tensile Characteristics of Several High-Strength Titanium Sheet Alloys at Room and Cryogenic Temperatures. ASTM STP 287, ASTM, Philadelphia, Pennsylvania, 1960.

APPENDIX A

CRYOSTAT DRAWINGS

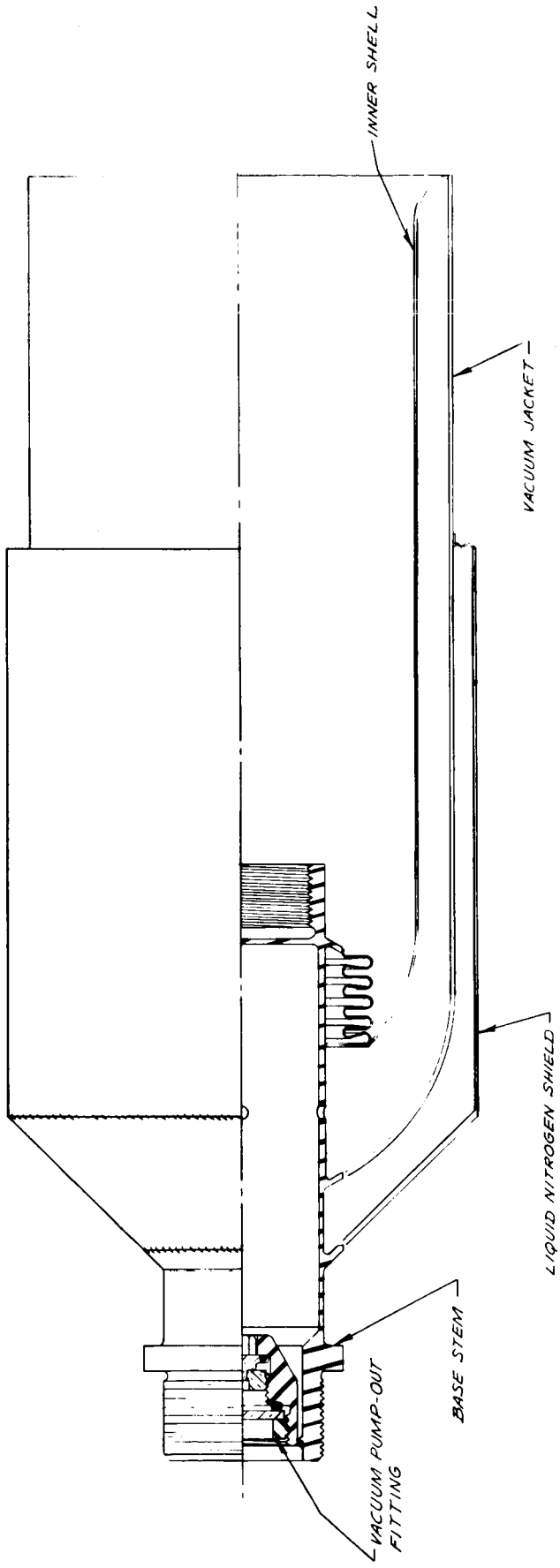

Fig. A-1 Fatigue Cryostat Assembly

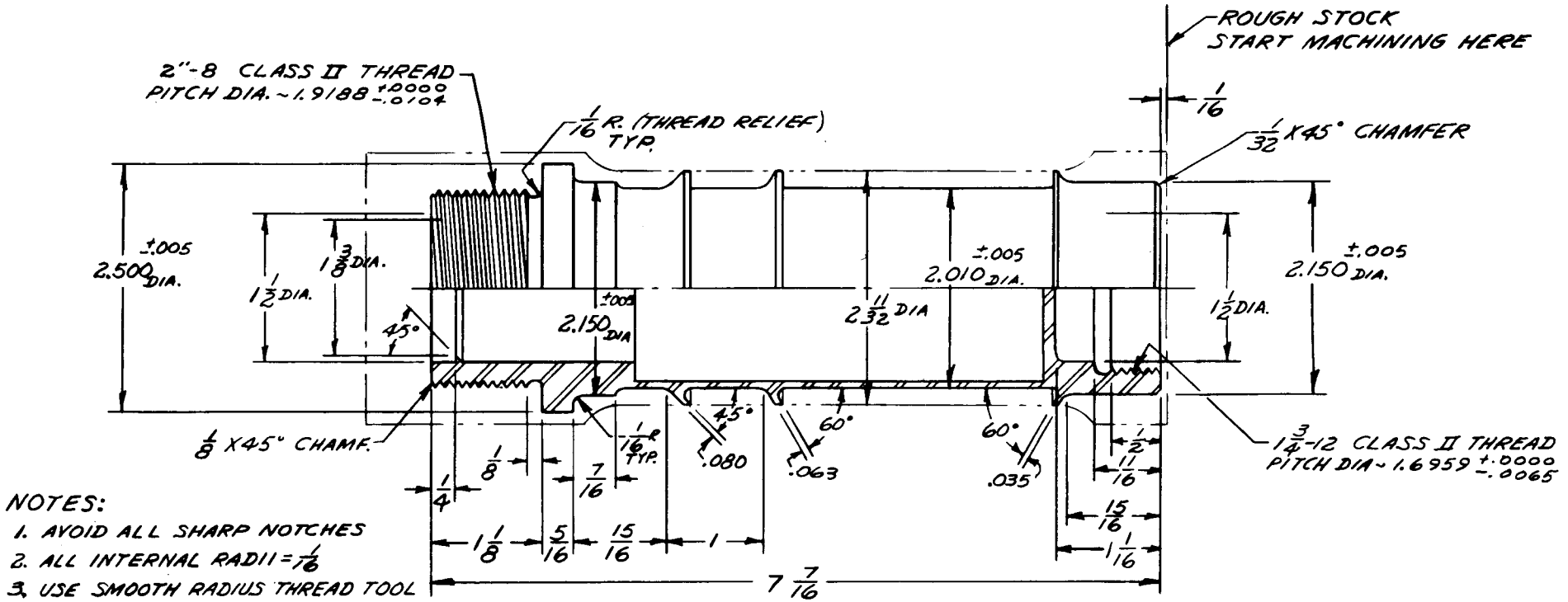

NOTES:

1. AVOID ALL SHARP NOTCHES
2. ALL INTERNAL RADII = 1/16
3. USE SMOOTH RADIUS THREAD TOOL
4. ROLL SHANK TO WORK HARDEN SURFACE. (PROTECT THREADS & END FACE)
5. PHANTOM OUTLINE INDICATES STOCK TO BE REMOVED.
6. THREAD DIAMETERS TO BE CONCENTRIC WITH ℄ WITHIN .002 T.I.R.

Fig. A-2 Cryostat Base Stem

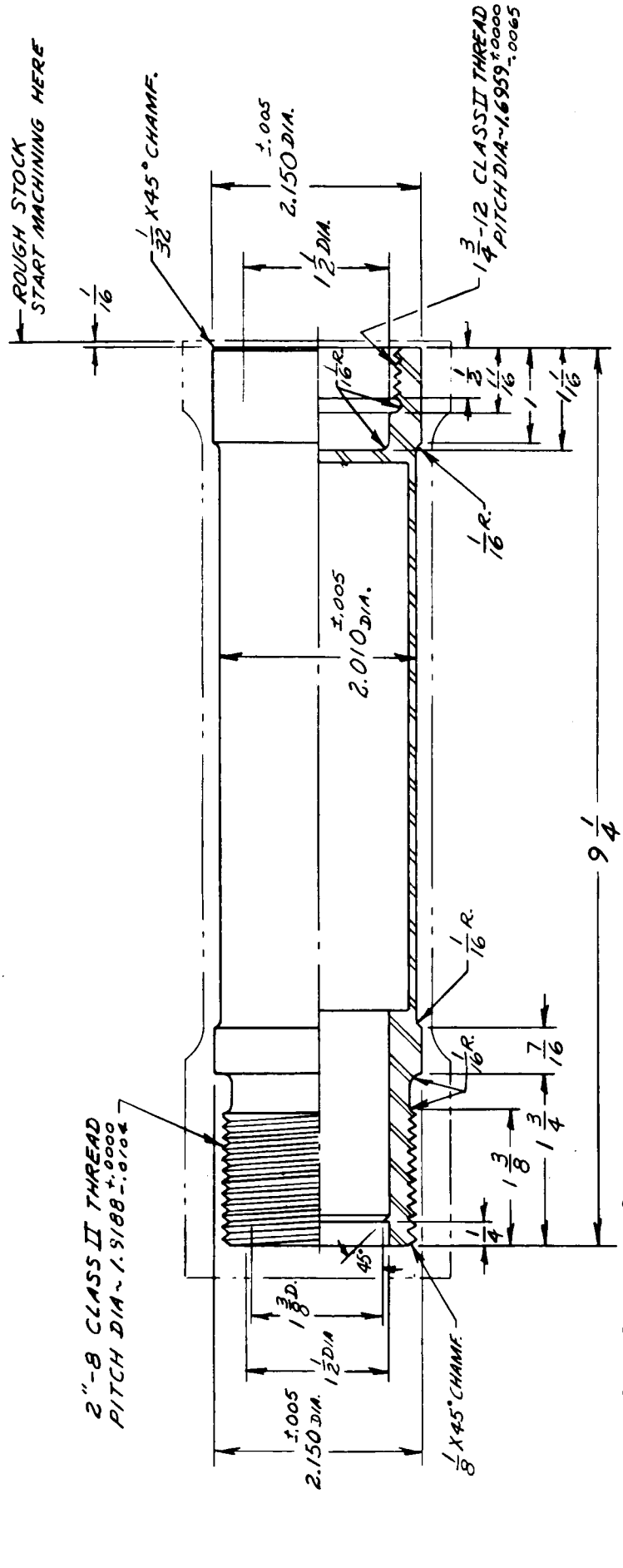

1. AVOID ALL SHARP NOTCHES
2. USE SMOOTH RADIUS THREAD TOOL
3. ROLL SHANK TO WORK HARDEN SURFACE. (PROTECT THREADS & END FACES)
4. PHANTOM OUTLINE INDICATES STOCK TO BE REMOVED.
5. THREAD DIAMETERS TO BE CONCENTRIC WITH Ø WITHIN .002 T.I.R.

Fig. A-3 Cryostat Top Stem

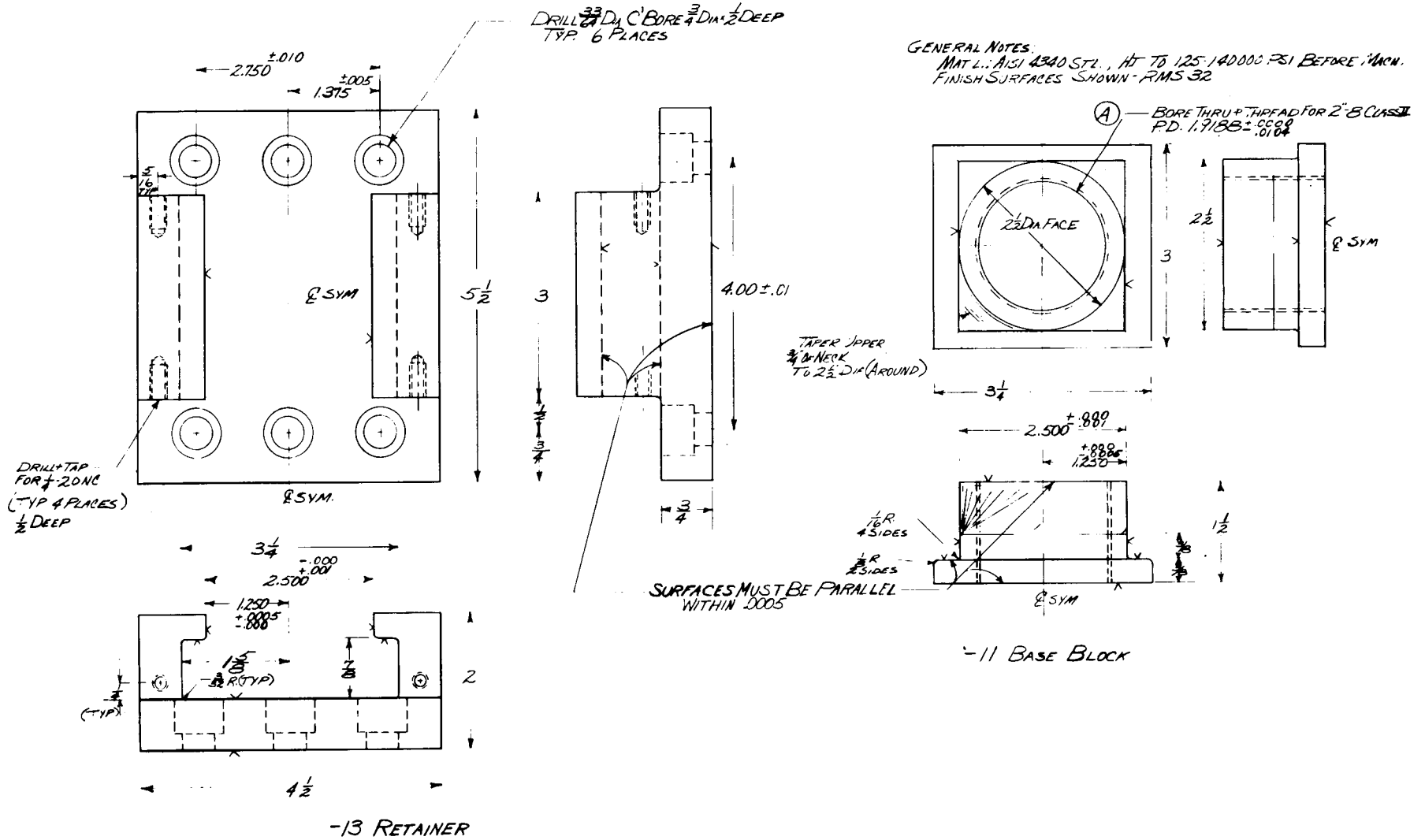

Fig. A-4 Lower Retainer Plate and Base Block

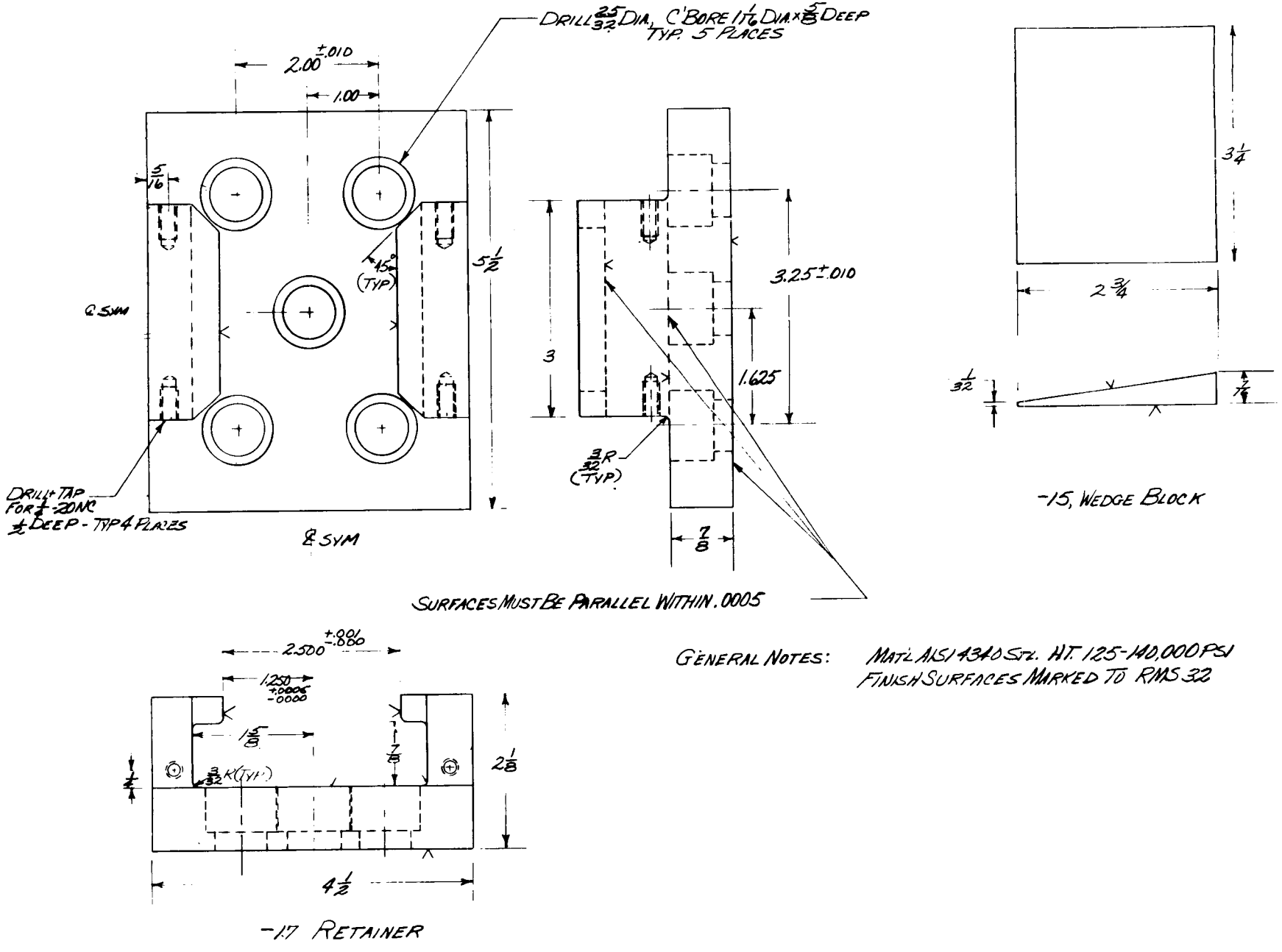

GENERAL NOTES: MAT'L AISI 4340 STL. HT. 125-140,000 PSI
FINISH SURFACES MARKED TO RMS 32

Fig. A-5 Upper Retainer Plate and Wedge Block

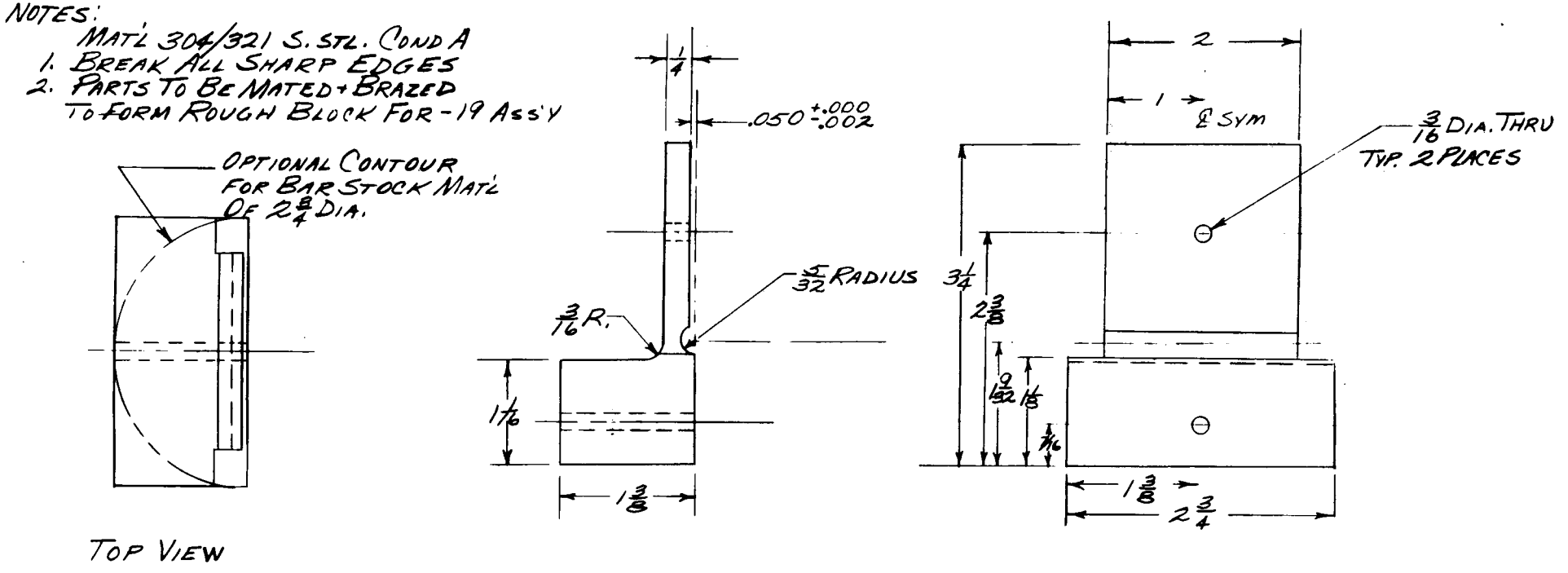

Fig. A-6 (a) Grip Block Half

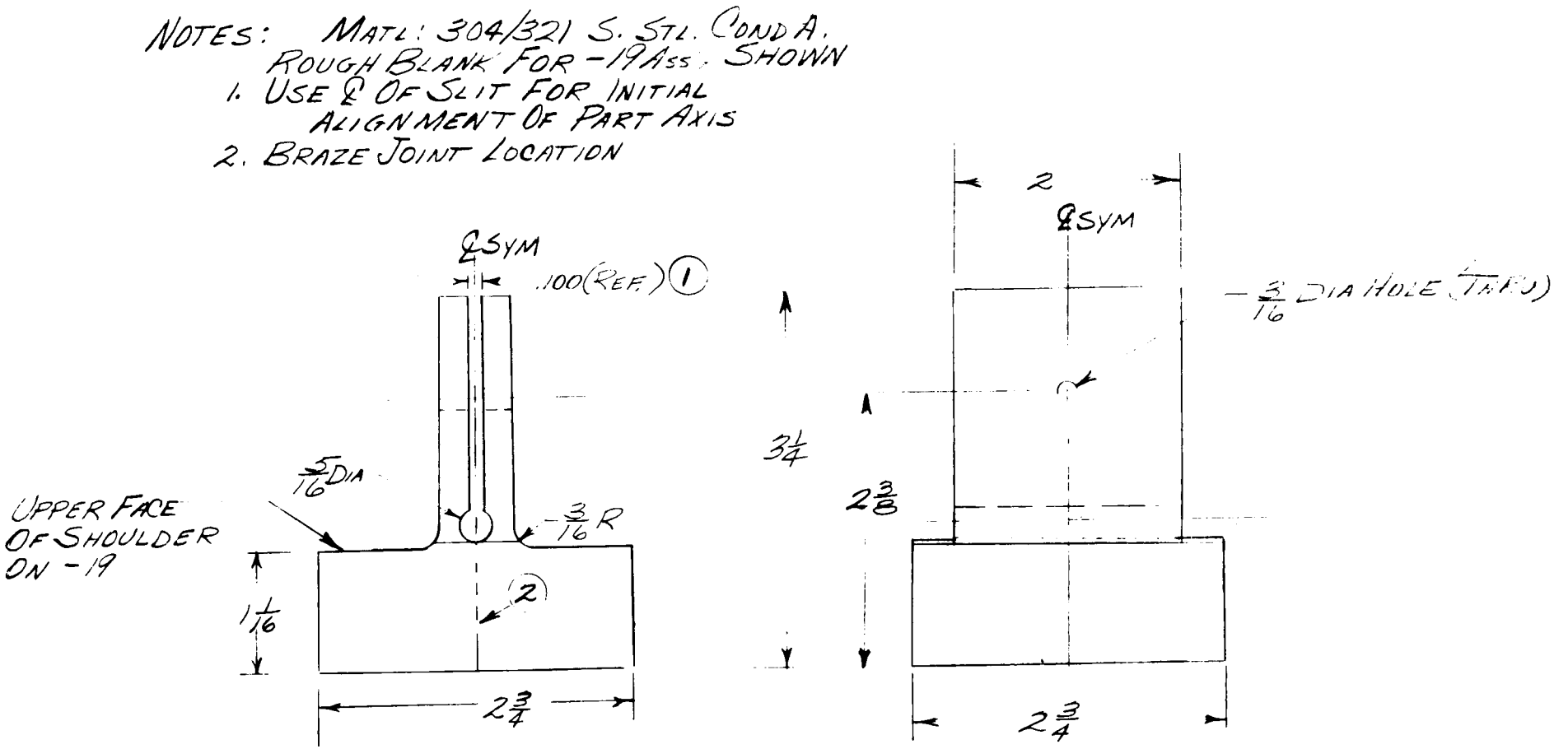

Fig. A-6 (b) Grip Block Assembly Rough Blank

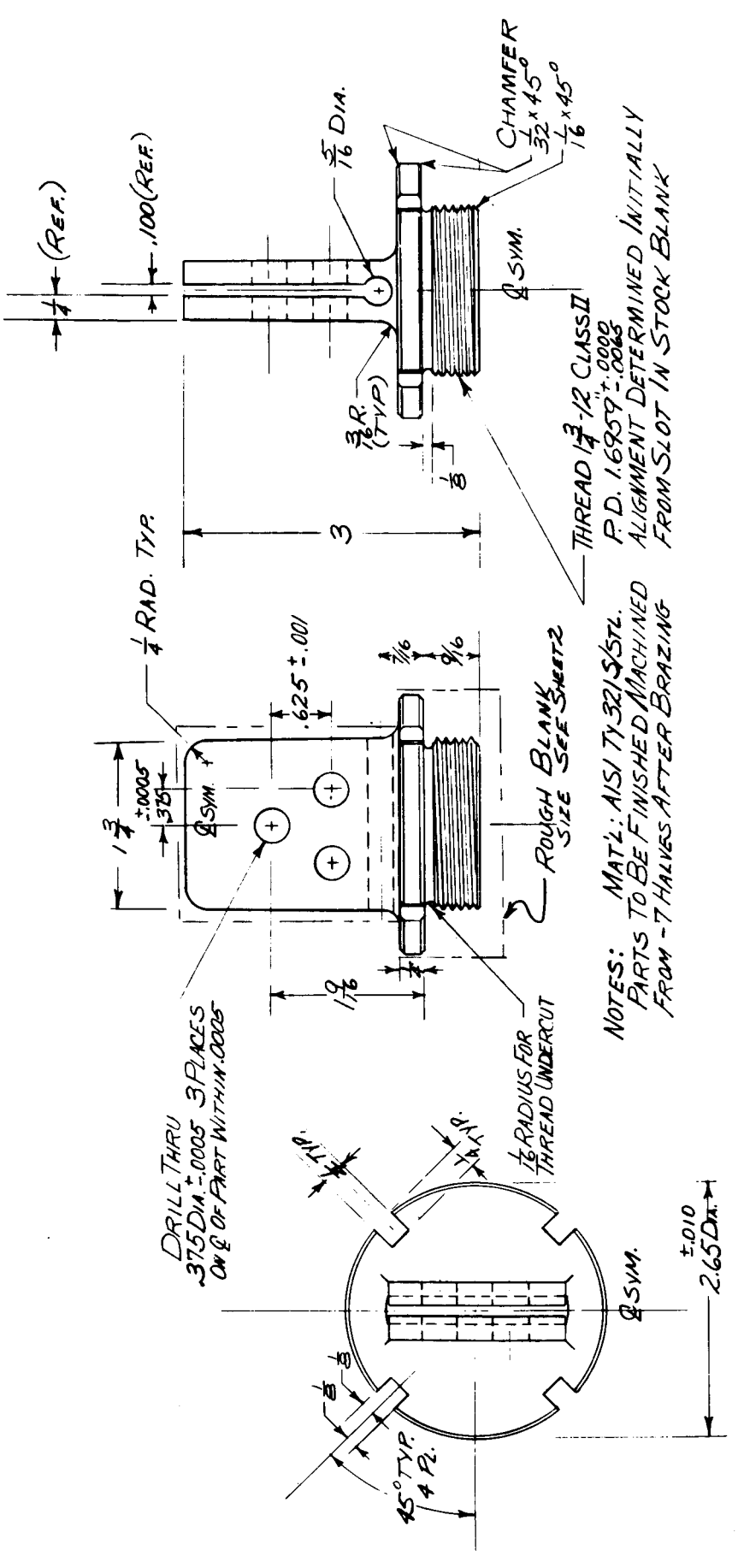

Fig. A-6 (c) Grip Block Assembly

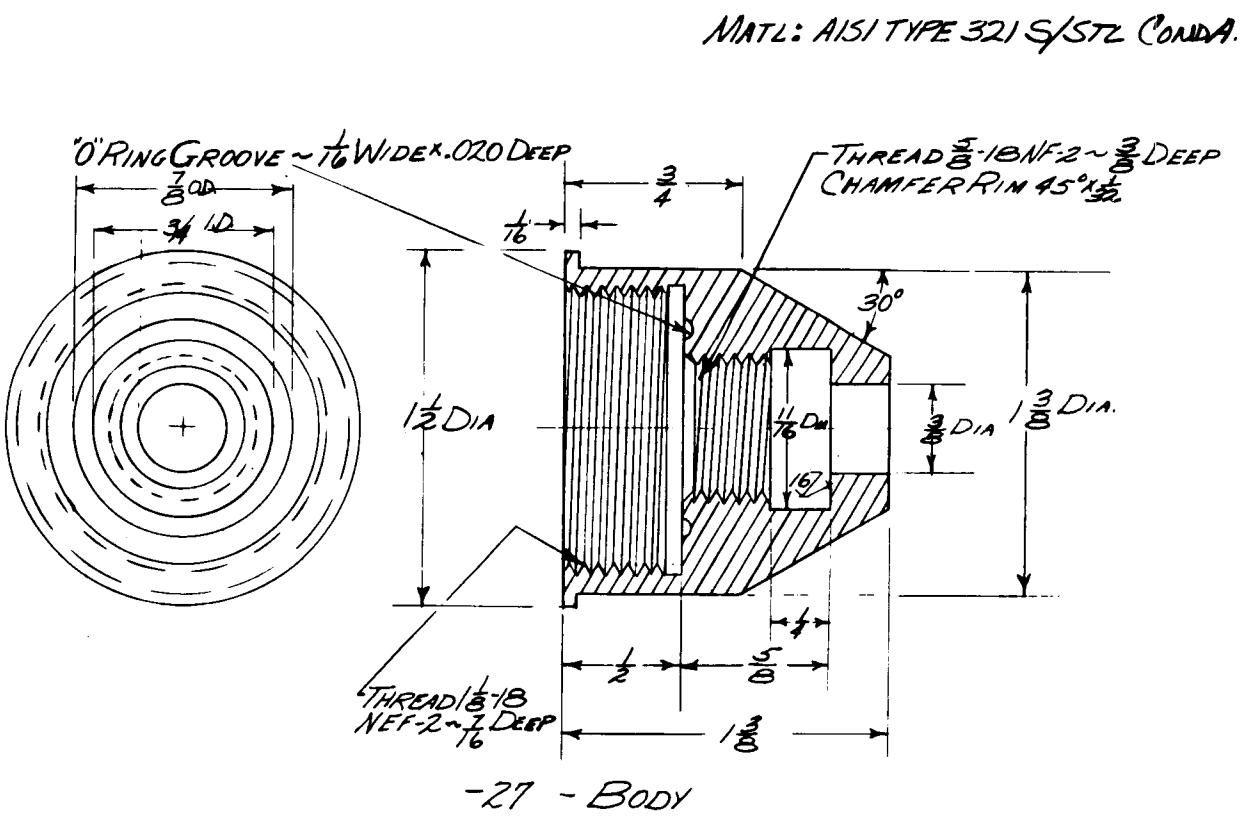

Fig. A-7 Vacuum Fitting-Cryostat Stem

APPENDIX B

TENSILE DATA

Table B-I Tensile Properties of 2014-T6 Aluminum Alloy at Cryogenic Temperatures

Temperature, °F	Ultimate Strength, ksi	Yield Strength (0.2% offset), ksi	Elongation in 2 in., %	Modulus of Elasticity, 10^6 psi	Weld Strength, ksi
70	71.8 70.4 70.9 71.0 Avg	67.3 66.3 65.9 66.5 Avg	10.5 10.0 9.5 10.0 Avg	10.6	55.1 55.3 59.0 56.5 Avg
-320	85.3 84.9 85.9 85.4 Avg	76.4 75.8 75.8 76.0 Avg	11.5 12.0 12.0 11.8 Avg	11.7	66.2 64.6 67.0 65.9 Avg
-423	100.0 99.0 96.3 98.4 Avg	83.0 82.8 80.7 82.2 Avg	14.0 13.5 13.5 13.7 Avg	12.3	74.3 72.2 69.5 68.5 71.2 70.5 71.1 Avg

Table B-II Tensile Properties of 2219-T87 Aluminum Alloy at Cryogenic Temperatures

Temperature °F	Ultimate Strength, ksi	Yield Strength (0.2% offset), ksi	Elongation in 2 in., %	Modulus of Elasticity, 10^6 psi	Weld Strength, ksi
70	66.6 66.9 66.5 66.7 Avg	55.2 55.7 55.2 55.4 Avg	11.0 11.0 10.5 10.8 Avg	10.5	45.2 50.4 50.6 48.7 Avg
-320	85.4 85.0 85.0 85.1 Avg	65.3 66.0 66.0 65.8 Avg	12.5 13.0 12.5 12.7 Avg	11.6	63.2 61.0 63.0 62.4 Avg
-423	100.4 101.0 96.1 99.2 Avg	71.0 70.6 68.5 70.0 Avg	15.0 15.0 13.5 14.5 Avg	12.5	72.2 65.9 70.0 65.5 68.7 64.2 67.7 Avg

Table B-III Tensile Properties of 5456-H343 Aluminum Alloy at Cryogenic Temperatures

Temperature, °F	Ultimate Strength, ksi	Yield Strength (0.2% offset), ksi	Elongation in 2 in., %	Modulus of Elasticity, 10^6 psi	Weld Strength, ksi
70	56.4 56.8 56.5 56.6 Avg	43.2 43.6 43.7 43.5 Avg	9.5 9.5 9.5 9.5 Avg	10.3	52.0 52.3 50.0 50.9 Avg
-320	72.8 70.8 73.4 72.3 Avg	50.7 50.7 50.5 50.6 Avg	9.5 7.0 11.0 9.2 Avg	11.4	58.5 61.9 57.8 59.4 Avg
-423	80.4 82.6 80.8 81.3 Avg	53.9 54.1 54.0 54.0 Avg	8.5 11.5 9.5 9.8 Avg	11.7	54.8 58.0 55.9 52.8 53.5 57.3 55.4 Avg

Table B-IV Tensile Properties of 2020-T6 Aluminum Alloy at Cryogenic Temperatures

Temperature, °F	Ultimate Strength, ksi	Yield Strength (0.2% offset), ksi	Elongation in 2 in., %	Modulus of Elasticity, 10^6 psi
70	82.7 82.3 82.7 82.6 Avg	78.9 77.7 79.1 78.6 Avg	8.0 8.0 8.0 8.0 Avg	11.1
-320	97.5 97.1 98.0 97.5 Avg	87.0 87.2 87.6 87.3 Avg	7.0 7.0 7.5 7.2 Avg	12.3
-423	110.3 110.0 128.0 116.1	94.8 94.6 100.9 96.8 Avg	10.0 10.0 12.5 10.8 Avg	13.6

Table B-V Tensile Properties of 7075-T6 Aluminum Alloy at Cryogenic Temperatures

Temperature, °F	Ultimate Strength, ksi	Yield Strength (0.2% offset), ksi	Elongation in 2 in., %	Modulus of Elasticity, 10^6 psi
70	78.6 79.2 78.5 78.8 Avg	71.4 72.5 70.8 71.6 Avg	10.5 10.5 10.5 10.5 Avg	10.2
-320	98.2 99.1 99.5 98.9 Avg	85.3 83.7 84.6 84.5 Avg	12.5 11.5 10.0 11.3 Avg	11.4
-423	100.2 95.5 105.9 100.8 Avg	88.4 82.1 87.8 86.1 Avg	11.5 2.5* 10.5 11.0 Avg of 2	11.9

*Failed through gage mark.

Table B-VI Tensile Properties of Annealed 5Al-2.5Sn Titanium Alloy at Cryogenic Temperatures

Temperature, °F	Ultimate Strength, ksi	Yield Strength (0.2% offset), ksi	Elongation in 2 in. %	Modulus of Elasticity, 10^6 psi	Weld Strength, ksi
70	114.5 116.3 115.9 115.8 Avg	106.7 106.9 108.9 107.8 Avg	16.5 16.0 16.5 16.3 Avg	15.8	113.1 111.7 112.8 112.5 Avg
-320	185.5 185.7 185.9 185.7 Avg	173.4 173.2 173.4 173.3 Avg	19.5 18.8 19.3 19.2 Avg	17.4	183.7 181.9 181.6 182.4 Avg
-423	226.9 237.4 236.7 233.6 Avg	* 211.3 * 211.3	2.0 2.0 1.5 1.8 Avg	---	245.2 216.9 220.1 227.4 Avg

*Strain gage failed.

Table B-VII Tensile Properties of Solution Treated and Aged 6Al-4V Titanium Alloy at Cryogenic Temperatures

Temperature, °F	Ultimate Strength, ksi	Yield Strength (0.2% offset), ksi	Elongation in 2 in., %	Modulus of Elasticity, 10^6 psi	Weld Strength, ksi
70	165.4 165.4 165.0 165.3 Avg	154.3 154.4 153.2 154.0 Avg	17.5 16.0 16.5 16.7 Avg	16.1	150.7 148.0 149.4 Avg
-320	242.7 242.7 243.7 243.0 Avg	____* 228.2 230.1 229.2 Avg	8.3 10.5 9.8 9.5 Avg	17.5	236.0 235.2 231.8 234.3 Avg
-423	297.7 295.7 296.5 296.6 Avg	282.1 ____* 284.9 283.5 Avg	2.5 2.5 2.5 2.5 Avg	----	277.5 280.4 268.3 275.4 Avg

*Strain gage failed.

Table B-VIII Tensile Properties of Solution Treated and Aged 13V-11Cr-3Al Titanium Alloy at Cryogenic Temperatures

Temperature, °F	Ultimate Strength, ksi	Yield Strength (0.2% offset), ksi	Elongation in 2 in., %	Modulus of Elasticity, 10^6 psi	Weld Strength, ksi
70	206.0 197.2 195.2 199.5 Avg	184.3 181.3 182.8 Avg of 2	5.5 7.0 7.0 6.5 Avg	16.1	143.8 143.5 145.9 144.4 Avg
-320	218.0 185.0 201.0 201.3 Avg	—	—* —* —**	16.8	125.6 95.7 129.8 127.7 Avg of 2
-423	—	—	—	—	81.3 88.3 49.5 84.8 Avg of 2

*Failed through pinhole.
**Failed outside gage mark.

APPENDIX C

FATIGUE DATA

Table C-I Fatigue Properties[a] of Parent Metal 2014-T6 Aluminum Alloy

Temperature, °F	Maximum Tension Stress, ksi	Number of Cycles to Failure
70	50.0	3.00×10^3
	50.0	4.00×10^3
	50.0	5.00×10^3
	40.0	2.00×10^4
	40.0	2.50×10^4
	40.0	3.30×10^4
	30.0	1.30×10^5
	30.0	1.57×10^5
	30.0	3.95×10^5
	25.0	1.26×10^5
	25.0	1.76×10^5
	25.0	5.63×10^5
	20.0	1.20×10^7 (Disc)
	20.0	1.19×10^7 (Disc)
	17.5	6.62×10^5
	17.5	1.03×10^6
	15.0	5.41×10^5
	15.0	1.28×10^6
	15.0	7.00×10^6 (Disc)
	15.0	8.59×10^6 (Disc)
-320	65.0	1.80×10^3
	65.0	2.00×10^3
	65.0	2.60×10^3
	50.0	3.33×10^4
	50.0	4.17×10^4
	50.0	6.96×10^4
	40.0	8.89×10^4
	40.0	9.50×10^4
	40.0	1.10×10^5
	30.0	2.06×10^5

Table C-I (concl)

Temperature, °F	Maximum Tension Stress, ksi	Number of Cycles to Failure
-320	30.0	2.58×10^5
	30.0	2.73×10^5
	25.0	1.07×10^6
	25.0	2.54×10^6
	25.0	5.02×10^6 (Disc)
-423	65.0	1.00×10^3
	65.0	1.00×10^3
	65.0	8.00×10^3 [b]
	62.5	1.50×10^4
	62.5	2.60×10^4
	62.5	3.50×10^4
	50.0	2.76×10^5
	50.0	3.70×10^5
	50.0	4.17×10^5
	45.0	1.22×10^6
	45.0	1.12×10^6 (Disc)
	45.0	1.00×10^6 (Disc)

[a] Axial load; R = -1.

[b] Specimen previously run at 45,000 psi for 1.12×10^6 cycles without failure.

Table C-II Fatigue Properties[a] of Parent Metal 2219-T87 Aluminum Alloy

Temperature, °F	Maximum Tension Stress, ksi	Number of Cycles to Failure
70	50.0	9.00×10^2
	46.0	3.00×10^3
	46.0	3.00×10^3
	46.0	4.00×10^3
	40.0	9.90×10^3
	40.0	1.49×10^4
	40.0	2.27×10^4
	35.0	2.43×10^4
	35.0	2.82×10^4
	35.0	3.19×10^4
	30.0	4.86×10^4
	30.0	1.40×10^5
	30.0	1.66×10^5
	25.0	1.80×10^5
	25.0	3.08×10^5
	25.0	6.76×10^5
	22.5	3.56×10^5
	22.5	9.52×10^5
	22.5	3.40×10^6
	20.0	4.45×10^6
	20.0	1.24×10^7 (Disc)
-320	55.0	6.00×10^2
	55.0	1.70×10^3
	55.0	1.90×10^3
	35.0	4.51×10^4
	35.0	6.46×10^4
	35.0	8.02×10^4
	35.0	1.16×10^5
	30.0	1.01×10^5
	25.0	1.05×10^6[b]

Table C-II (concl)

Temperature, °F	Maximum Tension Stress, ksi	Number of Cycles to Failure
-320	25.0	2.05×10^6 [b]
	20.0	5.21×10^6 (Disc)
	15.0	1.05×10^6
	15.0	2.21×10^6
	15.0	2.31×10^6
-423	62.5	1.50×10^3
	62.5	3.00×10^3
	62.5	4.00×10^3 [c]
	62.5	7.00×10^3
	62.5	7.50×10^3
	55.0	4.40×10^4
	55.0	6.60×10^4
	55.0	8.90×10^4
	50.0	1.24×10^5
	47.5	1.73×10^5
	47.5	1.74×10^5
	47.5	3.05×10^5
	40.0	7.95×10^5
	40.0	1.40×10^6 (Disc)
	40.0	1.46×10^6 (Disc)

[a] Axial load; R = -1.

[b] Failed through pinholes.

[c] Specimen previously run at 40,000 psi for 1.46×10^6 cycles without failure.

Table C-III Fatigue Properties[a] of Parent Metal 5456-H343 Aluminum Alloy

Temperature, °F	Maximum Tension Stress, ksi	Number of Cycles to Failure
70	40.0	1.50×10^3
	38.5	4.00×10^3
	38.5	5.00×10^3
	38.5	5.00×10^3
	35.0	8.00×10^3
	35.0	1.10×10^4
	35.0	1.40×10^4
	30.0	2.83×10^4
	30.0	4.30×10^4
	30.0	5.25×10^4
	25.0	5.25×10^4
	20.0	1.70×10^5
	20.0	4.59×10^5
	20.0	5.33×10^5
	15.0	1.00×10^6
	15.0	1.69×10^6
	15.0	4.96×10^6 (Disc)
-320	52.0	1.50×10^3
	52.0	4.50×10^3
	52.0	4.60×10^3
	50.0	9.10×10^3
	50.0	1.64×10^4
	50.0	1.65×10^4
	40.0	3.42×10^4
	40.0	4.37×10^4
	40.0	6.21×10^4
	30.0	6.87×10^4
	30.0	1.32×10^5
	30.0	2.38×10^5
	25.0	7.94×10^5

Table C-III (concl)

Temperature, °F	Maximum Tension Stress, ksi	Number of Cycles to Failure
-320	25.0	1.10×10^6
	25.0	4.43×10^6 (Disc)
-423	55.0	7.00×10^3
	55.0	8.00×10^3
	55.0	1.00×10^4
	50.0	1.60×10^4
	50.0	3.20×10^4
	50.0	3.30×10^4
	45.0	8.90×10^4
	42.5	3.05×10^5
	42.5	3.20×10^5
	42.5	5.19×10^5
	40.0	8.86×10^5 (Disc)
	40.0	9.07×10^5
	40.0	1.52×10^6 (Disc)

[a]Axial load; R = -1.

Table C-IV Fatigue Properties[a] of Parent Metal 2020-T6 Aluminum Alloy

Temperature, °F	Maximum Tension Stress, ksi	Number of Cycles to Failure
70	50.0	2.00×10^3
	50.0	2.00×10^3
	50.0	4.00×10^3
	40.0	3.00×10^3
	40.0	9.00×10^3
	40.0	1.00×10^4
	30.0	4.80×10^4
	30.0	8.50×10^4
	30.0	9.30×10^4
	20.0	1.25×10^5
	20.0	1.49×10^5
	20.0	1.60×10^5
	18.0	1.76×10^6
	18.0	3.90×10^6
	18.0	1.03×10^7 (Disc)
-320	70.0	1.00×10^3
	70.0	1.20×10^3
	70.0	2.30×10^3
	50.0	2.90×10^4
	50.0	4.31×10^4
	50.0	9.23×10^4
	40.0	7.42×10^4
	40.0	7.70×10^4
	40.0	1.22×10^5
	40.0	1.97×10^5
	30.0	1.16×10^5
	30.0	1.49×10^5
	30.0	3.27×10^5
	30.0	1.22×10^6
	22.5	1.37×10^6

Table C-IV (concl)

Temperature, °F	Maximum Tension Stress, ksi	Number of Cycles to Failure
-320	22.5	2.13×10^6
	22.5	4.16×10^6
-423	70.0	3.00×10^3 [b]
	67.5	4.00×10^3
	67.5	1.50×10^4
	60.0	1.70×10^4
	60.0	2.10×10^4 [c]
	60.0	2.90×10^4
	60.0	4.30×10^4
	57.3	8.60×10^4
	50.0	1.16×10^5
	50.0	1.53×10^5
	50.0	1.99×10^5
	42.5	7.75×10^5
	40.0	1.09×10^6
	40.0	1.41×10^6 (Disc)
	40.0	1.50×10^6 (Disc)

[a] Axial load; R = -1.

[b] Specimen previously run at 40,000 psi for 1.50×10^6 cycles without failure.

[c] Specimen previously run at 40,000 psi for 1.41×10^6 cycles without failure.

Table C-V Fatigue Properties[a] of Parent Metal 7075-T6 Aluminum Alloy

Temperature, °F	Maximum Tension Stress, ksi	Number of Cycles to Failure
70	63.0	1.50×10^3
	63.0	1.80×10^3
	63.0	2.00×10^3
	40.0	1.40×10^4
	40.0	1.80×10^4
	40.0	1.90×10^4
	30.0	2.80×10^4
	30.0	3.20×10^4
	30.0	4.10×10^4
	17.5	3.06×10^5
	17.5	3.44×10^5
	17.5	4.20×10^5
	12.5	2.07×10^6
	12.5	2.57×10^6
	12.5	1.03×10^7 (Disc)
-320	60.0	2.20×10^3
	60.0	5.50×10^3
	60.0	6.70×10^3
	40.0	7.12×10^4
	40.0	7.98×10^4
	40.0	9.32×10^4
	30.0	1.32×10^5
	30.0	2.67×10^5
	30.0	6.58×10^5
	20.0	1.34×10^6
	20.0	3.44×10^6
	20.0	4.30×10^6
	17.5	5.12×10^6 (Disc)
	17.5	5.35×10^6 (Disc)

Table C-V (concl)

Temperature, °F	Maximum Tension Stress, ksi	Number of Cycles to Failure
-423	80.0	1.00×10^3
	80.0	1.00×10^3
	80.0	1.00×10^3 [b]
	80.0	2.00×10^3
	65.0	4.20×10^4
	60.0	4.20×10^4
	60.0	7.10×10^4
	60.0	8.80×10^4
	50.0	1.42×10^6
	50.0	4.35×10^5
	50.0	4.35×10^5
	42.5	4.63×10^5
	37.5	4.05×10^6
	35.0	1.08×10^6
	35.0	1.11×10^6 (Disc)
	35.0	1.20×10^6 (Disc)

[a] Axial load; R = -1.

[b] Specimen previously run at 35,000 psi for 1.11×10^6 cycles without failure.

Table C-VI Fatigue Properties[a] of Welded 2014-T6 Aluminum Alloy

Temperature, °F	Maximum Tension Stress, ksi	Number of Cycles to Failure
70	30.0	2.00×10^3
	30.0	7.00×10^3
	30.0	1.00×10^4
	22.0	1.50×10^4
	22.0	2.10×10^4
	22.0	6.90×10^4
	15.0	1.70×10^5
	15.0	3.29×10^5
	15.0	5.14×10^5
	9.0	1.02×10^6 (Disc)
	9.0	1.03×10^6 (Disc)
	9.0	1.03×10^6 (Disc)
-320	35.0	1.00×10^2
	32.0	2.00×10^3
	30.0	1.05×10^4
	30.0	2.74×10^4
	30.0	2.75×10^4
	20.0	2.51×10^5
	20.0	3.42×10^5
	20.0	5.51×10^5
	10.0	1.59×10^6 (Disc)
	10.0	3.30×10^6 (Disc)
	10.0	5.29×10^6 (Disc)
-423	50.0	5.00×10^2
	40.0	2.00×10^3
	40.0	3.00×10^3
	40.0	6.00×10^3
	40.0	6.00×10^3[b]
	35.0	1.80×10^4

Table C-VI (concl)

Temperature, °F	Maximum Tension Stress, ksi	Number of Cycles to Failure
-423	35.0	6.80×10^4
	35.0	8.40×10^4
	30.0	1.82×10^5
	30.0	2.65×10^5
	30.0	3.18×10^5
	25.0	3.44×10^5
	17.5	1.01×10^6 (Disc)
	17.5	1.03×10^6
	17.5	1.06×10^6

[a]Axial load; R = -1.

[b]Specimen previously run at 17,500 psi for 1.01×10^6 cycles without failure.

Table C-VII Fatigue Properties[a] of Welded 2219-T87 Aluminum Alloy

Temperature, °F	Maximum Tension Stress, ksi	Number of Cycles to Failure
70	30.0	1.00×10^3
	30.0	6.00×10^3
	30.0	9.00×10^3
	20.0	2.40×10^4
	20.0	3.30×10^4
	20.0	5.30×10^4
	15.0	7.90×10^4
	15.0	1.94×10^5
	15.0	2.09×10^5
	10.0	2.04×10^6
	10.0	1.22×10^6
	10.0	1.04×10^7 (Disc)
-320	32.0	3.10×10^3
	32.0	5.50×10^3
	32.0	5.70×10^3
	25.0	4.10×10^4
	25.0	4.74×10^4
	25.0	5.14×10^4
	17.5	1.89×10^5
	17.5	3.19×10^5
	17.5	5.91×10^5
	12.5	9.93×10^5
	12.5	3.27×10^6
	12.5	4.57×10^6
-423	45.0	1.00×10^3
	45.0	1.00×10^3
	45.0	2.00×10^3
	45.0	2.00×10^3[b]
	45.0	5.00×10^3[c]

Table C-VII (concl)

Temperature, °F	Maximum Tension Stress, ksi	Number of Cycles to Failure
-423	42.5	1.70×10^4
	40.0	3.50×10^4
	35.0	5.50×10^4
	35.0	7.40×10^4
	35.0	1.17×10^5
	30.0	2.13×10^5
	30.0	2.36×10^5
	30.0	4.22×10^5
	22.5	7.78×10^5
	22.5	1.04×10^6 (Disc)
	22.5	1.13×10^6 (Disc)

[a]Axial load; R = 1.

[b]Specimen previously run at 22,500 psi for 1.04×10^6 cycles without failure.

[c]Specimen previously run at 22,500 psi for 1.13×10^6 cycles without failure.

Table C-VIII Fatigue Properties[a] of Welded 5456-H343 Aluminum Alloy

Temperature, °F	Maximum Tension Stress, ksi	Number of Cycles to Failure
70	30.0	2.00×10^3
	30.0	2.00×10^3
	30.0	3.00×10^3
	20.0	1.60×10^4
	20.0	2.20×10^4
	20.0	4.50×10^4
	13.8	2.45×10^5
	13.8	3.33×10^5
	13.8	3.90×10^5
	10.0	5.35×10^5
	10.0	2.44×10^6
	10.0	3.71×10^6
-320	32.0	2.60×10^3
	32.0	4.80×10^3
	32.0	8.40×10^3
	25.0	1.44×10^4
	25.0	2.54×10^4
	25.0	4.94×10^4
	17.0	2.04×10^5
	17.0	2.62×10^5
	17.0	4.21×10^5
	12.0	1.41×10^6
	12.0	2.58×10^6
	12.0	5.23×10^6 (Disc)
-423	40.0	1.20×10^4
	35.0	3.00×10^3
	35.0	6.00×10^3
	35.0	2.70×10^4
	30.0	2.40×10^4

Table C-VIII (concl)

Temperature, °F	Maximum Tension Stress, ksi	Number of Cycles to Failure
-423	30.0	8.70×10^4
	30.0	9.90×10^4
	25.0	3.30×10^5
	25.0	4.12×10^5
	17.5	1.00×10^6 (Disc)
	17.5	1.07×10^6 (Disc)
	17.5	1.19×10^6

[a]Axial load; R = -1.

Table C-IX Fatigue Properties[a] of Annealed Parent Metal 5Al-2.5Sn Titanium Alloy

Temperature, °F	Maximum Tension Stress, ksi	Number of Cycles to Failure
70	125.0	6.00×10^2
	125.0	1.00×10^3
	115.0	6.00×10^3
	115.0	8.00×10^3
	115.0	1.30×10^4
	100.0	2.00×10^4
	100.0	5.30×10^4
	100.0	8.10×10^4
	75.0	1.88×10^5
	75.0	2.04×10^5
	75.0	2.71×10^5
	70.0	1.36×10^6 (Disc)
	70.0	2.00×10^6 (Disc)
	70.0	2.00×10^6 (Disc)
-320	180.0	1.00×10^3
	180.0	3.10×10^3
	180.0	4.80×10^3
	175.0	3.00×10^3
	160.0	6.90×10^3
	160.0	4.53×10^4
	150.0	1.35×10^4
	150.0	2.55×10^4
	150.0	3.31×10^4
	120.0	6.46×10^4
	120.0	7.40×10^4
	120.0	1.34×10^5
	119.5	6.75×10^4
	119.0	2.05×10^6

Table C-IX (concl)

Temperature, °F	Maximum Tension Stress, ksi	Number of Cycles to Failure
-423	220.0	1.00×10^3 [b]
	220.0	1.00×10^3 [c]
	220.0	1.00×10^3 [d]
	220.0	3.00×10^3
	220.0	3.00×10^3
	220.0	1.30×10^4
	180.0	3.00×10^4
	170.0	4.00×10^4
	160.0	2.20×10^4
	140.0	9.00×10^4
	130.0	1.15×10^5
	130.0	1.61×10^5
	130.0	2.85×10^5
	125.0	1.05×10^6 (Disc)
	115.0	1.08×10^5
	105.0	3.79×10^5
	105.0	1.11×10^6 (Disc)
	105.0	1.12×10^6 (Disc)
	105.0	1.13×10^6 (Disc)

[a] Axial load; R = 0.01.

[b] Specimen previously run at 105,000 psi for 1.11×10^6 cycles without failure.

[c] Specimen previously run at 105,000 psi for 1.12×10^6 cycles without failure.

[d] Specimen previously run at 105,000 psi for 1.13×10^6 cycles without failure.

Table C-X Fatigue Properties[a] of Solution-Treated and Aged Parent Metal 6Al-4V Titanium Alloy

Temperature, °F	Maximum Tension Stress, ksi	Number of Cycles to Failure
70	150.0	7.50×10^3
	150.0	9.50×10^3
	150.0	1.40×10^4
	135.0	1.70×10^4
	135.0	1.90×10^4
	135.0	2.00×10^4
	85.0	1.00×10^5
	85.0	1.32×10^5
	85.0	3.24×10^5
	70.0	2.59×10^5
	70.0	1.97×10^6 (Disc)
	70.0	2.04×10^6 (Disc)
-320	182.0	2.50×10^3
	182.0	4.80×10^3
	182.0	1.02×10^4
	160.0	1.22×10^4
	160.0	1.86×10^4
	160.0	2.44×10^4
	118.0	2.79×10^4
	100.0	5.19×10^4
	100.0	8.01×10^4
	100.0	8.31×10^5
	98.0	7.32×10^4
	96.0	6.29×10^4
	90.0	1.60×10^5
	90.0	3.60×10^5 (Disc)

Table C-X (concl)

Temperature, °F	Maximum Tension Stress, ksi	Number of Cycles to Failure
-423	180.0	1.00×10^3
	180.0	8.00×10^3 [b]
	180.0	1.30×10^4 [c]
	180.0	1.90×10^4 [d]
	170.0	2.30×10^4 [e]
	160.0	1.60×10^4
	160.0	2.20×10^4
	160.0	3.10×10^4
	145.0	3.40×10^4
	140.0	3.90×10^4
	135.0	3.30×10^4
	135.0	3.40×10^4
	130.0	2.70×10^4
	130.0	2.34×10^5
	130.0	1.02×10^6 (Disc)
	125.0	1.21×10^6 (Disc)
	110.0	5.50×10^4
	110.0	1.12×10^6 (Disc)
	110.0	1.13×10^6 (Disc)

[a] Axial load; R = 0.01.

[b] Specimen previously run at 110,000 psi for 1.12×10^6 cycles without failure.

[c] Specimen previously run at 110,000 psi for 1.13×10^6 cycles without failure.

[d] Specimen previously run at 130,000 psi for 1.02×10^6 cycles without failure.

[e] Specimen previously run at 125,000 psi for 1.21×10^6 cycles without failure.

Table C-XI Fatigue Properties[a] of Solution-Treated and Aged Parent Metal 13V-11Cr-3Al Titanium Alloy

Temperature, °F	Maximum Tension Stress ksi	Number of Cycles to Failure
70	175.0	4.50×10^3
	175.0	7.00×10^3
	175.0	7.80×10^3
	120.0	1.70×10^4
	120.0	2.10×10^4
	120.0	2.50×10^4
	79.3	1.04×10^5
	79.3	1.19×10^5
	79.3	4.95×10^6 (Disc)
	79.0	5.14×10^6 (Disc)
	77.5	1.00×10^6 (Disc)
-320	175.0	2.00×10^3
	160.0	7.00×10^3
	140.0	9.00×10^3
	137.5	1.30×10^4
	135.0	2.10×10^4
	130.0	1.10×10^4
	125.0	8.17×10^5
	122.0	5.98×10^5
	120.0	1.40×10^4
	120.0	3.94×10^5
	115.0	6.00×10^4
	115.0	9.80×10^4
	105.0	4.14×10^5
	97.5	4.08×10^5
-423	160.0	1.00×10^3[b]
	160.0	2.00×10^3
	160.0	6.00×10^3

Table C-XI (concl)

Temperature, °F	Maximum Tension Stress, ksi	Number of Cycles to Failure
-423	145.0	2.00×10^3
	125.0	5.00×10^3
	125.0	1.00×10^4
	125.0	1.10×10^4
	110.0	1.39×10^5
	105.0	4.42×10^5
	105.0	1.05×10^6 (Disc)
	100.0	8.71×10^5
	100.0	1.10×10^6 (Disc)

[a] Axial load; R = 0.01.

[b] Specimen previously run at 105,000 psi for 1.05×10^6 cycles without failure.

Table C-XII Fatigue Properties[a] of Annealed Welded 5Al-2.5Sn Titanium Alloy

Temperature, °F	Maximum Tension Stress, ksi	Number of Cycles to Failure
70	105.0	5.00×10^3
	105.0	1.00×10^4
	105.0	1.20×10^4
	90.0	1.10×10^4
	90.0	2.30×10^4
	90.0	3.00×10^4
	72.0	6.40×10^4
	70.0	4.79×10^5
	70.0	1.13×10^6
	70.0	2.30×10^6
-320	155.0	5.00×10^3
	150.0	6.00×10^3[b] (Disc)
	125.0	1.80×10^4
	110.0	2.60×10^4[c] (Disc)
	95.0	2.60×10^4
	85.0	1.24×10^5
	82.5	5.90×10^4
	82.5	6.70×10^4
	80.0	6.90×10^4
	80.0	1.15×10^6
	77.5	1.09×10^5
	77.5	1.10×10^6
	75.0	4.30×10^4
-423	144.0	9.00×10^3
	130.0	8.00×10^3[d]
	120.0	5.00×10^3
	100.0	1.90×10^4
	90.0	2.06×10^5

Table C-XII (concl)

Temperature, °F	Maximum Tension Stress, ksi	Number of Cycles to Failure
-423	85.0	5.40×10^4
	75.0	6.80×10^4
	70.0	4.60×10^4
	70.0	1.71×10^5
	60.0	1.41×10^5
	60.0	1.12×10^6 (Disc)

[a] Axial load; R = 0.01.

[b] Specimen previously run at 77,500 psi for 1.10×10^6 cycles without failure.

[c] Specimen previously run at 80,000 psi for 1.15×10^6 cycles without failure.

[d] Specimen previously run at 60,000 psi for 1.12×10^6 cycles without failure.

Table C-XIII Fatigue Properties[a] of Solution Treated and Aged Welded 6Al-4V Titanium Alloy

Temperature, °F	Maximum Tension Stress, ksi	Number of Cycles to Failure
70	140.0	3.00×10^3
	140.0	4.00×10^3
	140.0	4.00×10^3
	100.0	2.30×10^4
	100.0	3.40×10^4
	100.0	4.50×10^4
	90.0	6.00×10^4
	90.0	8.30×10^4
	90.0	1.29×10^5
	85.0	5.04×10^4
	85.0	1.10×10^5
	85.0	1.82×10^6
-320	160.0	7.00×10^3
	150.0	5.00×10^3
	145.0	5.00×10^{3b}
	140.0	1.00×10^3
	140.0	1.90×10^{4c}
	135.0	1.70×10^4
	130.0	7.00×10^3
	120.0	2.70×10^{4d}
	115.0	2.80×10^4
	110.0	3.40×10^4
	100.0	2.10×10^4
	95.0	1.80×10^4
	90.0	4.70×10^4
	90.0	8.00×10^4
	87.5	2.04×10^5
	85.0	1.10×10^6 (Disc)
	80.0	1.03×10^6 (Disc)
	80.0	1.12×10^6 (Disc)

Table XIII (concl)

Temperature, °F	Maximum Tension Stress, ksi	Number of Cycles to Failure
-423	130.0	7.00×10^3
	130.0	1.10×10^4
	130.0	2.00×10^3[e]
	125.0	8.00×10^3[f]
	120.0	7.00×10^3[g]
	110.0	1.30×10^4
	105.0	1.70×10^4
	100.0	5.90×10^4
	95.0	2.20×10^4
	90.0	9.00×10^4
	85.0	1.79×10^5
	82.5	1.22×10^5
	80.0	1.03×10^6 (Disc)
	80.0	1.15×10^6 (Disc)
	80.0	1.50×10^6 (Disc)

[a] Axial load; R = 0.01.

[b] Specimen previously run at 85,000 psi for 1.10×10^6 cycles without failure.

[c] Specimen previously run at 80,000 psi for 1.03×10^6 cycles without failure.

[d] Specimen previously run at 80,000 psi for 1.12×10^6 cycles without failure.

[e] Specimen previously run at 80,000 psi for 1.03×10^6 cycles without failure.

[f] Specimen previously run at 80,000 psi for 1.50×10^6 cycles without failure.

[g] Specimen previously run at 80,000 psi for 1.15×10^6 cycles without failure.

DISTRIBUTION

Copies	To
1 thru 12	National Aeronautics and Space Administration George C. Marshall Space Flight Center Huntsville, Alabama Attn: M-P&C-CA
Remaining Copies	Martin Company Denver Division Denver, Colorado 80201 Attn: Libraries Section